

# **SANDIA REPORT**

SAND2006-6590

Unlimited Release

Printed November 2006

## **Fusion Transmutation of Waste: Design and Analysis of the In-Zinerator Concept**

Benjamin B. Cipiti, Virginia D. Cleary, Jason T. Cook, Samuel Durbin, Rodney L. Keith, Thomas A. Mehlhorn, Charles W. Morrow, Craig L. Olson, Gary E. Rochau, James D. Smith, Matthew C. Turgeon, Michael F. Young, Laila El-Guebaly, Ryan Grady, Phiphat Phruksarojanakun, Igor Sviatoslavsky, Paul Wilson, A. B. Alajo, Avery Guild-Bingham, Pavel Tsvetkov, Mahmoud Youssef, Wayne Meier, Francesco Venneri, Terry R. Johnson, Jim L. Willit, Tom E. Drennen, Will Kamery

Prepared by  
Sandia National Laboratories  
Albuquerque, New Mexico 87185 and Livermore, California 94550

Sandia is a multiprogram laboratory operated by Sandia Corporation, a Lockheed Martin Company, for the United States Department of Energy's National Nuclear Security Administration under Contract DE-AC04-94AL85000.

Approved for public release; further dissemination unlimited.



**Sandia National Laboratories**

Issued by Sandia National Laboratories, operated for the United States Department of Energy by Sandia Corporation.

**NOTICE:** This report was prepared as an account of work sponsored by an agency of the United States Government. Neither the United States Government, nor any agency thereof, nor any of their employees, nor any of their contractors, subcontractors, or their employees, make any warranty, express or implied, or assume any legal liability or responsibility for the accuracy, completeness, or usefulness of any information, apparatus, product, or process disclosed, or represent that its use would not infringe privately owned rights. Reference herein to any specific commercial product, process, or service by trade name, trademark, manufacturer, or otherwise, does not necessarily constitute or imply its endorsement, recommendation, or favoring by the United States Government, any agency thereof, or any of their contractors or subcontractors. The views and opinions expressed herein do not necessarily state or reflect those of the United States Government, any agency thereof, or any of their contractors.

Printed in the United States of America. This report has been reproduced directly from the best available copy.

Available to DOE and DOE contractors from

U.S. Department of Energy  
Office of Scientific and Technical Information  
P.O. Box 62  
Oak Ridge, TN 37831

Telephone: (865)576-8401  
Facsimile: (865)576-5728  
E-Mail: [reports@adonis.osti.gov](mailto:reports@adonis.osti.gov)  
Online ordering: <http://www.osti.gov/bridge>

Available to the public from

U.S. Department of Commerce  
National Technical Information Service  
5285 Port Royal Rd  
Springfield, VA 22161

Telephone: (800)553-6847  
Facsimile: (703)605-6900  
E-Mail: [orders@ntis.fedworld.gov](mailto:orders@ntis.fedworld.gov)  
Online order: <http://www.ntis.gov/help/ordermethods.asp?loc=7-4-0#online>



## **Fusion Transmutation of Waste: Design and Analysis of the In-Zinerator Concept**

B.B. Cipiti<sup>1</sup>, V.D. Cleary<sup>1</sup>, J.T. Cook<sup>1</sup>, S. Durbin<sup>1</sup>, R.L. Keith<sup>1</sup>, T.A. Mehlhorn<sup>1</sup>, C.W. Morrow<sup>1</sup>, C.L. Olson<sup>1</sup>, G.E. Rochau<sup>1</sup>, J.D. Smith<sup>1</sup>, M. Turgeon<sup>1</sup>, M. Young<sup>1</sup>, L. El-Guebaly<sup>2</sup>, R. Grady<sup>2</sup>, P. Phruksarojanakun<sup>2</sup>, I. Sviatoslavsky<sup>2</sup>, P. Wilson<sup>2</sup>, A.B. Alajo<sup>3</sup>, A. Guild-Bingham<sup>3</sup>, P. Tsvetkov<sup>3</sup>, M. Youssef<sup>4</sup>, W. Meier<sup>5</sup>, F. Venneri<sup>6</sup>, T.R. Johnson<sup>7</sup>, J.L. Willit<sup>7</sup>, T.E. Drennen<sup>8</sup>, W. Kamery<sup>8</sup>

<sup>1</sup>Sandia National Laboratories, P.O. Box 5800, Albuquerque, NM 87185-0748

<sup>2</sup>University of Wisconsin, 1500 Engineering Dr, Madison, WI 53706

<sup>3</sup>Texas A&M University, 129 Zachry Engineering Center, College Station, TX 77843-3133

<sup>4</sup>University of California, 46-128C Engr IV, Los Angeles, CA 90095-1597

<sup>5</sup>Lawrence Livermore National Laboratory, P.O. Box 808, L-641, Livermore, CA 94551

<sup>6</sup>General Atomics, P.O. Box 85608, San Diego, CA 92186-5608

<sup>7</sup>Argonne National Laboratory, 9700 S. Cass Ave, Argonne, IL 60439

<sup>8</sup>Hobart & William Smith College, 300 Pultney St, Geneva, NY 14456

### **Abstract**

Due to increasing concerns over the buildup of long-lived transuranic isotopes in spent nuclear fuel waste, attention has been given in recent years to technologies that can burn up these species. The separation and transmutation of transuranics is part of a solution to decreasing the volume and heat load of nuclear waste significantly to increase the repository capacity. A fusion neutron source can be used for transmutation as an alternative to fast reactor systems. Sandia National Laboratories is investigating the use of a Z-Pinch fusion driver for this application. This report summarizes the initial design and engineering issues of this "In-Zinerator" concept. Relatively modest fusion requirements on the order of 20 MW can be used to drive a sub-critical, actinide-bearing, fluid blanket. The fluid fuel eliminates the need for expensive fuel fabrication and allows for continuous refueling and removal of fission products. This reactor has the capability of burning up 1,280 kg of actinides per year while at the same time producing 3,000 MW<sub>th</sub>. The report discusses the baseline design, engineering issues, modeling results, safety issues, and fuel cycle impact.

## **Acknowledgement**

The authors would like to acknowledge the support of Laboratory Directed Research and Development Project 81753 under the guidance of Tom Mehlhorn and Dan Sinars, and Project 102362 under the guidance of Craig Olson and Gary Rochau for this research.

# Contents

Abstract .....	3
Acknowledgement .....	4
Contents .....	5
Figures.....	7
Tables .....	8
Executive Summary .....	9
Acronyms.....	12
1.0 Introduction.....	13
2.0 Background.....	14
2.1 Spent Nuclear Fuel.....	14
2.2 Reprocessing .....	16
2.3 Transmutation .....	17
2.4 Z-Pinch Facility .....	18
2.5 References.....	20
3.0 In-Zinerator Concept & Design Parameters .....	21
3.1 Chamber Design.....	23
3.1.1 Shock Mitigation.....	24
3.1.2 Material Choice.....	24
3.1.3 Chamber Component Lifetime .....	25
3.1.4 Activation.....	27
3.1.5 RTL Options .....	28
3.2 Blanket Design.....	32
3.2.1 Actinide Mixture.....	32
3.2.2 Primary Coolant.....	33
3.2.3 Tritium Breeding.....	34
3.2.4 Safety Issues.....	35
3.3 Extraction Systems.....	36
3.3.1 Continuous Reprocessing.....	36
3.3.2 Tritium & Fission Product Gas Recovery.....	46
3.3.3 Safety Issues.....	52
3.4 Thermal Analysis .....	53
3.4.1 Heat Generation .....	53
3.4.2 Other Thermal Issues .....	54
3.5 References.....	55
4.0 Advanced Nuclear Fuel Cycle .....	58
4.1 GNEP Fuel Cycle.....	58
4.2 Integration of the In-Zinerator in the Fuel Cycle.....	59
4.2.1 Complete TRU Burning.....	59
4.2.2 Alternative Burning Strategies.....	60
4.2.3 In-Zinerator vs. Fast Reactor Technical Comparison .....	61
4.2.4 In-Zinerator vs. Fast Reactor Economic Comparison.....	62
4.2.5 Summary Comparison .....	66
4.3 References.....	67
5.0 Modeling Methodology .....	68

5.1 MCNP Model.....	68
5.1.1 Modeling Data .....	70
5.1.2 MCNP Transmutation Modeling .....	72
5.2 MCise Transmutation Model .....	73
5.2.1 Theory .....	73
5.2.2 Modeling Requirements .....	74
5.2.3 MCise Model .....	75
5.2.4 Analysis Methodology .....	78
5.3 Activation and Heat Load Reduction Calculations .....	79
5.4 References .....	79
6.0 Modeling & Transmutation Results .....	80
6.1 Neutron Spectrum Analysis .....	80
6.1.1 Neutron Energy Spectrum.....	80
6.1.2 Pulse Modeling .....	81
6.2 Transmutation Rates .....	83
6.2.1 Actinide Inventory Change .....	83
6.2.2 Actinide Burnup/Buildup Rates .....	85
6.2.3 Fission Product Buildup.....	88
6.2.4 Net Transmutation Effectiveness .....	90
6.3 Design Optimization Variables .....	92
6.2.1 <sup>6</sup> Li Enrichment .....	93
6.2.2 First Wall Thickness .....	95
6.4 References .....	96
7.0 Conclusion .....	97
7.1 References .....	99

## Figures

Figure 2-1: Heat Load of Spent Fuel by Element .....	15
Figure 2-2: Heat Load of Spent Fuel as a Function of Time .....	15
Figure 2-3: UREX+1a Reprocessing .....	16
Figure 2-4: Fission to Capture Cross-Section .....	18
Figure 2-5: Z-Pinch Wire Array and Target .....	19
Figure 2-6: Current Z-Pinch Experiment at Sandia National Laboratories .....	19
Figure 3-1: In-Zinerator Power Plant.....	21
Figure 3-2: Neutron Damage to the First Wall .....	26
Figure 3-3: Neutron Damage as a Function of Radius .....	26
Figure 3-4: Specific Activity of Chamber Components after Removal .....	27
Figure 3-5: Pressure Loading of the RTL .....	29
Figure 3-6: Outer RTL Cone with Stiffening Rings .....	30
Figure 3-7: Steel RTL Cost for the In-Zinerator.....	31
Figure 3-8: Cast Tin RTL Cost .....	32
Figure 3-9: Tritium Breeding Ratio vs. $^6\text{Li}$ Enrichment .....	34
Figure 3-10: Conceptual Actinide Mixture Treatment Flowsheet.....	38
Figure 3-11: Zirconium Removal Steps.....	40
Figure 3-12: Overall Actinide Loss Relative to Zirconium Removal Steps .....	41
Figure 3-13: Actinide Extraction and Fuel Reconstitution Steps .....	42
Figure 3-14: Fission Product Removal .....	43
Figure 3-15: Tritium Recovery from Argon .....	48
Figure 3-16: Tritium Recovery from $(\text{LiF})_2\text{-AnF}_3$ .....	49
Figure 3-17: Distillation and Storage.....	51
Figure 4-1: GNEP Fuel Cycle.....	58
Figure 4-2: Advanced Fuel Cycle with Complete In-Zineration of TRU .....	60
Figure 4-3: MOX Fuel Cycle with In-Zineration of Minor Actinides.....	61
Figure 4-4: Allowable In-Zinerator LCOE to be Competitive with FRs.....	65
Figure 5-1: In-Zinerator MCNP Model .....	69
Figure 5-2: Schematic of In-Zinerator MCise Model .....	75
Figure 6-1: Neutron Energy Spectrum with Initial Core Loading Isotopics .....	80
Figure 6-2: In-Zinerator Neutron Pulse .....	81
Figure 6-3: Relative Energy Deposition vs. Time .....	82
Figure 6-4: Power vs. Time .....	82
Figure 6-5: Actinide Ratio Change in the In-Zinerator .....	84
Figure 6-6: Beginning of Life and End of Life Comparison of Blanket Radioactivity .....	85
Figure 6-7: Actinide Burnup/Buildup after 1 Year of Operation .....	86
Figure 6-8: Actinide Burnup/Buildup after 50 Years of Operation.....	87
Figure 6-9: Actinide Burnup/Buildup as a Function of $k_{\text{eff}}$ .....	88
Figure 6-10: In-Zinerator Net Transmutation Capability .....	91
Figure 6-11: Effect of TRU Buildup and Cs/Sr .....	92
Figure 6-12: Energy Multiplication vs. Time with and without $^6\text{Li}$ Replenishment .....	93
Figure 6-13: $k_{\text{eff}}$ vs. Time with and without $^6\text{Li}$ Replenishment.....	94
Figure 6-14: Tritium Breeding Ratio (TBR) with and without Replenishment of $^6\text{Li}$ .....	95
Figure 6-15: Effect of First Wall Thickness on Criticality .....	96

## Tables

Table 3-1: In-Zinerator Design Parameters .....	23
Table 3-2: Fission Yields – Characterized by Fluoride Chemistry.....	37
Table 3-3: Estimated Composition of Salt Entering Process.....	39
Table 3-4: Diameters of Packed Columns .....	45
Table 3-5: Entrained Elements in Helium Sparge Gas .....	49
Table 3-6: Nuclear Heating and Temperature Rise .....	54
Table 4-1: Reactor Cost Assumptions .....	63
Table 4-2: Fleet Average LCOE (cents/kWh) .....	64
Table 4-3: In-Zinerator vs. FR vs. Thermal Recycle .....	66
Table 5-1: TRU Vectors as a Function of Burnup.....	71
Table 5-2: TRU Vectors as a Function of Fuel Age .....	72
Table 5-3: Loading Rates.....	77
Table 5-4: Analysis Parameters .....	79
Table 6-1: Fission Product Production in 50 Years (Moles) .....	89



## Executive Summary

A scoping level analysis of a transmutation reactor driven by Z-Pinch fusion has been initiated. The “In-Zinerator” concept burns up long-lived actinides from light water reactor waste in a sub-critical blanket driven by high energy fusion neutrons. Significant power is produced while at the same time providing a repository benefit by transmuting actinides into shorter-lived fission products that produce much less radioactive heat.

A D-T fusion target yield of 200 MJ fired once every ten seconds will be adequate to design a reactor capable of transmuting 1,280 kg of actinides per year while at the same time producing 3,000 MW<sub>th</sub>. This defines the requirements of a Z-Pinch pulsed power fusion source for use as a transmutation reactor. It also provides guidance to the Z-Pinch experimental program at Sandia National Laboratories as to what extrapolations from current capabilities will be required to enable this mission application. This research has focused on the design of the transmutation blanket surrounding a future Z-Pinch fusion source. The fusion source initiates a burn and energy multiplication in the blanket which contains actinides in a fluid fuel form.

The In-Zinerator effectively converts actinides into fission products. Figure 1 shows the effectiveness of transmuting actinides for 50 years. The blue line shows the total heat production from 64 metric tons of actinides. The green line shows the heat production from the sum of the all the fission products produced as a result of fissioning the 64 metric tons of actinides. After 10 years of cooling the heat load is decreased by a factor of 10, and after 50 years the heat load is reduced by a factor of 500.

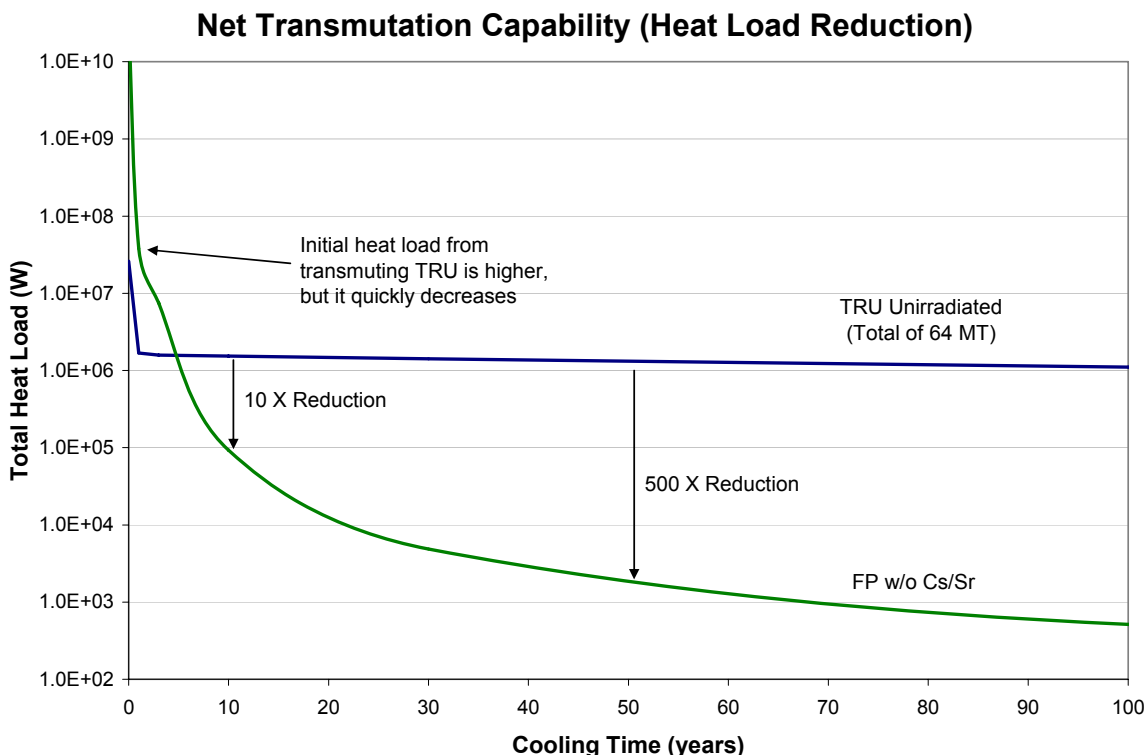


**Figure 1: Net Transmutation Effectiveness of the In-Zinerator Concept**

The Yucca Mountain nuclear waste repository capacity is currently limited by heat load, so the reduction of heat production by transmuting actinides into fission products could lead to much more effective use of repository space. The ultimate goal of transmutation technologies (along with reprocessing) is to prevent the need for additional costly repositories for a couple hundred years.

The In-Zinerator blanket consists of an annular array of 5 cm pipes containing a lithium fluoride eutectic that forms with actinide fluorides. This mixture is in a fluid form, and will be recycled continuously for fission product separation and fuel replenishment. Lead coolant surrounds the actinide channels to remove the heat and drive a power plant loop. The engineering design of this system is described, and key engineering issues were examined as part of this work.

There are five key advantages of transmuting actinides with this type of design:

1. A sub-critical blanket driven by fusion makes the burning of actinides safer without the possibility of a prompt-critical excursion. In addition, a sub-critical configuration allows unique actinide mixtures to be burned safely without the need to worry about reactor control issues.
2. The In-Zinerator can operate with the lowest possible support ratio. The support ratio is the ratio of transmutation reactors to light water reactors required to burn up the transuranic actinides as fast as the current light water reactor fleet produces them. The In-Zinerator does not require any fertile material, like  $^{238}\text{U}$ , which would otherwise breed additional actinides. This allows the In-Zinerator concept to reach a much lower support ratio than fast reactors (FRs).
3. The fluid fuel form allows for the actinides to be continuously reprocessed and prevents the need for costly fuel fabrication (as compared to FRs). The continuous refueling also eliminates the need for fueling shutdowns.
4. Compared to other fusion designs, Z-Pinch may offer the most compact fusion source due to the unique power delivery system. The solid transmission lines come in from the top of the reactor, which means that the sides and bottom are left clear for installation of a blanket. Unique shock mitigating techniques using aerosols will be possible since the chamber atmosphere does not need to be clean for the driver to function.
5. A fusion-driven transmuter provides valuable operating experience for a fusion system which could provide a path to a pure fusion power plant in the future.

There are a number of challenges that must be overcome in order for this concept to be realized:

1. Z-Pinch must continue to make strides in fusion yield production.
2. More theoretical and experimental validation will be required for the shock mitigation technique.
3. The bottom portion of the transmission line that delivers the energy pulse to the fusion target will be blown apart after each shot. A recyclable transmission line has been designed for this purpose. However, the recyclable transmission line destruction, remanufacturing, repetitive installation, and interaction with the solid first wall all need to be investigated further.

4. The energy deposition from the fusion pulse and subsequent fission energy multiplication occurs almost instantaneously. Removing the heat, and engineering the device for large temperature changes will be challenges for future work.
5. The high neutron flux will cause damage to the chamber first wall and actinide pipes over time which could require periodic replacement of components. This issue will need to be addressed by either limiting the power level or examining high temperature operation that extends the lifetime of components.
6. There are a number of safety and control concerns with using a fluid fuel (even in a sub-critical configuration) that will need to be more fully explored. Also, the thermal properties and materials compatibility of the liquid fuel will have to be determined experimentally.
7. This concept will have all the components and challenges of FR technology, plus the added cost of the fusion driver. Compared side by side, the In-Zinerator will likely cost more than a FR of the same power output. It is not clear if the better transmutation efficiency of the In-Zinerator will make up for this deficit.

The integration of the In-Zinerator design in the fuel cycle was also of interest in this work. The In-Zinerator support ratio in the fuel cycle is 1:5, meaning that one In-Zinerator will be required for every 5 light water reactors in order to burn up the transuranic actinides as fast as the light water reactor fleet produces them. The current fleet of light water reactors would then require about 20 In-Zinerators, each producing 1,000 MW<sub>e</sub> to stabilize transuranic levels.

Although it is too early to estimate the cost of the In-Zinerator, an economic analysis was performed to set the goals in comparison to the cost of transmuting actinides using a FR fleet. Due to the better support ratio offered by the In-Zinerator, this concept can cost up to 25% more than a FR and still be competitive. Whether FRs or In-Zinerators are used, reprocessing and transmutation are likely to add at least 2.0 mil/kWh to the cost of nuclear power across the entire fleet.

Although the added cost is very small compared to what the average consumer pays for electricity, it adds up to a very large sum of money to help build a fleet of transmutation systems. It will be up to policy-makers to determine if the benefits of these technologies are worth the cost.

Fusion transmutation of waste is a useful application for a technology that has a difficult time reaching economical competitiveness. The In-Zinerator provides an intermediate step on the path towards pure fusion energy development, which will be required for long-term energy sustainability. Only fusion has the long-term potential to provide sustainable energy without criticality concerns and without the production of large amounts of high level waste.

# Acronyms

ADS	Accelerator Driven Systems
AE	Alkaline Earth
AFCI	Advanced Fuel Cycle Initiative
ALARA	As Low As Reasonably Achieved
ALWR	Advanced Light Water Reactor
AM	Alkali Metal
An	Actinide
ANL	Argonne National Laboratory
DPA	Displacement Per Atom
FG	Fission Gas
FP	Fission Product
FPY	Full Power Year
FR	Fast Reactor
FSV	Fort Saint Vrain
FW	First Wall
GNEP	Global Nuclear Energy Partnership
HLW	High Level Waste
IFE	Inertial Fusion Energy
ITER	International Thermonuclear Experimental Reactor
LCOE	Levelized Cost of Electricity
LOCA	Loss of Coolant Accident
LLW	Low Level Waste
LWR	Light Water Reactor
MA	Minor Actinides
MCise	Monte Carlo Inventory Simulation Engine
MCNP	Monte Carlo Neutron Transport (code)
MOX	Mixed Oxide
MSBR	Molten Salt Breeder Reactor
MT	Metric Ton
MTIHM	Metric Ton of Initial Heavy Metal
MWD	Mega-Watt Day
NM	Noble Metal
ORNL	Oak Ridge National Laboratory
PDF	Probability Distribution Function
PRISM	Power Reactor – Innovative, Small Module
RE	Rare Earth
RTL	Recyclable Transmission Line
SNL	Sandia National Laboratory
TBR	Tritium Breeding Ratio
TRU	Transuranic Isotopes (Np, Pu, Am, Cm)
UREX	Uranium Extraction (Aqueous Processing of Spent Fuel)

# **Fusion Transmutation of Waste: Design and Analysis of the In-Zinerator Concept**

## **1.0 Introduction**

Nuclear waste transmutation is possible with the use of any fast neutron source. The Z-Pinch fusion program at Sandia National Laboratories uses an intense pulsed power source to generate x-rays which in turn heat a fusion target. The high-energy neutrons liberated from the fusion reaction can be used to induce fission in an actinide-bearing blanket to burn up long-lived actinides. The goal of this research was to design a baseline transmutation reactor driven by Z-Pinch fusion.

Transmutation of actinides along with reprocessing can dramatically reduce the volume, heat load, and radiotoxicity of nuclear waste from light water reactors (LWRs). The waste generation and lack of a sustainable solution to disposing of the waste is one of the major roadblocks of the continued use of nuclear power. Reprocessing and transmutation make it possible to ensure that only one waste repository will be needed for the next couple centuries. In addition, continued research in these technologies may one day allow for a future without the need for deep geologic nuclear waste disposal.

The “In-Zinerator” concept can be designed to burn up any combination of minor actinides depending on the desired fuel cycle of the future. This report will focus on the burning of all transuranics (TRU) which includes Np, Pu, Am, and Cm. The actinides are contained in a liquid form to allow for continuous on-line removal of fission products and to prevent the need for costly fuel fabrication and fuel characterization. This liquid actinide blanket is designed to be slightly sub-critical to allow for a substantial neutron and energy multiplication. The In-Zinerator can be designed to burn up 1,280 kg of actinides per year while at the same time producing 1,000 MWe.

The advantage of using fusion for transmutation is that the fusion yield requirement is modest and makes the engineering issues much less challenging. In addition, this application provides fusion with an intermediate step on the path to a pure fusion power plant. An In-Zinerator can generate revenue both by producing power and destroying actinides, which may make it an economic application of fusion well before pure fusion energy is economic.

This report discusses the baseline design that was chosen including the associated engineering issues. The modeling of the neutronics of the actinide blanket and chamber is presented along with the modeling methodology of the transmutation calculations. The continuous processing loop and power plant loop are examined. Safety issues in key areas of concern are examined. Finally, attention was given to integration into the nuclear fuel cycle and how this option competes with fast reactor (FR) transmutation.

## 2.0 Background

Before the In-Zinerator design is described, a discussion will be presented here on nuclear waste, reprocessing and transmutation options, and the Z-Pinch facility. The composition of nuclear waste and the effect on the repository are important to understand to show which species should be transmuted. Nuclear fuel reprocessing will be required to separate out the different components in waste. A brief background on transmutation science will be presented. The final part of this chapter discusses the Z-Pinch experiment and how it can be used for transmutation.

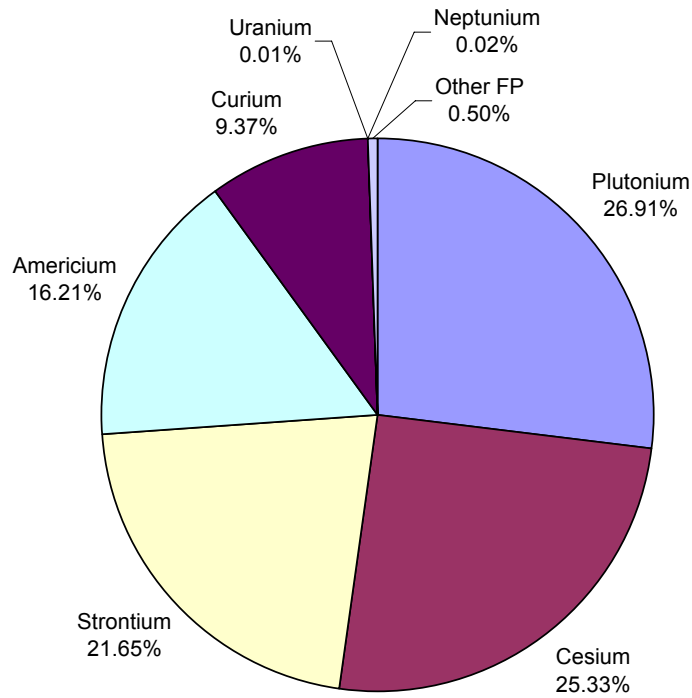
### 2.1 Spent Nuclear Fuel

The current U.S. LWR fleet produces about 2,000 MT of spent fuel per year. The Yucca Mountain Project is designed to hold 70,000 MT of spent fuel and other high level wastes (HLW) with 63,000 MT making up commercial spent fuel [1]. About 45,000 MT of spent fuel has been accumulated to date, which means that by 2015 the repository will be full.

The repository is not limited by space, but rather by the heat load and radiotoxicity of the fuel [2]. The heat load determines how closely the waste can be packed without causing changes in water flow in the surrounding rock, but the radiotoxicity and mobility of isotopes are also important since they affect long-term dose rates. Currently, the repository is limited by temperature, so a reduction in heat load means more waste can go into the repository. The Advanced Fuel Cycle Initiative (AFCI) has done extensive research on alternative fuel cycles that extend the capacity of the repository [3,4].

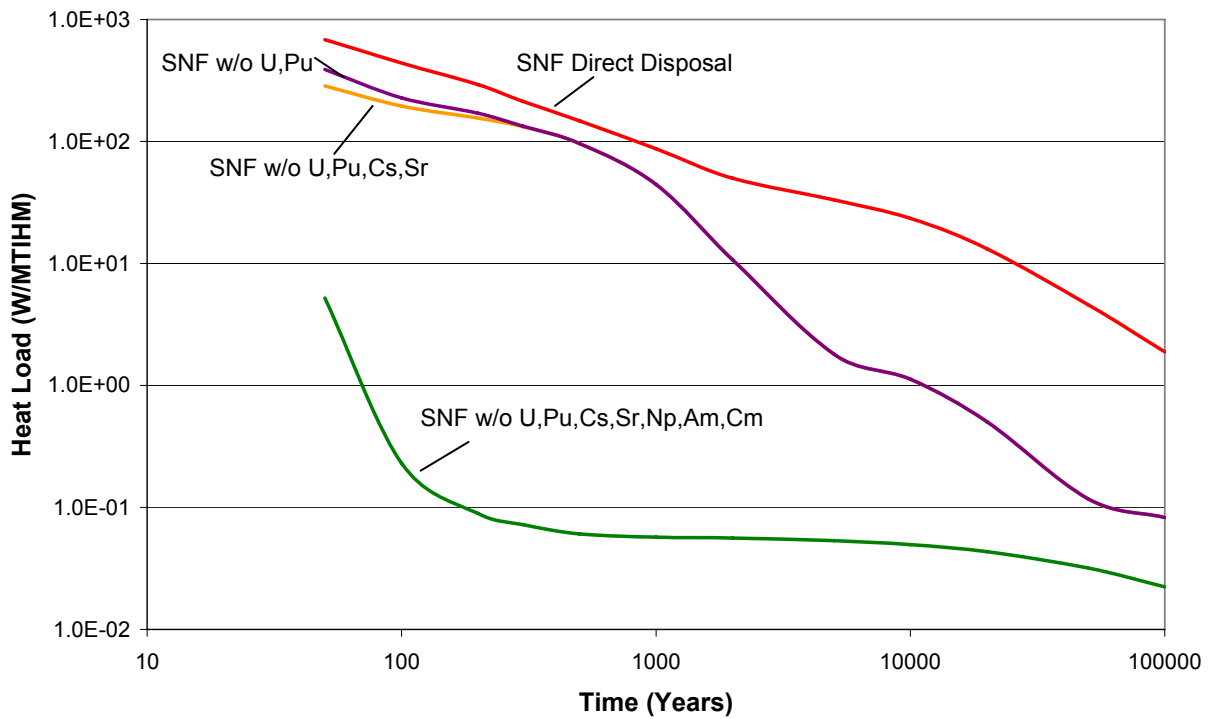
As shown in Figure 2-1 the dominant heat producers in spent fuel are Pu, followed by the fission products Cs/Sr, followed by the minor actinides Am/Cm. This figure is representative of 50 year-old spent pressurized water reactor fuel with a burnup of 60,000 MWD/MT and initial enrichment of 4.03 %. Although U makes up the majority of the mass of spent fuel, it has a very small contribution to heat load. The rest of the fission products only make up 0.5 % of the heat load.

Figure 2-2 shows the heat load contribution as a function of time on a log-log scale, which shows the long-term implications on the repository. The graph is plotted in units of Watts per metric ton of initial heavy metal (W/MTIHM), so it is normalized to the mass of the original fuel as would be disposed directly in the once-through cycle. The top line in red is the total heat load of spent fuel. The purple line demonstrates the effect of removing Pu and U from spent fuel. The drop in heat load is almost all due to Pu removal, but in any reprocessing scheme U will also be removed for volume reduction. The orange line is the effect of removing the fission products Cs and Sr. Because of their thirty-year half-lives, their removal is more important in the early years. The green line shows the dramatic effect of also removing the minor actinides Np, Am, and Cm. Np has little impact on heat-load, but Np-237 is the major contributor to dose in the surrounding areas of the repository over 10,000-year-plus time frames [2]. Many of the other actinides also contribute to the dose, so removing the actinides also decreases the long term dose concerns of the repository.



**Figure 2-1: Heat Load of Spent Fuel by Element**

### Heat Load Contributors in Spent Fuel



**Figure 2-2: Heat Load of Spent Fuel as a Function of Time**

Figures 2-1 and 2-2 demonstrate which elements are important to remove in an advanced reprocessing plant. U is extracted as a strategic resource and to reduce volume. Pu, also a strategic resource and proliferation concern, and the other minor actinides (Np, Am, Cm) are extracted due to their long-term contribution to heat load and dose. Cs and Sr are extracted due to their short-term contribution to heat load. All of these separations have the potential to decrease the heat load by a factor of 100 at the time of emplacement and a factor of 1,000 after 100 years depending on separation efficiency. This could mean that based on the thermal limits, the repository could hold the reprocessed waste from 100 times as much fuel as with the direct disposal plan.

## 2.2 Reprocessing

The UREX+ reprocessing concept has been studied by the AFCI program extensively for the purpose of improving waste management [3,4,5]. The basic UREX reprocessing concept removes uranium from spent fuel, but other separation steps can be added to remove the major contributors to the heat load and radiotoxicity of nuclear waste. The UREX+1a scheme has a separation step for U, Cs/Sr, and all the TRU (Pu, Np, Am, Cm). Additional processing steps have been investigated to separate Am/Cm from the Pu/Np in the TRU, and even isolation of specific species. However, the current plans are focusing on the UREX+1a process so that Pu is not separated from the rest of the minor actinides (for proliferation concerns) [3]. Figure 2-3 shows a simplified flow diagram of UREX+1a showing all of the different product and waste streams generated.

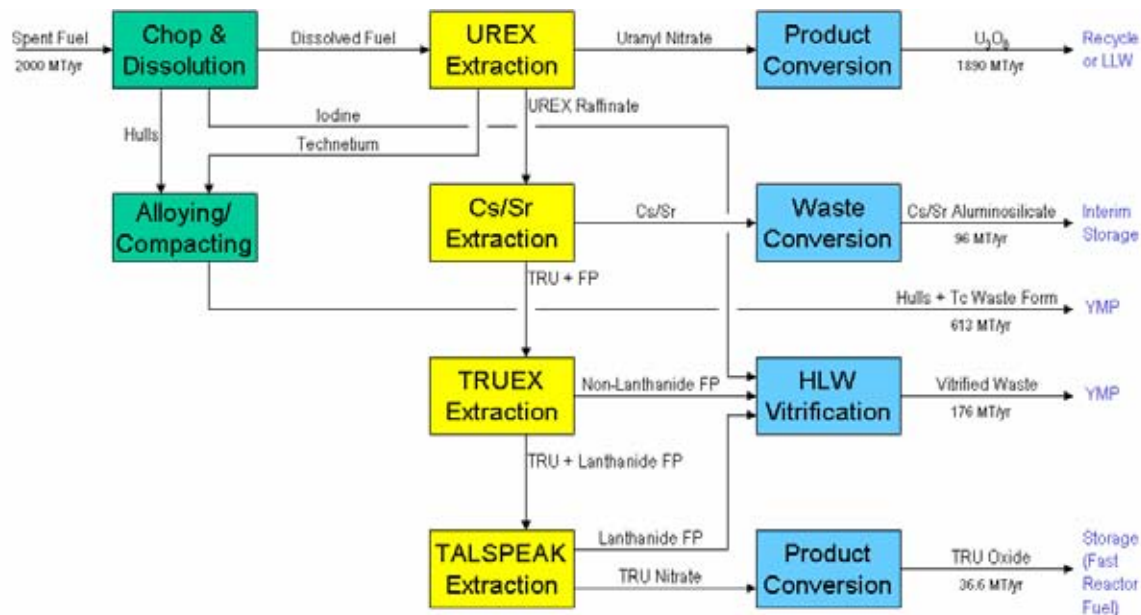


Figure 2-3: UREX+1a Reprocessing [4,5]



The two major product streams are U<sub>3</sub>O<sub>8</sub> (which could be stored for re-enrichment, for breeding, or disposed as low level waste) and the TRU oxide (which could be stored for future use as FR fuel or as fuel for other potential burners).

There are five major waste streams in addition to small amounts of low level waste that are produced: I, Tc, hulls, vitrified fission products, and Cs/Sr. The short-lived isotopes of Cs/Sr are placed into a solid waste form and could go to a temporary waste storage facility for natural decay. The I and Tc could potentially be transmuted into stable species, though it is uncertain whether this is a cost-effective option.

The UREX+1a process is able to partition all of the major contributors to heat load and long term dose in spent fuel. This process must be in place in order to provide the fuels for fast-spectrum reactors or transmuters to transform long-lived species into safer or more stable forms.

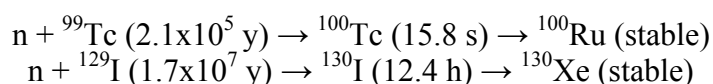
## 2.3 Transmutation

The term ‘transmutation’ spans many nuclear processes, but the main goal is to turn a long-lived isotope into a short-lived or stable species. Transmutation of actinides refers to the fissioning or ‘burning’ of these species. Although fission produces a spectrum of radioactive fission products, the long-term radioactivity and heat load of the fission products is much less than the actinides, so there is a net gain to burning up actinides. In addition, due to the high energy content in the actinides, transmutation produces a great deal of power.

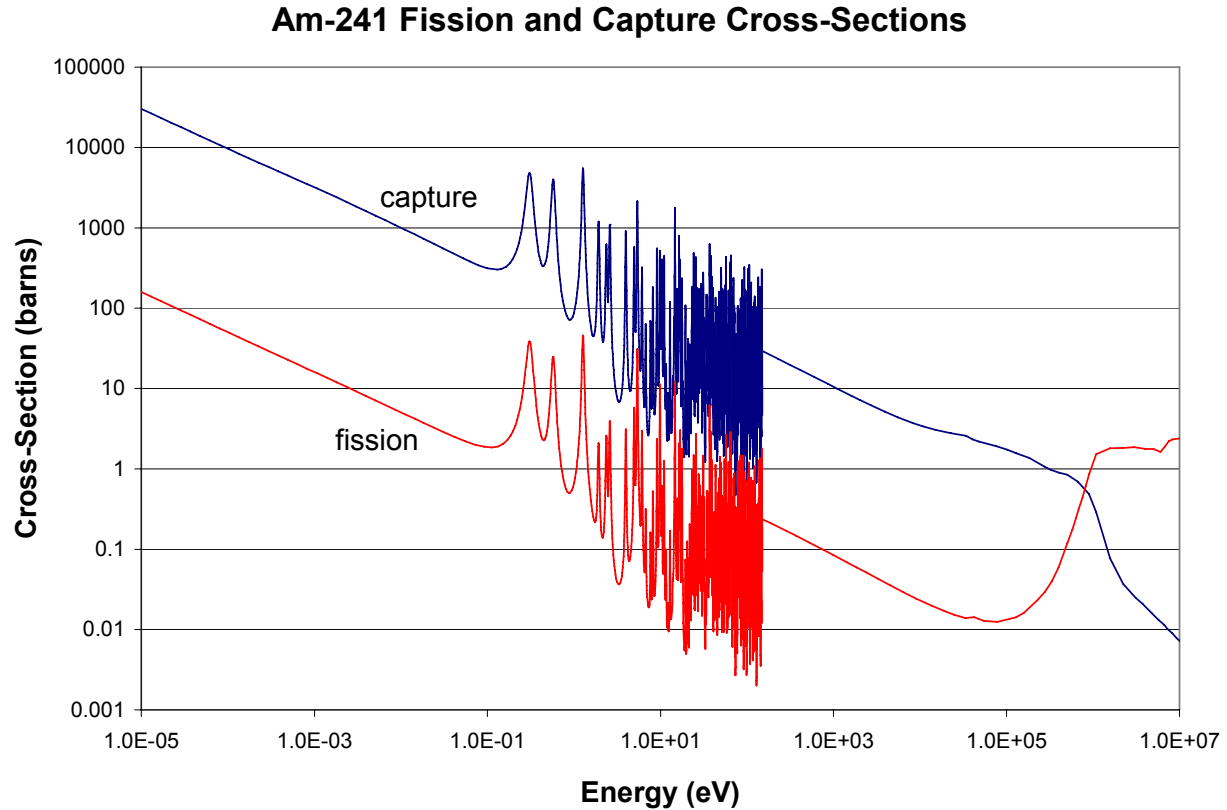
Neutrons are used to initiate the fission reactions needed to transmute actinide species. When bombarded with a neutron, an actinide can either capture the neutron and create a heavier actinide, or it can absorb the neutron and fission. The trick with actinide fissioning is to operate at neutron energies such that fission occurs more often than capture. For most of the TRU isotopes, a high neutron energy (fast spectrum) is required to optimize this fission to capture probability.

Figure 2-4 shows an example of the fission and capture cross-sections for <sup>241</sup>Am. The capture cross-section is always higher until above 1 MeV neutron energy. This graph demonstrates the value of moving to fast spectrums with neutron energies greater than 1 MeV for burning up the minor actinides. Many of the other actinides that build up in spent fuel show similar trends. There are three different methods for generating a fast neutron spectrum: fast reactors (FR), fusion, and accelerator-driven systems.

It is also possible to transmute fission products into short-lived or stable species. In contrast to actinide transmutation, transmutation of fission products is accomplished through neutron capture reactions. Two ideal examples are the transmutation of <sup>99</sup>Tc and <sup>129</sup>I:



For both of these species, the absorption of a neutron creates a very short-lived isotope that then decays into a stable species. Thermal neutron energies are required to achieve the highest cross-section for fission product transmutation. These two species may be ideal candidates for transmutation since they contribute to the repository dose, have very long half-lives, and have high cross-sections for neutron absorption. However, transmutation of Tc and I has not yet been investigated in detail for this work.



**Figure 2-4: Fission to Capture Cross-Section [6]**

## 2.4 Z-Pinch Facility

The Z-Pinch facility at Sandia National Laboratories uses an intense x-ray source to heat and compress a fusion target to the energies and densities required to initiate fusion. Extremely high powers are delivered to a tungsten wire array surrounding a D-T fusion target (see Figure 2-5) on the order of nanoseconds. The rapid power delivery through the tungsten wires generates the intense x-ray source that heats the fusion fuel. A transmission line is attached to the top and bottom of the target to deliver the energy pulse through the wires. When the fusion yield occurs, the result is the production of a point source of 14.1 MeV D-T neutrons, which can be used to burn minor actinides.

There are a few advantages to using Z-Pinch to drive a fusion system. The driver cost is expected to be \$30/J of x-rays delivered as compared to \$1000/J for laser or heavy-ion driven fusion [8]. The driver efficiency is high for a fusion system. Repetitive operation of the driver using magnetic switches has already been demonstrated. That being said, Z-Pinch is the youngest of the major fusion concepts.

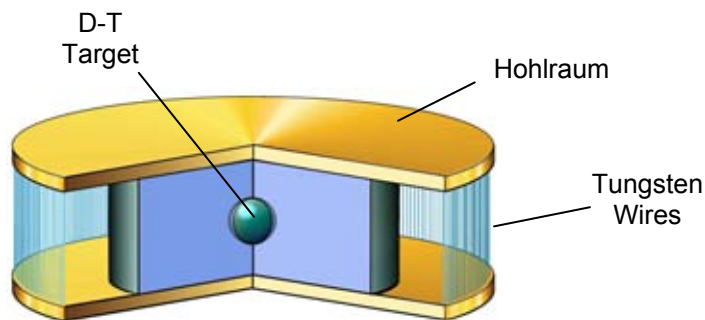


**Figure 2-5: Z-Pinch Wire Array and Target [7]**

The current Z-Pinch chamber is shown in Figure 2-6. Marx generators (a parallel bank of capacitors) produce the pulse of power delivered by water lines to a magnetically insulated transmission line in the center of the device. The current machine has 36 Marx generators that store a total of 11.4 MJ. The water section contains intermediate storage capacitors and pulse forming lines to help create the correct pulse shape. The pulse then passes through an insulator stack to a vacuum transmission section with about 3 MJ of energy. From there the pulse travels through a vacuum magnetically-insulated transmission line to the wire array. The wire array compresses the pulse to produce a much shorter x-ray pulse. The current experiment can deliver 1.8 MJ of x-rays to the target in about 5 ns; however, the experiment is currently being upgraded to increase the power. Using gas targets, yields of close to  $4 \times 10^{13}$  neutrons per target from D-D have been achieved [9]. The current machine can only fire once or twice per day because it was not designed for higher repetition rate.

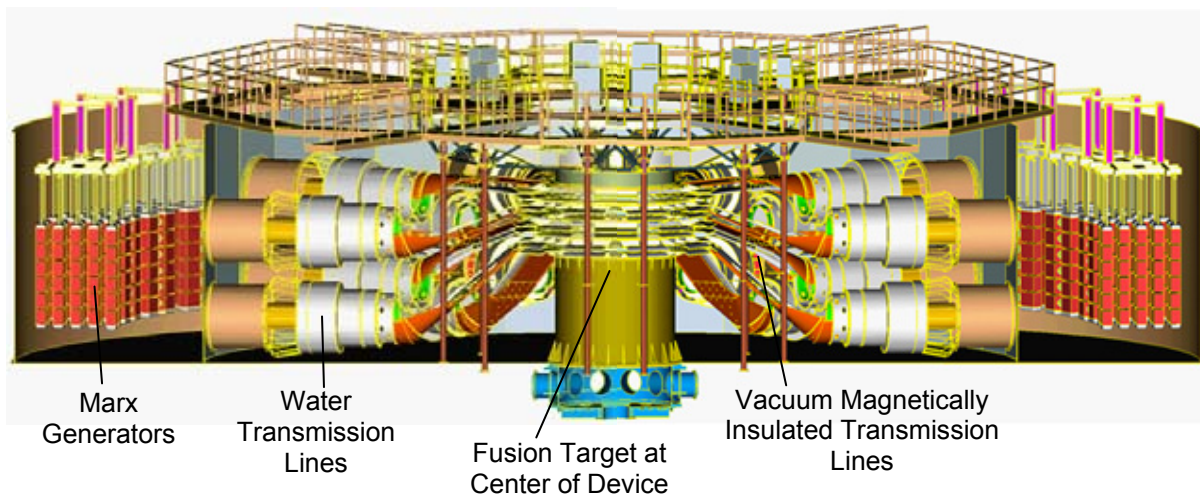


**Figure 2-6: Current Z-Pinch Experiment at Sandia National Laboratories [7]**

A reactor concept based on a Z-Pinch driver will need to make some changes. It is likely that the driver would be a Linear Transformer Driver (LTD) which is more compact than the Marx water line technology [8]. The current experiment uses robust transmission lines that must be rebuilt after each shot, but for high repetition rates, a recyclable transmission line (RTL) is envisioned. The majority of the transmission line will be permanent, but a portion of the transmission line near the target (1-2 m) will be designed to be destroyed on each shot—the debris then would be captured and recycled.

There are at least three major engineering challenges of using Z-Pinch as a reactor. The first is making the RTL/target components in a manner that is reliable and cost effective. The second challenge revolves around reaching the high repetition rate (one shot every ten seconds)—this includes charging the capacitors, replacing the RTL and target, and clearing the chamber. The third challenge is to design systems to mitigate the intense energy release.

The major advantage of using Z-Pinch for transmutation is that the geometry is much more suited for placing a blanket around the target as compared to most other fusion energy systems. The transmission line can come in from the top, but the rest of the area around the target can be open. In addition, the chamber atmosphere does not have to be as clean as other inertial confinement fusion systems. The next chapter discusses the In-Zinerator concept in detail.

## 2.5 References

1. “Final Environmental and Impact Statement for a Geological Repository for the Disposal of Spent Nuclear Fuel and High-Level Radioactive Waste at Yucca Mountain,” Nye County, Nevada, U.S. Department of Energy, Office of Civilian Radioactive Waste Management, DOE/EIS-0250 (February, 2002).
2. “Total System Performance Assessment, Viability Assessment of a Repository at Yucca Mountain, Vol. 3,” TRW Environmental Safety Systems, Inc., Las Vegas, NV (Sept. 10, 1998).
3. “Spent Nuclear Fuel Recycling Program Plan,” Report to Congress, U.S. Department of Energy (March, 2006).
4. “Advanced Fuel Cycle Initiative, Quarterly Report – Volume II (January-March 2005),” SAND2005-3988P (June, 2005).
5. “Scoping Study for the Spent Fuel Treatment Facility,” Washington Group International (January, 2004).
6. Evaluated Nuclear Data File, [www.nndc.bnl.gov/exfor3/endf01.htm](http://www.nndc.bnl.gov/exfor3/endf01.htm) (February 16, 2006).
7. C.L. Olson et al. “Z-Pinch IFE Program Final Report for FY04,” SAND2005-2742P (April, 2005).
8. C.L. Olson, “Z-Pinch Inertial Fusion Energy,” in Landholt-Boernstein Handbook on Energy Technologies (Editor in Chief; W. Martienssen), Volume VIII/3, Fusion Technologies (Edited by K. Heinloth), Springer-Verlag, Berlin-Heidelberg, (2004).
9. C.A. Coverdale et al., “Neutron Production and Implosion Characteristics of a Deuterium Gas Puff Z-Pinch,” to be submitted to *Physics of Plasmas*.

### 3.0 In-Zinerator Concept & Design Parameters

The In-Zinerator uses the Z-Pinch concept to design a transmutation and power reactor. This design was largely based on the Z-Pinch Power Plant design [1], but it was modified to reflect the differences required with the sub-critical blanket. A brief summary of the concept will be given here followed by more detailed designs and analyses of the individual components.

Figure 3-1 shows what the reactor chamber of an In-Zinerator power plant might look like. The pulse for the fusion target is delivered through a magnetically insulated transmission line. The bottom portion of the transmission line (shown in yellow) is destroyed with each shot, so it is designed to be recyclable so that the fragments can be captured and reused. The recyclable transmission line (RTL) is formed from two nested thin-walled cones. This geometry minimizes the inductance through the RTL. The RTL and target debris will be removed from the chamber after each shot.

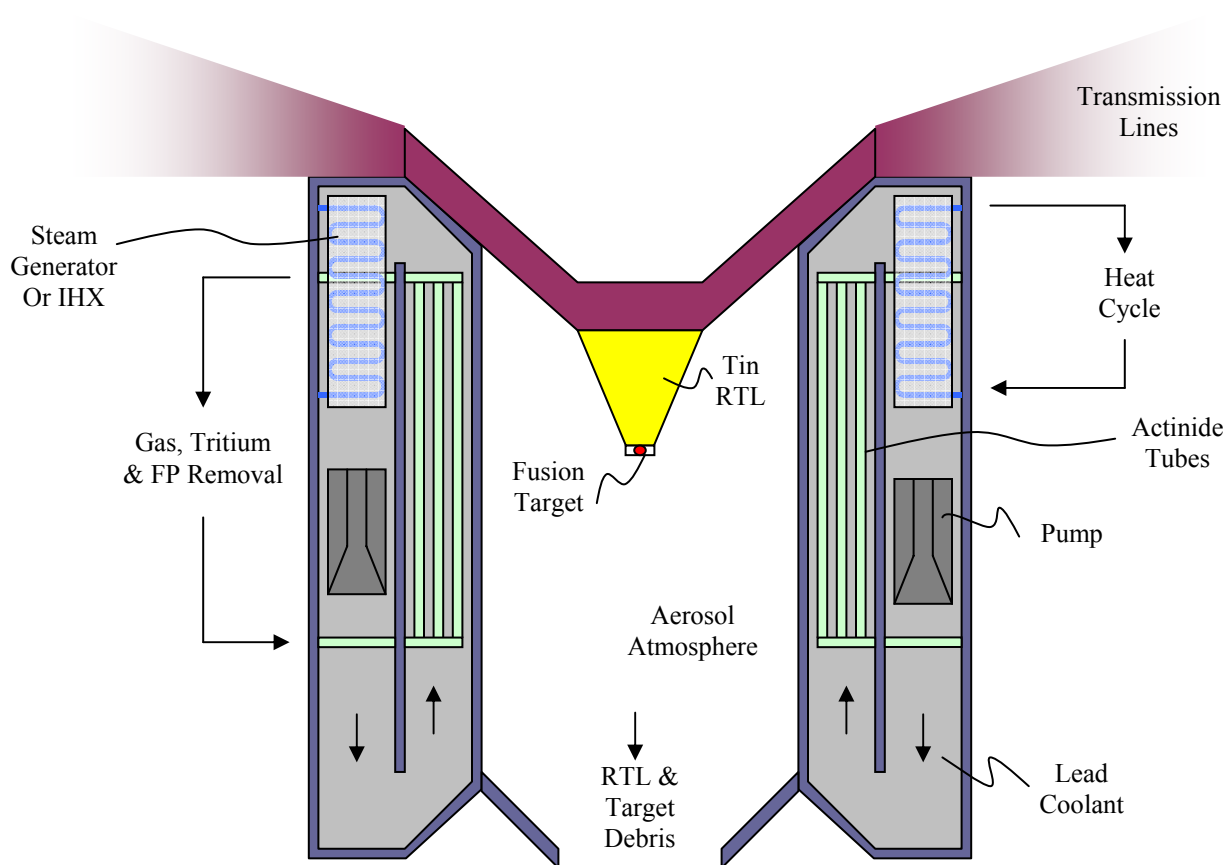


**Figure 3-1: In-Zinerator Power Plant**

The chamber is cylindrically symmetric with a 2 m standoff from the target to the first wall and 5 m in height. The first wall separates the Z-Pinch driver from the blanket and coolant. The chamber material must be able to withstand high temperatures, and the most likely candidate is Hastelloy-N. The chamber will contain a 10 torr Argon atmosphere for x-ray mitigation with

liquid metal sprays or aerosols to absorb energy and prevent excessive first wall heating. The sprays or aerosols minimize the required chamber radius. A low melting temperature metal like tin will likely be used for both the RTL and sprays for easy collection after the shot.

The fusion target has a yield around 200 MJ for a shot rate once every ten seconds. The fusion neutrons drive a sub-critical blanket containing the actinides in a cylindrical geometry. The actinides are contained in a fluid form within a hexagonal array of pipes using a LiF eutectic. A lead coolant circulates through the chamber (as shown by the arrows in Figure 3-1) to remove the energy from the fissioning of the actinides. There is a thick lead coolant region outside of the actinide array which borrows heavily from the pool-type reactors designs. An intermediate heat exchanger removes energy from the lead to power either a Rankine or Brayton cycle.

The actinide mixture is circulated slowly to remove fission products and tritium. The rate of circulation is such that the entire actinide mixture volume is processed once per day. Tritium is bred from the lithium to sustain the fusion reaction. The fission products will be continuously removed and either converted to a waste form, or converted to a form suitable for shipment back to a reprocessing plant.

Table 3-1 summarizes the design parameters of the In-Zinerator Power Plant. The original Z-Pinch Power Plant baseline parameters are also given to help show the changes when moving towards the transmutation application. The baseline design produces 3,000 MW<sub>th</sub> while burning 1,280 kg of minor actinides per year. The fusion source requirement is met by firing a 200 MJ target once every 10 seconds. The  $k_{\text{eff}}$  for this design is 0.97 which leads to a high energy multiplication of 150.

The engineering advantage of moving towards the In-Zinerator concept is that only one chamber is required, and the fusion yield requirement is an order of magnitude lower. The blanket design also changed considerably due to the presence of the actinides. A first wall separates the fusion chamber from the actinide and coolant region which may make the RTL insertion and recovery system simpler. The tritium generation in the In-Zinerator is significantly lower. These advantages all provide cost savings and ease up on the engineering challenges of generating power from Z-Pinch. The destruction of TRU along with energy production gives the concept another service that can be charged for, so the economics may be better as compared to a pure fusion energy plant.

An engineering disadvantage of the In-Zinerator is that the presence of the actinides and fission products adds additional safety and environmental concerns. Also, the energy deposition rate from each shot in the In-Zinerator is ten times higher than for the Z-Pinch power plant. (However, it should be noted that the Z-Pinch Power Plant baseline design spread out the energy to ten chambers—the added cost of dealing with the higher energy deposition in the In-Zinerator is much more desirable than having to build ten chambers). Lastly, it is unclear if a solid first wall will be able to withstand the RTL and target debris. The following sections go into more detail about the parameters in Table 3-1.

<u>Parameter</u>	<u>Z-Pinch Power Plant</u>	<u>In-Zinerator</u>
Fusion Target Yield	3,000 MJ	<b>200 MJ</b>
Repetition Rate	0.1 Hz	<b>0.1 Hz</b>
Power per Chamber	390 MWth	<b>3,000 MWth</b>
Transmutation Rate	N/A	<b>1,280 kg/yr</b>
$k_{\text{eff}}$	N/A	<b>0.97</b>
Energy Multiplication	N/A	<b>150</b>
Number of Chambers	10	<b>1</b>
<i>RTL &amp; Target</i>		
RTL Material	1006 carbon steel	<b>Tin</b>
Cone Dimensions	1m Ø x 0.1m Ø x 2m H	<b>1m Ø x 0.1m Ø x 1m H</b>
Mass per RTL	34 kg	<b>65 kg</b>
Tritium per Target	16 mg	<b>1.35 mg</b>
<i>Chamber Design</i>		
Shape	Spherical	<b>Cylindrical</b>
Dimension	5.9 m outer radius	<b>3.2 m outer radius</b>
Chamber Material	F82H	<b>Hastelloy-N</b>
Wall Thickness	35 cm	<b>5 cm</b>
<i>Blanket</i>		
Actinide Mixture	N/A	<b>(LiF)<sub>2</sub>-AnF<sub>3</sub></b>
Coolant	Flibe	<b>Lead</b>
Coolant Configuration	Jet and Pool	<b>Shell &amp; Tube (contained)</b>
First Wall Configuration	Thick liquid wall	<b>Structural Wall</b>
Shock Mitigation	Thick, voided coolant	<b>Argon gas &amp; Aerosol</b>
Coolant Operating Temperature	950 K	<b>950 K</b>
Heat Cycle	Rankine	<b>Rankine or Brayton</b>
<i>Extraction Systems</i>		
Tritium Breeding Ratio	1.2	<b>1.2</b>
Tritium production	553 g/day	<b>3.8 g/day</b>
Fission Product Removal	N/A	<b>On-Line Removal</b>

**Table 3-1: In-Zinerator Design Parameters [1]**

### 3.1 Chamber Design

The In-Zinerator chamber is a cylindrical annulus to separate the fusion chamber from the actinide fuel and coolant region. The separation adds protection to the actinide fuels from the Z-Pinch energy pulse. The Z-Pinch chamber is 200 cm in radius to the first wall and 500 cm in height. The fuel and coolant region is 107 cm thick to the outer chamber wall. The walls are 5 cm thick. The actinide tubes will probably be the same material as the chamber wall and are 2 mm thick.

### 3.1.1 Shock Mitigation

One of the key engineering challenges of using Z-Pinch for any type of reactor is to adequately contain the fusion yield within the chamber. Extensive work has been done this year on investigating different methods for containing or mitigating the shock.

The fusion target yield produces neutrons, ions, and x-rays. The high energy fusion neutrons will be practically unaffected by any type of gas or aerosol in the chamber. Very little neutron energy is deposited in the first wall as well. (The neutrons will be stopped by the thick fuel and coolant region). The main concern with shock mitigation is the x-ray pulse released from the fusion target, equal to about 30% of the fusion target yield.

For the In-Zinerator concept, a 200 MJ target will be required (as discussed in future sections). The x-ray pulse then will be 65 MJ. If there were no material in the chamber, this energy would be deposited in a very thin layer of the first wall of the chamber. Such an intense energy deposition would cause melting, ablation, and the formation of a shock wave. A heavy gas can be used to absorb the energy from the x-ray pulse; however, the gas temperature would rise to unreasonable temperatures. The high gas temperature may cause too much heating of the chamber wall.

An alternative that has been explored in related work is to use an aerosol in the chamber to absorb the x-rays [2]. The liquid in suspension will absorb energy by evaporation, thus preventing a large temperature rise. Calculations were performed on the pressure pulse delivered to the chamber wall due to the use of aerosols, and results have found that this pressure pulse is reasonable for target yields up to 1000 MJ. Therefore, an aerosol or liquid spray in the chamber could adequately mitigate the shock. It should be noted that due to the cyclic nature of the Z-Pinch pulse, the maximum allowable pressure pulse is due to cyclic loading limits rather than static loading limits. See reference 2 for additional information.

### 3.1.2 Material Choice

Due to the desired use of a molten salt mixture for the actinides, the nickel super alloy Hastelloy was chosen as the reference material for the chamber design. This material is ideally suited for use with molten salts up to high temperatures, and has good mechanical properties up to 1,100 K. A great deal of experience is available on the use of Hastelloy alloys from the Molten Salt Breeder Reactor (MSBR) at Oak Ridge National Laboratory [3].

Hastelloy-N was used in the design of the MSBR for improved corrosion resistance using a LiF-BeF<sub>2</sub>-ZrF<sub>4</sub>-UF<sub>4</sub> fuel. The fuel temperature in the reactor core was 650 °C. The original Hastelloy-N alloy consisted of 17% Mo, 7% Cr, 5% Fe, and the balance Ni, but later, additions of Ti or Nb were used to prevent radiation embrittlement and inter-granular cracking by the tellurium fission products [3].



A detailed mechanical analysis of Hastelloy was not conducted for this design, although parallel research did examine the mechanical properties for use in a Z-Pinch reactor [2]. This material was used to define all chamber components (first wall, actinide tubes, outer wall, top, and bottom) in the MCNP model.

### **3.1.3 Chamber Component Lifetime**

The constant neutron bombardment on the first wall damages the structure of the chamber over time; this in turn limits the life of these components. The life-limiting criterion for Hastelloy-N is a key factor in determining the service lifetime of the first wall (FW) and tube walls. There are no firm guidelines for Hastelloy as for the ferritic steel (FS) components of fusion systems where the life-limiting criterion has traditionally been the displacement of atoms (dpa), ranging between 100 and 200 dpa. In this analysis, a dpa limit of 200 for the Hastelloy structure was assumed.

Figure 3-2 shows the total damage due to neutron bombardment on the first wall from both the fusion neutrons and the fission neutrons in the system (for the baseline design of 3,000 MWth). The neutron damage is plotted as a function of vertical height, with the peak at the chamber centerline. In absence of actinides and fission neutrons, the FW would be a permanent component that performs properly during the entire life of the plant, 40 full power years (FPY), with a peak dpa of 100. The actinides change the neutron environment and result in a notable increase in the dpa level to a maximum of 550 dpa. This could result in a requirement to replace the chamber wall after 15 and 30 FPY of operation.

The radial variation of the peak dpa is displayed in Figure 3-3. This figure indicates a higher dpa level in the center of the blanket region containing the actinide mixture. This means the tubes might have to be replaced more frequently than the first wall. Well-protected by the blanket, the damage to the back wall is relatively low and remains below the 200 dpa limit at all times.

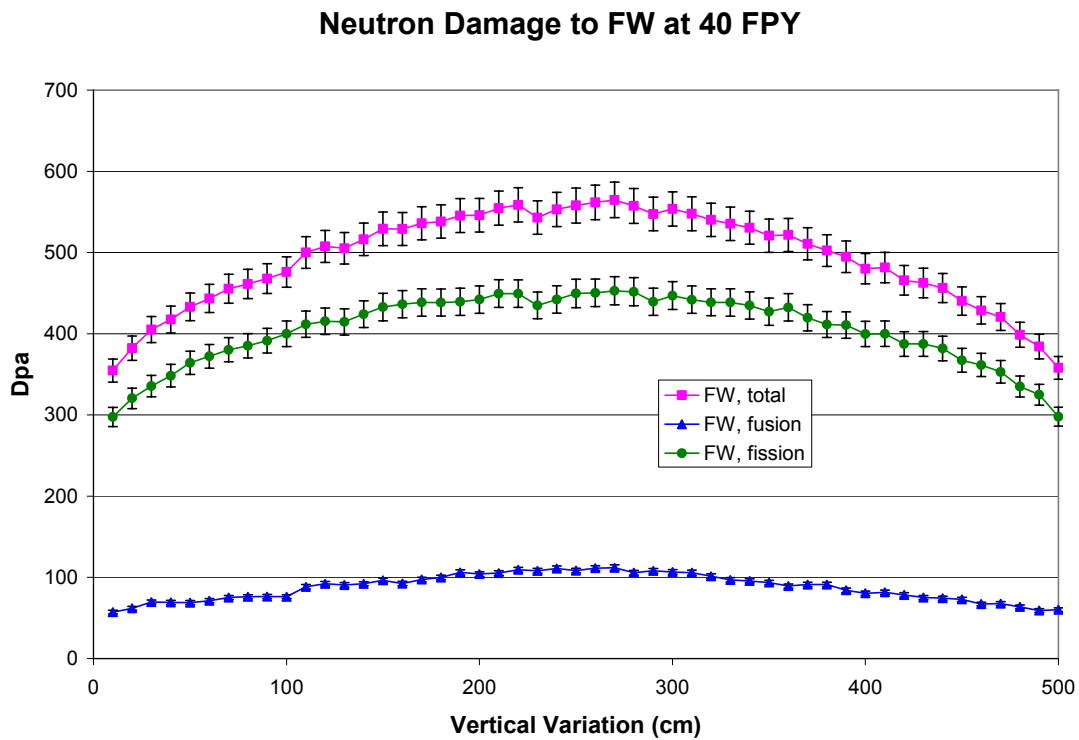


Figure 3-2: Neutron Damage to the First Wall

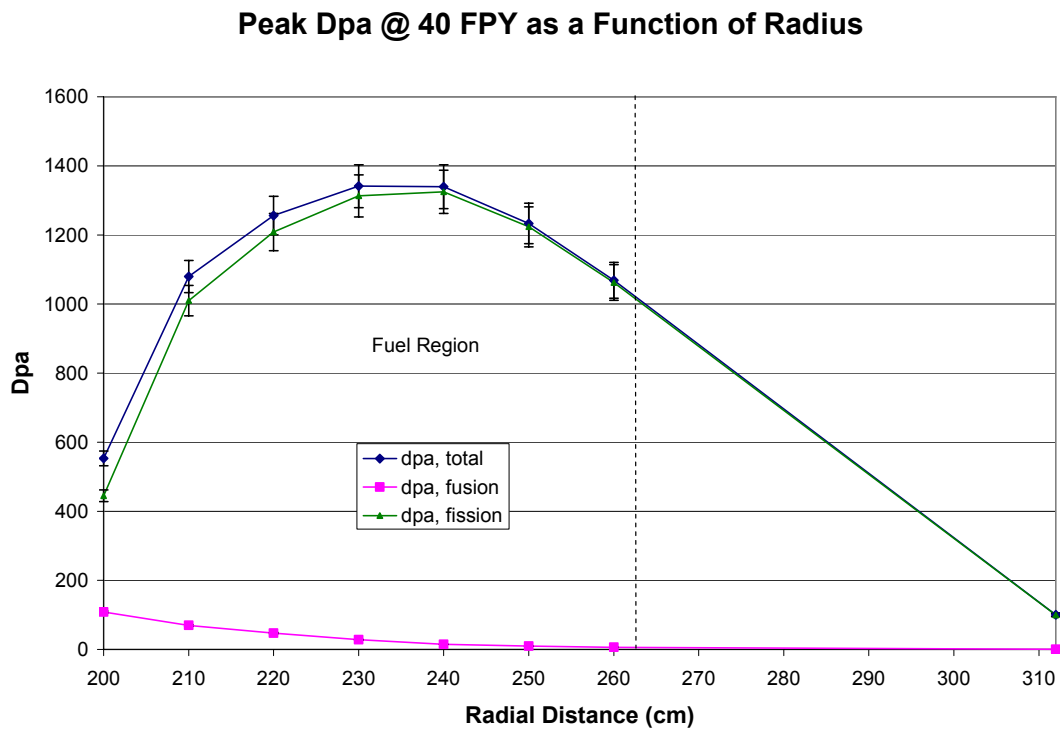
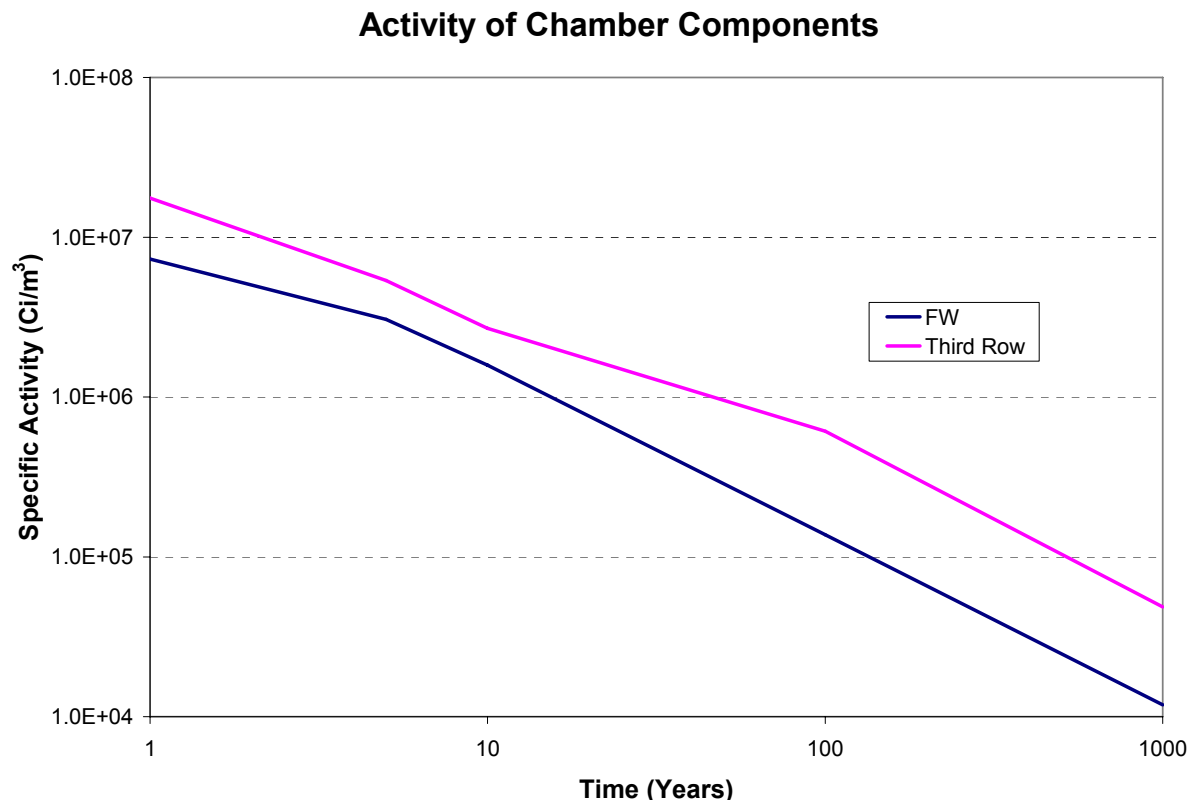


Figure 3-3: Neutron Damage as a Function of Radius

The frequent replacement of chamber components like the first wall and actinide tubes will have negative effects on economics and waste production. Methods for minimizing the damage rate include increasing the reactor size or decreasing the design power level, which may not be practical. It may be possible that the high temperature operation could partially anneal the chamber components during operation. This annealing could occur in between pulses. If this effect occurs, it could lead to an extension of the maximum dpa that can be reached. Future work will investigate this effect in more detail.

### 3.1.4 Activation

The activation of the chamber components was analyzed to evaluate the radiological hazards of the individual components. Figure 3-4 shows the specific activity of the first wall and the actinide tubes assuming these components were removed (and replaced) after the 200 dpa limit was reached.



**Figure 3-4: Specific Activity of Chamber Components after Removal**

Using the results shown in Figure 3-4, the waste disposal rating (WDR) was evaluated for a fully compacted waste using the most conservative waste disposal limits developed by Fetter [4] and NRC-10CFR61 [5]. By definition, the WDR is the ratio of the specific activity at 100 y after shutdown to the allowable limit summed over all radioisotopes. If the waste were fully compacted, it would have to be disposed as a high level waste. As an intact vessel, it could qualify as low level waste. However, the fact that the tubes are exposed to actinides and fission products will complicate matters. This issue should be investigated further in future work.

### **3.1.5 RTL Options**

To achieve repetitive firing of Z-Pinch targets, a recycle transmission line (RTL) is required that can be destroyed on each shot. The RTL fragments then are recovered and remanufactured into new RTLs. Past work has investigated the design and cost of the manufacturing plant for steel RTLs for a pure fusion power plant [6]. These costs were scaled down to those required for the In-Zinerator concept.

The original choice of steel as the RTL material was based on an exposed thick liquid blanket, so this material choice was re-examined for the In-Zinerator concept. With a solid first wall, steel probably does not make the most sense since any fragments from the fusion yield could damage the first wall. However, it was still evaluated for cost since the estimate was performed in previous years.

A new idea for this year is to produce the RTL from tin. The major reason for choosing tin is for its low melting temperature. The melting temperature of tin, at 232 °C, is well below the operating temperature of the first wall. Any fragments of tin in the chamber will melt and collect at the bottom. This could make collection and remanufacturing much easier. In addition, tin may be easy to cast into the desired RTL shape, which could save considerable costs in the remanufacturing process. The disadvantage of tin is that more material is required to have the same strength as steel.

The breakup of the RTL after a Z-Pinch shot has not been examined yet in detail. Portions of the RTL may fragment, melt, or vaporize from the fusion energy release. Of particular importance is the effect that fragments could have on the first wall if they are ejected with a high velocity. This analysis will need to be completed in the next year.

#### **Structural Analysis of the Tin RTL**

The operating conditions of the RTL are such that a differential pressure is applied to the surface of the conical shell, promoting a buckling failure mode of the structure that would interfere with the fusion process. The outer cone of the RTL is subjected to a vacuum on the interior surface and 10-20 torr of Argon gas pressure on the outside (see Figure 3-5). The RTL may buckle if this pressure differential is great enough. The purpose of the RTL structural analysis was to determine the thickness of material required to withstand buckling.

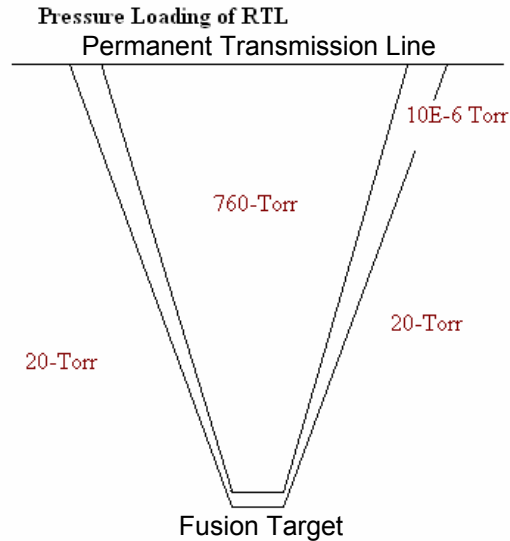


**Figure 3-5: Pressure Loading of the RTL**

### *Finite Element Analysis*

The commercial finite element analysis program, ABAQUS, was used to analyze the conical shell structure. The method estimated the critical buckling load, which in this case was pressure. This analysis was more idealized as it did not take into account the presence of imperfections or dents in the cone, but it was useful for this level of effort.

As such in the case of a full sized RTL, “perfect” conical geometry was used in the Eigenbuckling analyses. This translates into a conical frustum with the larger radius of 50 cm, the smaller radius of 5 cm, and a cone angle of 12.68 degrees. The “perfect” geometry represented the outer shell of the RTL cone, with an added flange at the top for support (boundary conditions). While this geometry was fairly easy to incorporate into the analyses, actual experimental results performed as a part of Z-Pinch IFE on steel RTL cones indicate that the experimental results tend to be less than 2/3 of the analytical results [1].

Stiffening rings were also examined as a way to increase the strength of the cone while minimizing the total mass needed (See Figure 3-6). Note that the effects of stiffening rings on the manufacturability of the cones has not been examined yet.

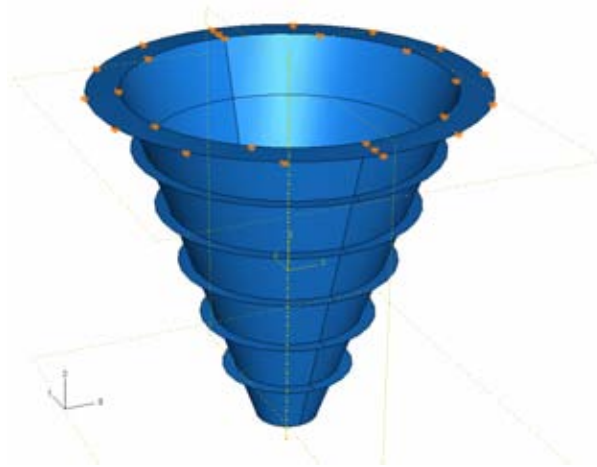


**Figure 3-6: Outer RTL Cone with Stiffening Rings**

For a target critical buckling pressure of 1.5 psi, Tin required a 0.30 cm wall thickness, which resulted in an overall mass of 162.11 kg, which is a substantial increase over the steel baseline design (25 kg). However, by adding a few stiffeners in optimal locations, an increase factor of 2.5 could be achieved for a Tin RTL. If the stiffeners were chosen to be embedded into the structural wall, the mass increase would be insignificant. Therefore, the Tin RTL mass could be reduced to 64.8 kg, or still nearly twice that of steel without the addition of stiffeners. However, it is believed this can be reduced even further with more analysis.

### **Steel RTL Cost Estimation**

The steel RTL examined for the Z-Pinch Power Plant concept was 2 m tall and 25 kg in mass for the combined inner and outer cone assembly. This 25 kg was an optimized mass. If this size RTL is required for the In-Zinerator, the remanufacturing plant would process approximately 100,000 metric tons of steel per year. If the RTL required height is only 1 m, the throughput would drop to 30,000 metric tons per year. These numbers are believed to be high and low estimates for the size of the remanufacturing facility required.

The details of the remanufacturing plant are shown in reference 6. This cost analysis was scaled to the 100,000 and 30,000 metric ton per year sizes using the 7/10 scaling law (costs are multiplied by the ratio of throughputs raised to the 7/10 power). Though in some cases, direct scaling was more appropriate.

The total project costs for the 100,000 and 30,000 metric tons per year plants were \$136.6 and \$79.8 million respectively at 80% confidence. The energy requirements to run the plant are 9.0 MWe and 2.7 MWe respectively. Operating costs scale to \$3.3 and \$2.9 million per year. The final RTL cost is shown in Figure 3-7 as a function of confidence interval. The expected RTL cost will be between \$3.10 and \$5.40 per RTL depending on the size of the cone. This range equates to a fuel cost between \$1.12 and \$1.94 per MWhr, which is comparable to a portion of the fuel cost for nuclear reactors. This cost is much more reasonable than the RTL cost for the Z-Pinch Power Plant due to the reduced number of shots required.

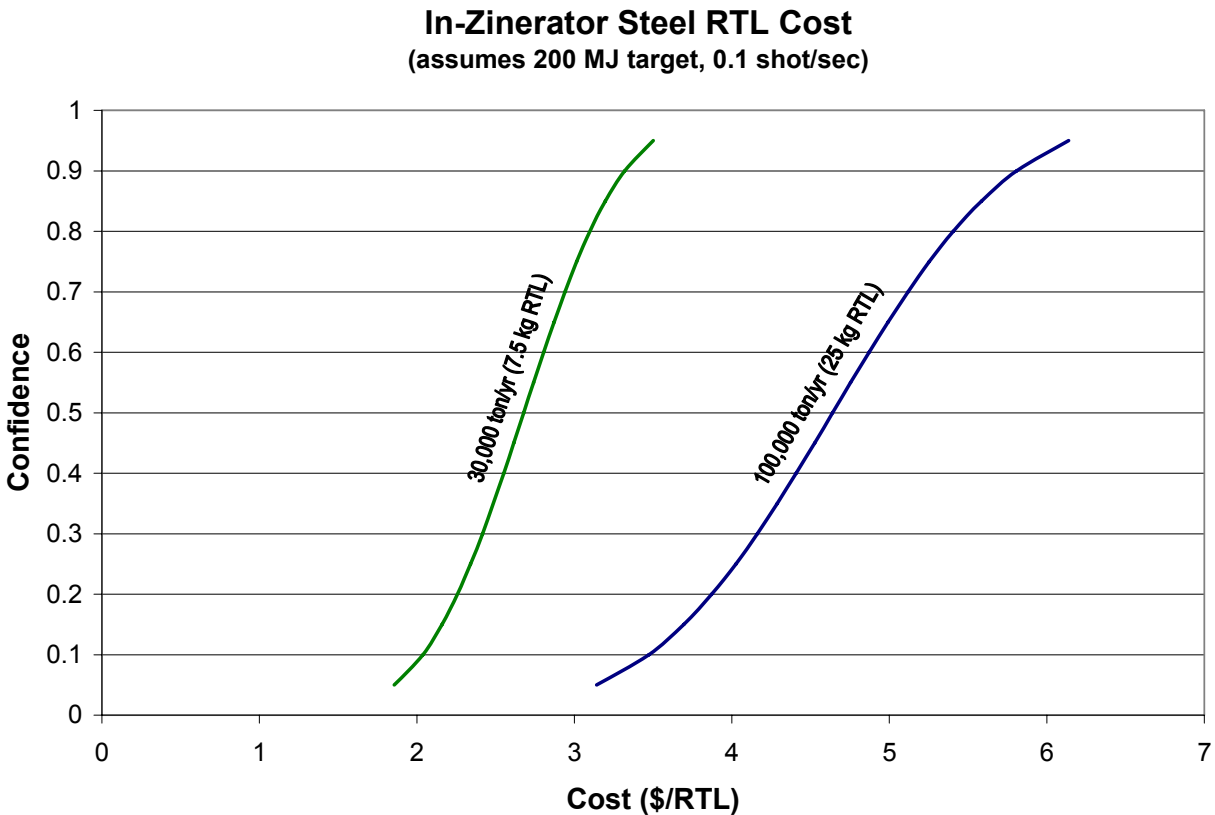


**Figure 3-7: Steel RTL Cost for the In-Zinerator**

### Tin RTL Cost Estimation

The cast tin RTL cost estimation has considerably more uncertainty since tin is not used on such a large scale for manufacturing anymore. However, work in the previous year investigated the costs for a cast flibe RTL. It will be assumed that the cast tin costs will scale since the process is equivalent.

The mass of the cast flibe RTL and the cast tin RTL are coincidentally about the same, but 1/10 of the amount of tin will be required for the In-Zinerator over a year. The scaled total project cost to build the tin casting plant would be about \$25 million. The energy use would be minimal since the tin will already be molten as it comes out of the Z-Pinch chamber. At 80% confidence, the cast tin RTL is expected to cost \$1.21 per RTL, which is equal to \$0.44 per MWh (see Figure 3-8). This cost would be minor compared to the rest of the In-Zinerator Plant cost and other fuel costs.

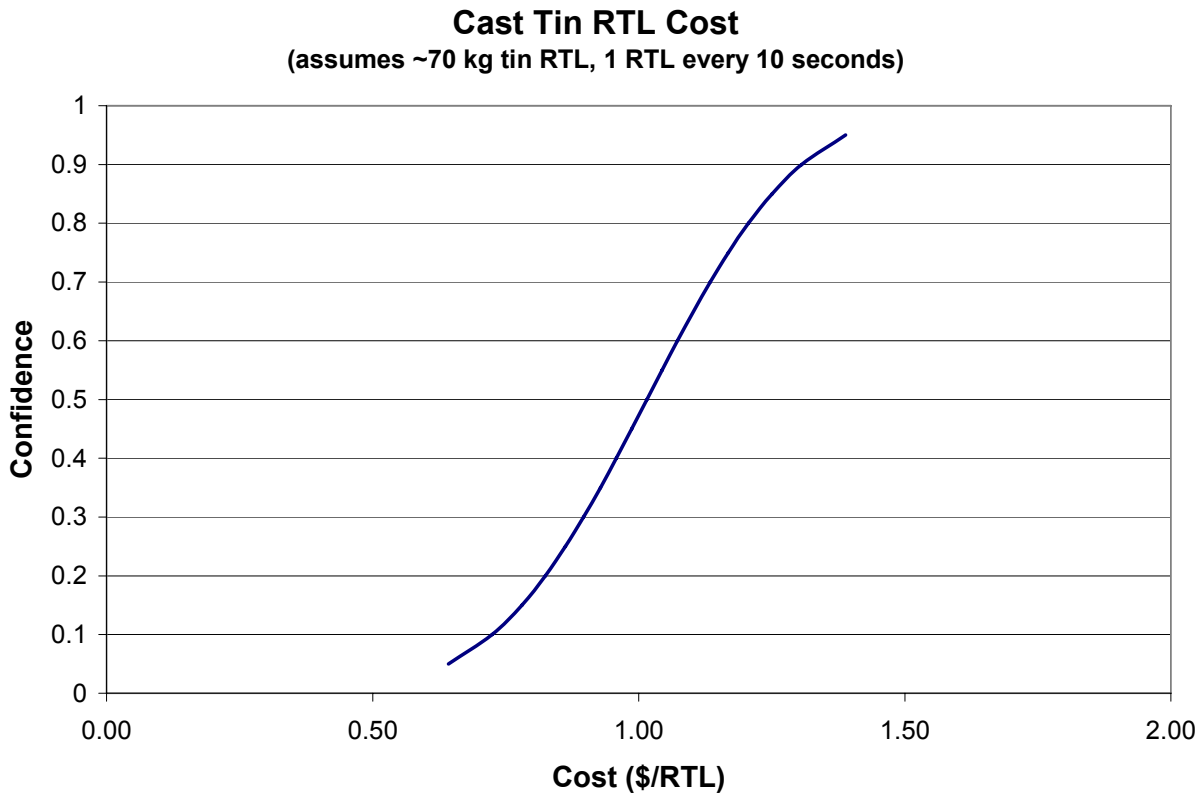


**Figure 3-8: Cast Tin RTL Cost**

The cast tin RTL cost is lower than the steel RTL cost, though this analysis will need to be done in much more detail when it is more appropriate to do so. The reason tin costs less though more material is required is because the manufacturing process of direct casting is much easier than casting, rolling, stamping, and pressing steel.

## 3.2 Blanket Design

### 3.2.1 Actinide Mixture

Several different materials were examined for use as the actinide mixture, but the design constraints made the process challenging. The goals for the actinide mixture were as follows:

- 1) Be liquid at a reasonable operating temperature
- 2) Have a high solubility for actinides to achieve high multiplication
- 3) Contain lithium for tritium breeding
- 4) Consist of a favorable material that is not reactive with structural components

The actinide mixture is in a fluid form during operation. The use of a fluid fuel eliminates the need for solid fuel fabrication and allows for continuous processing of the fluid to remove fission products and add actinides to maintain constant inventories.



Materials that were examined included any that had been used in past fusion designs (Flibe, Pb-Li), or in past FR designs (Na, Pb, NaF-ZrF<sub>4</sub>). All of these materials have very low solubilities for actinides. In fact, many of these materials were chosen for FRs because they would not dissolve out any actinides in the event of a cladding breach. There is a design for a molten salt reactor that examined flibe and NaF-ZrF<sub>4</sub> [7], but a lower solubility was acceptable since the reactor core was compact. One of the disadvantages of a fusion-fission hybrid concept is that it has a poor neutron economy due to the large hole in the center.

The (LiF)<sub>2</sub>-AnF<sub>3</sub> eutectic was chosen for being able to meet all of the above requirements; however, there are many uncertainties with this unique mixture, and chemical experiments will be required in the future to verify properties and determine thermodynamic characteristics. This eutectic was studied in a paper by van der Meer et al. [8] using theoretical methods and comparison to the LiF-LnF<sub>3</sub> series. The theoretical LiF-AmF<sub>3</sub> eutectic forms at 33 mole% AmF<sub>3</sub> and is liquid at 675 °C, while the theoretical LiF-PuF<sub>3</sub> eutectic forms at 20 mole% PuF<sub>3</sub> and is liquid at 730 °C. It is uncertain how a mixture of actinides would behave. The actinide mixture in the modeling was set at 33 mole% actinide fluorides, but based on the parametric analysis it would not be too difficult to modify the reactor design to 20 mole%. The area of more concern is the high operating temperature that would be required, but Hasteloy-N was designed to work with molten salts at high temperatures.

Other mixture ideas that could be investigated in more detail in the future include slurries of molten metals and particulate actinides. For example a suspension could be formed using actinides in the oxide form or fluoride form with an appropriate carrier fluid. This configuration could allow for lower operating temperatures, but it would complicate the continuous separations process. It also could have criticality concerns if the mixture does not stay well mixed.

### **3.2.2 Primary Coolant**

The primary coolant surrounding the actinide tubes is lead. This coolant removes the heat and provides a large thermal sink for accident scenarios. The coolant is circulated with pumps through the chamber to heat exchangers within the pool-type chamber design. The heat exchangers and heat cycle have not been investigated in detail this year, but it is seen as a secondary concern at this point.

Lead was chosen due to the experience with lead in FRs or fusion reactor designs of the past. The properties are well-defined. Lead has a low melting temperature to offer a range of operating conditions. With proper control of impurities, activation of lead is not an issue. It has a low solubility for actinides which is advantageous if there were a leak of an actinide tube. It is not reactive with most materials (especially oxygen and water). Lead has favorable safety features in FRs.

There are concerns about lead interactions with steel, but steel will probably not be used for the temperatures required in this reactor. Lead interactions with Hasteloy and other high-temperature materials will need to be investigated in more detail in the future.

### 3.2.3 Tritium Breeding

As described previously, one of the constraints on the choice of the actinide mixture was to contain Li for breeding of tritium. It has long been a goal of fusion reactor designs to use the intense neutron flux to breed tritium from the  ${}^6\text{Li}(n,t){}^4\text{He}$  reaction. With the proper design, it is easy to provide enough  ${}^6\text{Li}$  to generate sufficient tritium to sustain the fuel supply for the fusion targets. Natural Li contains 7.5%  ${}^6\text{Li}$  and 92.5%  ${}^7\text{Li}$ , but it can be enriched or depleted to get to a desired tritium breeding ratio (ratio of bred tritium to burned up tritium). The goal for this work was to design a blanket with a tritium breeding ratio (TBR) of 1.2 to allow for some loss in processing. However, it should be noted that a much smaller TBR will be required for an actual plant to minimize tritium leakage to the environment.

The effect of  ${}^6\text{Li}$  enrichment on the TBR is shown in Figure 3-9. The baseline design used a  ${}^6\text{Li}$  enrichment of 5% (slightly depleted), but this led to a high TBR. Future work will need to optimize this further. As the enrichment of  ${}^6\text{Li}$  increases, the breeding decreases. The reason for this effect is that  ${}^6\text{Li}$  acts as a poison in the actinide blanket by absorbing neutrons. Increased quantities of  ${}^6\text{Li}$  will decrease the net multiplication, in turn decreasing the TBR. This effect could be useful for control of the reactor neutronics with time.

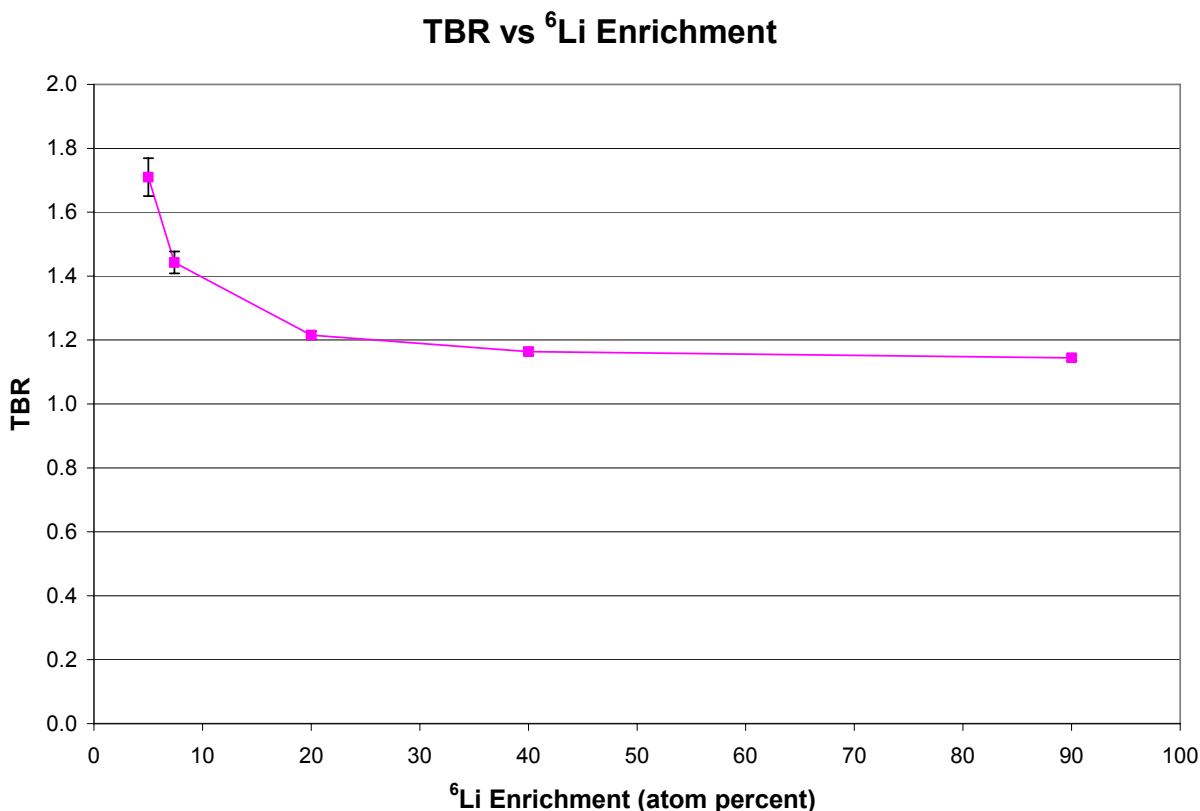


**Figure 3-9: Tritium Breeding Ratio vs.  ${}^6\text{Li}$  Enrichment**

### 3.2.4 Safety Issues

The decision to use a liquid fuel in the design introduces several safety issues that a solid fuel would not have considered. With liquid fuel the concentration of the actinides in the blanket will have to be monitored in order to ensure that localized actinide buildup does not occur and cause  $k_{\text{eff}}$  to become greater than or equal to 1.0. It is recommended that throughout the system, the concentration of actinides is monitored and liquid flow and mixing controls are applied to prevent localized actinide buildup [9]. More research needs to be done to adequately understand the use of a liquid fuel and the resulting criticality issues liquid fuel presents [10].

Another major safety concern in dealing with liquid fuel is fuel tube ruptures and breaks. Since the fuel will be channeled through multiple tubes, fuel tube ruptures and breaks could cause pooling of the fuel mixture and contamination of the lead coolant. Material considerations for the fuel tubes must be examined since molten salts can pose corrosion problems and lead to an increased amount of breaks/ruptures in the fuel tubes. Safety systems must be in place to ensure that any fuel tube ruptures are identified in an efficient and timely manner. It is recommended that a baseline is established to determine when the leak rate of the fuel tubes presents a fuel pooling criticality concern. It may be determined through analysis that small leaks will not amount to enough fuel pooling to be of an immediate concern. However, the potential for large breaks and contamination of the coolant will always exist and the pooling of fuel will remain a safety issue. It is recommended that criticality calculations be performed to analyze varying sizes of fuel pools. In addition, the contamination of the coolant must be more thoroughly examined to determine if the fuel will pool or if it will mix into the coolant. If pooling occurs, methods must be established to remove the fuel pool. However if mixing occurs, long-term effects of coolant contamination must be considered. This contamination could lead to concerns with cooling rates, material degradation, and possibly contamination of other systems (primarily the power plant side through ruptures in steam generator tubes). Shutdown systems must exist to immediately stop fuel flow to prevent excessive leakage.

The greatest concern with the LiF eutectic is the tremendous amount of radioactivity contained in the mixture. It will be necessary to contain the LiF fuel mixture to prevent human contamination. Also, safety gear that not only protects against radiation, but also the eyes, nose, throat, and skin must be available for personnel. Because of the high temperature the LiF will be operating at, it is also recommended that class D type fire extinguishing systems be installed. The class D type extinguishing systems will also be appropriate for the fires involving the lead coolant, since metal fires cannot be extinguished with water extinguishing systems.

In all plant designs, Loss of Coolant Accidents (LOCAs) are a major concern. Heat exchangers will remove heat from the lead, and pumps will keep the liquid lead cycling and prevent solidifying of the coolant in regions farthest from the heat source. Designing in redundant pump systems will decrease the likelihood of fuel solidification by ensuring that the loss of a pump does not prevent adequate coolant flow [11].

An advantage in this design is the use of the coolant as a reflector. In the event of a LOCA, loss of the lead will decrease the reactivity of the fuel. In addition, with the use of a pool design, the probability of a LOCA is reduced because major damage to the pool wall will have to occur for a

large scale LOCA to occur. However, small LOCAs are still possible; coolant could be lost in the event of a pipe break in the heat exchanger tubes or the fuel tubes (depending on pressure differences). Lead coolant inventory needs to be monitored on a small scale to ensure that coolant is not out of the system. In addition, a supplementary tank of lead coolant may need to be installed to make up lost coolant inventory in the event of a LOCA. The coolant tank can also allow for a rapid cooling of the system, especially in the event of a rapid shutdown.

## **3.3 Extraction Systems**

### **3.3.1 Continuous Reprocessing**

A conceptual process for removing fission products from the In-Zinerator fuel salt is described in this section. This design pulls on data and experience from the Molten Salt Breeder Reactor Project at Oak Ridge National Laboratory which used fluoride salt-bismuth systems. (For more information see references 12,13,14,15). The MSBR fuel recycle process required multistage contactors to achieve separation of actinides and fission products, and was complicated for reasons that are not pertinent to the In-Zinerator.

#### **In-Zinerator Flowsheet**

It was necessary to modify some aspects of the In-Zinerator requirements to simplify fuel salt reprocessing. At the start of this work, it was assumed that an In-Zinerator would be fueled solely with Am/Cm, so the work shown in this section works under this basis. Note that because of the chemical similarities between all of the TRU, this process will be very similar for TRU fueling. The fuel salt is nominally  $\text{LiF-33 mol\% (Am, Cm)F}_3$  with a fission product content of <2% of the actinide content. This salt mixture has a melting point of about 675°C. However, some streams in the conceptual process have all of the actinide fluorides removed and, thus, would have an excessively high melting point. One alternative is to use an initial fuel composition of  $\text{LiF-25\% CsF-33\% AnF}_3$  so that with the actinides removed, the salt has the composition of about  $\text{LiF-34\% CsF}$ , which has a melting point below 650°C. There is no phase diagram for the salt containing actinides, but judging from other fluoride salt mixtures of mono- and trivalent cations, the fuel salt will have a melting point below 650°C. The process operating temperature is between 650 and 670°C.

Alkali metal fission products, rubidium and cesium, can be removed adequately if their concentrations in the fuel salt are fairly high. In the conceptual process, their concentration is allowed to gradually displace the natural cesium but always maintaining a salt composition with a melting point below 650°C. The concentrations of the alkali metal fission products will exceed the nominal 2% of the actinide content. The total concentrations of zirconium, alkaline earths, and rare earths will be kept below 2% in this concept.

Based on the fission yields generated from the modeling data (see Chapter 6) the breakdown of fission products categorized by their chemistry is given in Table 3-2. For the calculations described below, the fission elements that form anions are included in the alkali metal category.

The fuel salt discharged from the reactor is first degassed to remove fission gases and filtered to remove insoluble materials that do not form fluorides, mainly noble metal fission products. It is assumed that the noble metals, except zirconium, remain as metallic particles suspended in the fuel salt, but experience with the Molten Salt Reactor Experiment does not rule out the formation of other noble metal fluorides. If some do form it is possible to volatilize them selectively by sparging fluorine through the salt.

Category	Elements	Average Mol. Wt.	Yield (mol./sec)
Alkali Metal (AM)	Rb, Cs	126	5.14E-05
Alkaline Earth (AE)	Sr, Ba	115	2.16E-05
Rare Earth (RE)	Y, La – Yb	138	8.68E-05
Zirconium (Zr)	Zr	93	3.59E-05
Noble Metals (NM)	Nb – Sb	100	1.36E-04
Fission Gas (FG)	Kr, Xe		4.63E-05
Anions	Se, Br, Te, I	126	1.12E-05
Totals			3.78E-04

**Table 3-2: Fission Yields – Categorized by Fluoride Chemistry**

As shown in Figure 3-10, the degassed and filtered salt is contacted in the first column with a bismuth-alkali metal solution to reduce  $ZrF_4$  and dissolve the zirconium metal. Because significant amounts of actinides are also transferred to the metal, the product metal is “scrubbed” with salt containing  $BiF_3$ . A fraction of the zirconium is transferred to the salt, but a larger fraction of actinides is transferred.

The salt leaving the zirconium extraction column is fed to the actinide extraction vessel where essentially all of the actinides and some of the rare earths and alkaline earths are reduced by Bi-AM and transferred to the metal phase. The fraction of rare earths left in the salt is sufficient to control their concentration in the fuel. The salt depleted of actinides is sent to the fission product removal column. Salt containing  $BiF_3$  is then charged to this vessel to transfer the actinides into the salt. The salt from the zirconium scrub step and makeup  $LiF$  and actinide fluorides are then added to this vessel to reconstitute the fuel, which is returned to the reactor.

In the fission product removal column, salt is again contacted with Bi-AM to remove a sufficient fraction of the alkaline earths to control their concentration in the fuel. The treated salt is transferred to the operations where Bi-Li solutions and salt with  $BiF_3$  are prepared for use in the process. An electrolytic cell produces fluorine and Bi-AM solutions; the fluorine is used to make salt containing  $BiF_3$ .

The metal streams leaving the zirconium scrub column and fission product extraction column are sent to the waste treatment process. Two options for converting the fission products to waste forms are discussed in a later section. In either case, clean bismuth is produced and recycled to the process.

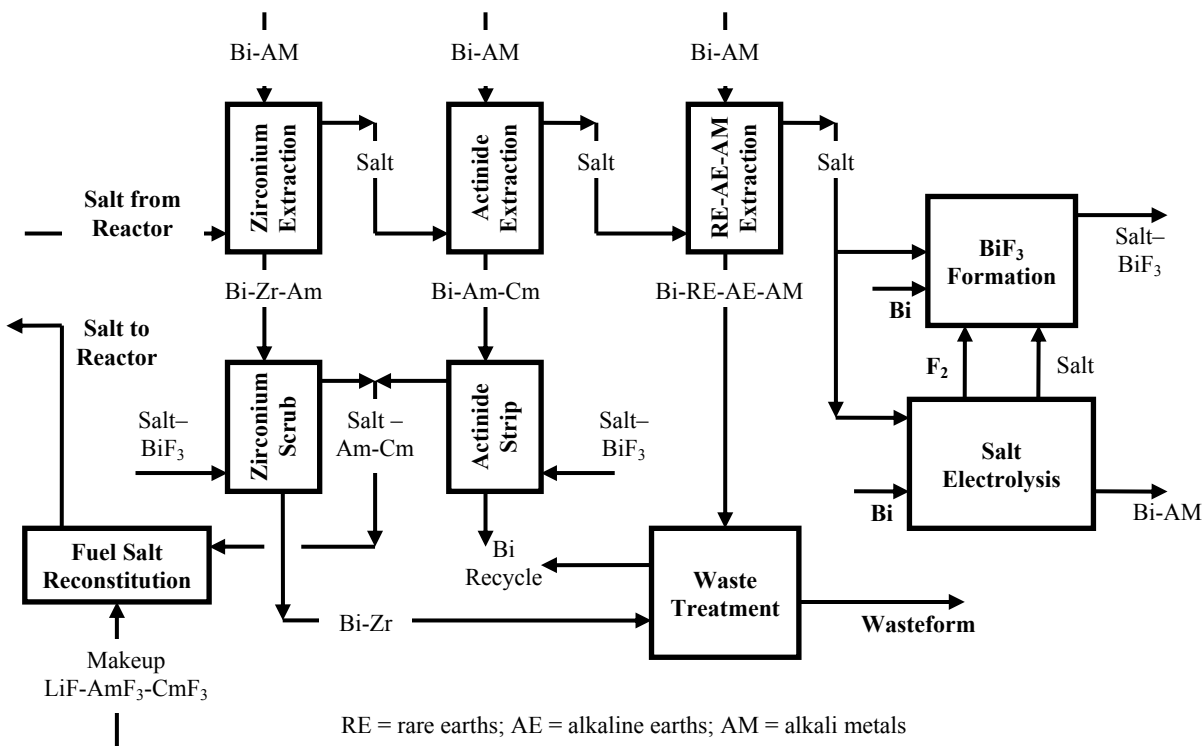


**Figure 3-10: Conceptual Actinide Mixture Treatment Flowsheet**

## Process Details

The process outlined above is discussed in more detail in this section. Approximate material balances have been calculated for the major steps to demonstrate the feasibility of the conceptual process and to highlight important parameters. Because the parameters used for this illustration were not optimized, better performance, e.g., lower actinide losses, can be expected. Salt and metal flow rates were determined by the requirement to remove 10% of zirconium, rare earth, and alkaline earth fission products from the incoming fuel salt and control their concentrations in the fuel.

The lack of data required that several assumptions be made. It is assumed that all alkali metal elements, lithium, rubidium, and cesium, behave chemically like lithium, and that their total content (mole fraction) in both phases is equivalent to lithium. Samarium valence can be either two or three in this fluoride-bismuth system depending on conditions: it is assumed to be two under all conditions. Samarium is included with europium and the alkaline earths, barium and strontium; all divalent cations have a distribution coefficient equal to that of europium (see Table 3-2). Elements that form anions in the salt, such as Br, I, Se, and Te, are included with the alkali metals. The distribution coefficients of all rare earths are assumed to be equal to that of lanthanum. All of the fission gases and noble metals are separated from the salt before entering

the process. The estimated composition of the filtered, degassed salt leaving the reactor and fed to the zirconium extraction step is shown in Table 3-3. The curium content is assumed to be 10% of the americium content.

The composition in Table 3-3 is determined from the fission product breakdown shown in Table 3-2 along with the requirement to limit the total concentration of zirconium, rare earths, and alkaline earths to 2% of the actinide content. Initially, the salt is 42 mol.% LiF – 25% CsF – 33%  $\text{AmF}_3$  to ensure a salt melting point below 650°C throughout the process. During reactor operation, fission product rubidium and cesium gradually replace the natural cesium.

Component	mol. frac.
(Li, AM)F	0.666
$\text{AmF}_3$	0.300
$\text{CmF}_3$	0.030
$(\text{AE})\text{F}_2$	0.0005
$(\text{RE})\text{F}_3$	0.0020
$\text{ZrF}_4$	0.0008

**Table 3-3: Estimated Composition of Salt Entering Process**

### *Zirconium Separation and Scrub*

Separation of zirconium from the actinides is the most difficult process, but adequate zirconium removal with low actinide losses can be made with one equilibrium extraction stage and one scrub stage as shown in Figure 3-11. The zirconium fraction extracted in the first step is sensitive to the amount of lithium fed. However, the overall actinide loss and zirconium removal are relatively insensitive to the conditions in the scrub step as illustrated in Figure 3-12. The relative actinide loss is the amount of americium and curium in the waste stream divided by the amount of zirconium in that stream. The bases for these calculations are a metal/salt ratio in the extraction stage of 0.1 and a zirconium extraction from the salt feed of 20%. Using a metal/salt ratio of 10 in the scrub column, half of the zirconium is removed from the metal and returned to the salt yielding an overall zirconium removal by the process of 10%.

The benefits of adding a second extraction stage were examined. With two stages of countercurrent salt-metal flow, the fraction of actinides transferred to the metal was reduced only 1% while the fraction zirconium transferred was increased 7%. Even with a second extraction stage, a scrub stage is required. Adding a second stage does not improve any of the salt-metal transfers in this process, which is an advantage as explained in the section on equipment concepts.

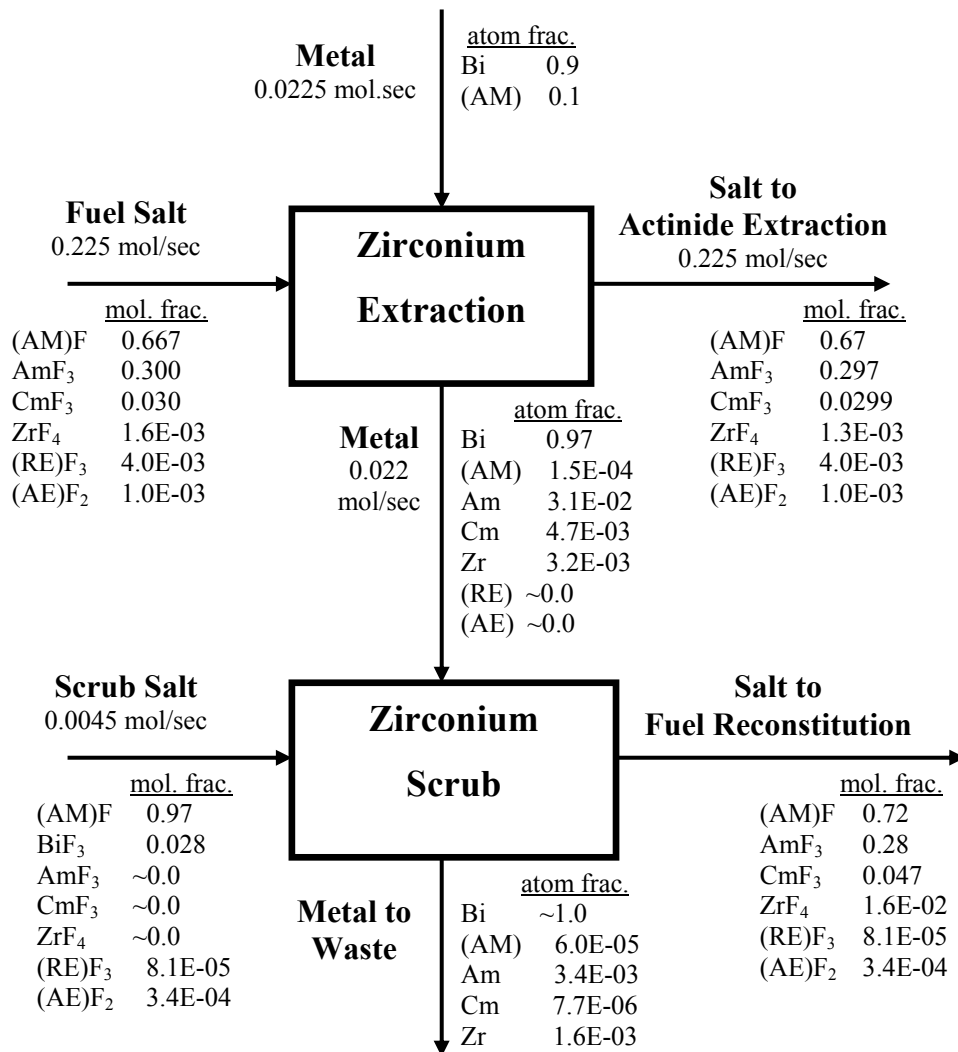
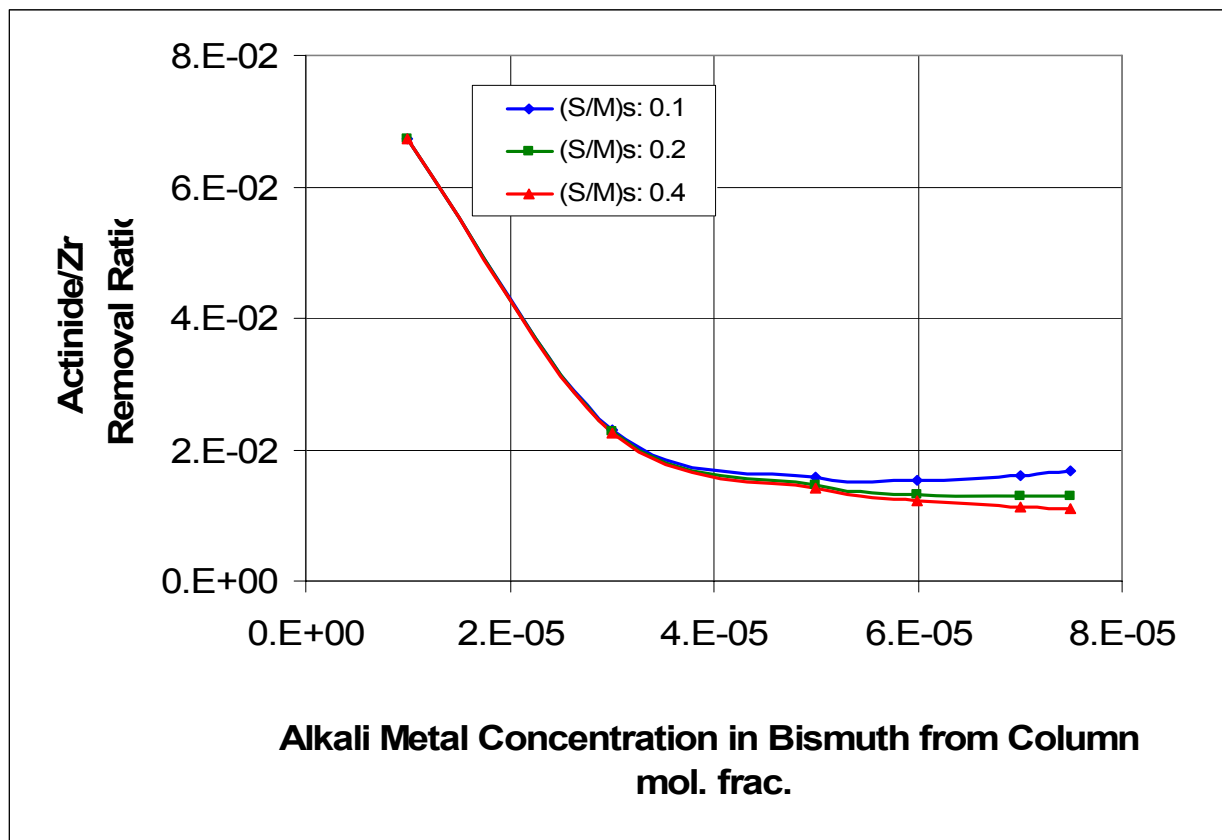


Figure 3-11: Zirconium Removal Steps





**Figure 3-12: Overall Actinide Loss Relative to Zirconium Removal Steps**

### *Actinide Extraction and Stripping*

Stream flows around the actinide extraction and stripping columns are shown in Figure 3-13. Salt from the zirconium extraction column is contacted with a Bi-AM solution in the actinide extraction column. Nearly all of the actinides and about 90% of the rare earths are reduced and dissolved in the metal phase. (The remaining 10% of the rare earths is removed in the fission product removal column.) The amount of bismuth is sufficient to dissolve all of the actinides and rare earths. The combined solubility of actinides in this complex bismuth solution is estimated to be 3 mol%. The alkali metals and alkaline earths are also assumed to be completely soluble in the metal phase.

The metal solution leaving the actinide extraction column is contacted in the stripping column with a salt containing  $\text{BiF}_3$  to oxidize the actinides into salt. Complete stripping of actinides from the metal phase is not necessary because any actinides remaining in the bismuth are recycled through the  $\text{BiF}_3$  step. Incomplete stripping avoids the possibility of introducing  $\text{BiF}_3$  into the fuel salt.

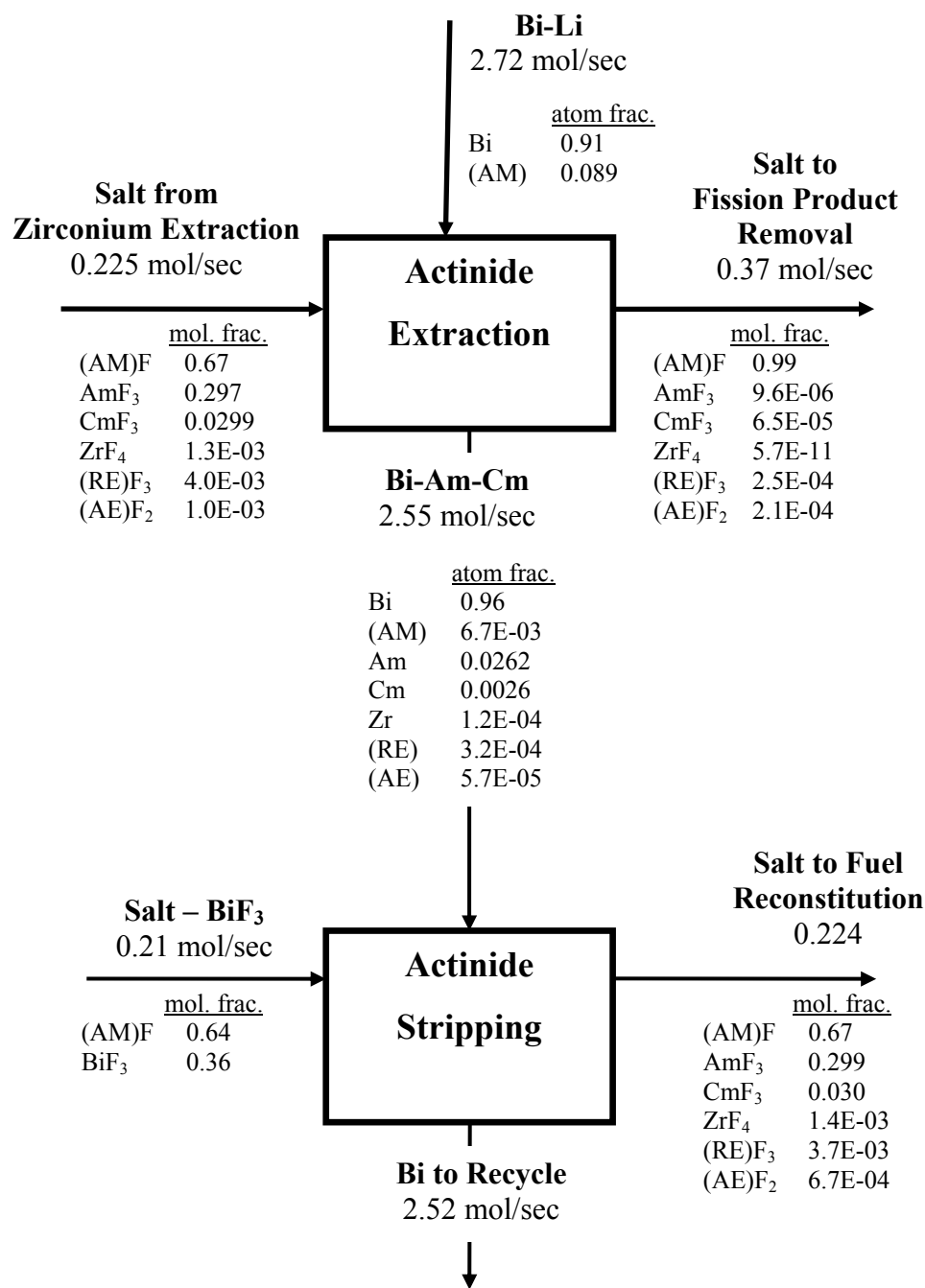


**Figure 3-13: Actinide Extraction and Fuel Reconstitution Steps**

The salt leaving this column is mixed with salt from the zirconium scrub column and makeup LiF, AmF<sub>3</sub> and CmF<sub>3</sub> to reconstitute the reactor fuel. The metal product is recycled to the process by feeding it to the vessel producing BiF<sub>3</sub>.

## Fission Product Removal

Salt from the actinide extraction step is contacted with a Bi-AM solution that reduces the alkaline earths into the metal phase. Stream flows around this step, shown in Figure 3-14, are predicated by the requirement to achieve an overall 10% removal of alkaline earths from the incoming fuel salt. The salt with essentially all of the actinides and the required amounts of fission products removed is divided between the electrolytic cell and the BiF<sub>3</sub> production step. The metal solution containing fission products is sent to the waste treatment operations.

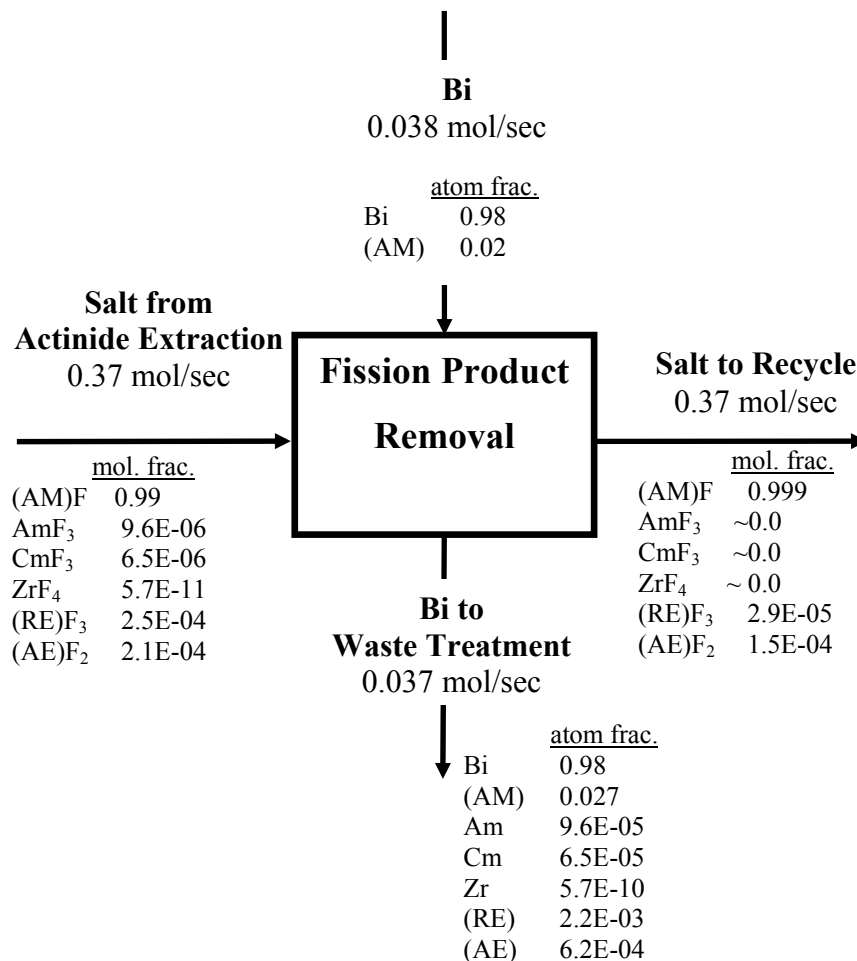


**Figure 3-14: Fission Product Removal**

## Waste Treatment

Two options, not shown in the previous figure, for treating the two metal streams containing fission product wastes are proposed. In the first, the fission products are extracted from the metal into a fluoride phase and converted to apatite by reaction with Ca<sub>3</sub>(PO<sub>4</sub>)<sub>2</sub>. [16,17,18]

In the second, the fission products are oxidized from the bismuth with HCl or Cl<sub>2</sub> into a LiCl-rich salt forming a mixture with a melting point about 550°C. This mixture is cooled to below 450°C to precipitate LiCl and concentrate fission products in the liquid phase. The liquid salt is contacted with the lithium-form of Zeolite A that sorbs the fission products into the zeolite lattice. Experimental measurements [19,20] show that rare earths and alkaline earths are strongly sorbed by the zeolite and, although the alkali metal fission products are less strongly sorbed, they can be adequately removed because of their high concentrations in the LiCl salt. The zeolite is separated from as much of the adhering salt as possible, combined with glass and additional zeolite, and heated to 900 – 925°C to transform it into glass-bonded sodalite. Tests at Argonne National Laboratory have demonstrated that this waste form would be acceptable for geologic disposal [21].

The fission gases can be placed in tanks for long-term storage. Since the gas volume at 200 atm is only 165 L per year of reactor operation, storage for up to 100 years to allow <sup>85</sup>Kr decay before release is not unreasonable.

The filters containing the noble metal fission products must be washed with fresh salt to remove adhering fuel salt. The filter assemblies with the noble metals are melted and cast, the salt is removed, and the metal ingot is encapsulated for geologic disposal.

## Equipment Concepts

The process flow rates are small, but the large quantity of actinides causes criticality problems. Because the actinides are diluted in salt or bismuth and the equipment configurations are poorly moderated and reflected, it is assumed that the maximum quantity of actinides in any vessel is limited to 5 kg to provide a margin against double-batching. Criticality analyses are required, but the general equipment design appears feasible.

The salt mass flow entering the zirconium extraction step is about 120 kg/hr, the volume rate is 30 L/h, if the density is 4.0 gm/cm<sup>3</sup>, and the salt is about 50 wt% actinides. The bismuth rate to the extraction step is less than 2 L/h. The zirconium extraction and scrub equipment are countercurrent packed columns of a height equivalent to at least one theoretical stage. Countercurrent packed columns are also proposed for the actinide extraction, actinide strip, and fission product removal; they also require one theoretical equilibrium stage. Because of the nature of the salt-metal contacts throughout this process, column length beyond one theoretical stage does not affect performance significantly.

ORNL data for bismuth and fluoride salts flowing through packed columns are used to size the units for the In-Zinerator process. That flooding correlation is [22]

$$(V_d)^{0.5} + (V_c)^{0.5} = 19.7 ,$$

where  $V_d$  = superficial velocity of discontinuous phase (metal), ft/hr and  
 $V_c$  = superficial velocity of continuous phase (salt), ft/hr.

Diameters of the process columns shown in Table 3-4 were determined for metal and salt flow rates well below this flooding line.

Column	Diameter (in.)	Maximum Actinide Content (kg/ft of height)
Zirconium Extraction	1.25	0.3
Zirconium Scrub	0.5	>0.1
Actinide Extraction	3.0	1.6
Actinide Strip	3.0	0.2
Fission Product Removal	1.5	>0.1

**Table 3-4: Diameters of Packed Columns**

There are scant experimental data on mass transfer rates in packed columns for metal-salt systems. ORNL determined values of height of a transfer unit in the range of 1 to 2 ft [23]. Similar transfer rates were determined for cadmium-chloride salts [24]. The height equivalent of a theoretical stage is estimated to be 2 ft for all columns in this process. Since additional height beyond 2 feet does not affect the extractive performance, all columns are 3 ft high.

However, the extra height does increase the criticality problems because the longer column can contain additional actinides. The maximum amount of actinides that could be contained in each column is shown in Table 3-4. The amounts are calculated assuming that the feed containing the actinides fills the column free volume, which is 50% of the geometric volume with the other half occupied by packing. To stay within the 5 kg limit, there should be two actinide extraction columns each with a diameter about 2.2 in. Because this column is coupled with the actinide stripping column, there should also be two stripping columns.

The electrolytic cell design is based on Argonne experience with the electrorefining of uranium in chloride salts. Cathode current densities of 0.2 amp/cm<sup>2</sup> and current efficiencies of >90% have been achieved with solid cathodes. Higher current densities and efficiencies can be expected with a stirred liquid cathode, such as bismuth. A total current of 24,000 amps must be supplied to the electrolytic cell to produce the 0.24 gm-moles/sec of alkali metals dissolved in bismuth that is required by the process. Assuming 1 amp/cm<sup>2</sup> and 80% efficiency, the surface area of the bismuth pool is 3 m<sup>2</sup> and its diameter is about 2 m. The vessel to produce salt with BiF<sub>3</sub> is considerably smaller based on experience at Argonne to produce LiCl-KCl-UCl<sub>3</sub> by introducing a dilute chlorine gas stream near the interface between a molten U-Cd alloy and LiCl-KCl.

Hold-up tanks would be required between the columns to provide buffers ensuring steady flow rates. The tanks holding salts with 33 mol% actinide fluorides could have a volume of only 2.5 L – only a 5 min. supply; multiple holding tanks are required. Although no estimates were made, fission product heat rates of fuel directly from the reactor are presumed to be excessive. Holding tanks must be provided before the zirconium extraction column, but their size is also limited by criticality.

## Discussion

The next phase of process development should be measurements of the behaviors of some important fission products, e.g., cesium, noble metals, alkaline earths, and several rare earths, determined for this specific salt composition. Sufficient material balance calculations were made to suggest that the conceptual process is feasible. They, however, are based on extrapolations of ORNL measurements with salts containing  $\text{BeF}_2$  and  $\text{ThF}_4$ . In addition, a criticality analysis must be done and fission product heat rates determined before the equipment can be properly sized. Lastly, the development and eventual qualification of a suitable fission product waste form should be pursued in parallel with refinement of the process and development of process equipment.

In order to significantly reduce the short-term heat generation rate, it is desirable to remove Cs/Sr from the waste stream. Future work will need to examine the separation of these isotopes and final disposition path. If Cs is required in the blanket, perhaps these fission products can be allowed to buildup and replace the natural Cs that would otherwise be used. This effect on the heat load and running of the In-Zinerator will need to be examined.

### 3.3.2 Tritium and Fission Product Gas Recovery

Breeding and recovery of tritium is required to fuel the fusion driver in the In-Zinerator. In addition, the control of fission product gases and tritium is important for safety and environmental concerns. Two recovery schemes are necessary to recover unburned tritium present in the Z-Pinch chamber after the shot and bred tritium contained within the actinide mixture. Fission product gases within the actinide mixture must also be removed with the tritium. Tritium is stored in absorber beds for use in target manufacturing, and fission product gases are stored in absorber beds for eventual disposal. The following sections describe the gas recovery systems in more detail.

#### Tritium Recovery Parameters

Tritium production and recovery within the In-Zinerator power plant is required for tritium self-sufficiency of the fusion driver. The mass of deuterium (D) and tritium (T) required for power plant operation is determined using the following baseline parameters:

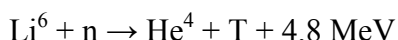
- 2.25 mg DT/capsule (burn efficiency of 1/3)
- 1:1 ratio of D to T (mass of T is 60% of total DT mass in capsule)
- Consumption of 6 capsule/min
- 5%  $^6\text{Li}$  enrichment

Each target contains 1.35 mg of tritium and 0.9 mg of deuterium, and 2/3 of the material is unburned. The masses of tritium and deuterium that must be recovered per day from the Z-Pinch chamber are:

- 7.8 g T/day (78,000 Curies per day)
- 5.2 g D/day

These isotopes are assumed to be contained as a gas within the Argon atmosphere in the Z-Pinch chamber after a shot. Therefore, the hydrogen isotopes must be separated from Argon.

Tritium breeding occurs in the actinide mixture due to the presence of lithium by the reaction:



The goal of the In-Zinerator design is to have a Tritium Breeding Ratio (TBR) within the actinide mixture of 1.2. This allows enough tritium to be bred to sustain the reaction while giving a margin for losses during extraction and processing. The estimated total amount of tritium bred per day in the mixture is:

4.7 g/day (47,000 Curies per day)

The tritium recovery design from  $(\text{LiF})_2\text{-AnF}_3$  mixture can support larger breeding ratios if the  $^6\text{Li}$  enrichment is modified. The baseline MCNP model uses an enrichment of 5%  $^6\text{Li}$  but may change slightly as the design evolves.

### **Gas Recovery from Argon**

Tritium and deuterium are recovered from the fusion chamber using the argon gas (10 torr, 640 g/shot). The exhaust exiting the chamber contains argon, helium, deuterium, and tritium since about 2/3 of the target fuel is not burned. The total flow rate of hydrogen isotopes is 13 g/day (7.8 g T + 5.2 g D). A diagram of the recovery process from the chamber is presented in Figure 3-15.

The fusion chamber is evacuated and replaced with 10 torr Argon after every shot. The exhaust exits the chamber at high temperature and passes through a particulate filter to remove RTL and target debris. The exhaust is then cooled to 110°C before introduction to a hydrogen gas membrane system.

The average concentration of hydrogen isotopes in the In-Zinerator fusion exhaust is calculated as:

5.2 mol D,T per day  
1.4 x 10<sup>5</sup> mol Ar per day  
37 ppm D,T concentration in Ar

In an effort to increase the single-pass effectiveness of the downstream hydrogen getter, a hydrogen gas filter such as the PRISM® hollow fiber membrane system currently marketed by Air Products, Inc. is proposed [26]. This is a robust, industrially proven system that is frequently utilized to separate hydrogen from argon in the ammonia industry. Reliability and ease of maintenance are attractive. It could be adapted to the radiological demands of tritium handling at substantial cost [27]. A practical balance between the number of stages and the effectiveness of the hydrogen getter will need to be determined.





[illegible]

<u>Monatomic Element</u>	<u>g/day</u>	<u>ppm</u>
Tritium (TBR = 1.2)	4.7	44
Hydrogen	7.2	200
Bromine	1.8	0.6
Krypton	23	7.6
Iodine	44	10
Xenon	501	106

49

Hydrogen isotopes are not readily soluble in flibe [34]. It is reasonable to extrapolate that hydrogen isotopes are also not readily soluble in this fluoride salt. Therefore, the addition of hydrogen to the helium sparge gas should enhance surface recombination and facilitate tritium release as predicted for flibe [35].

The gas recovery system takes place in the following steps:

1. The gas stream passes through an intermediate hot gas exchanger (exit 400°C).
2. The cooled gas is introduced into a high temperature charcoal adsorber. Iodine and bromine are removed at this stage.
3. The gas stream passes through a water-cooled heat exchanger (exit 50°C) and then through an intermediate cold gas exchanger (exit -180°C).
4. The cold gas stream enters a liquid nitrogen-chilled cold temperature charcoal adsorber (exit -190°C). Krypton and xenon are removed at this stage.
5. The gas stream proceeds through a final heat exchanger process to raise the temperature before passing over a titanium sponge gettering bed at ~400°C to scavenge hydrogen and tritium [28].
6. The purified helium is heated in the intermediate hot gas exchanger.
7. The heated helium is mixed with hydrogen and reintroduced into the sparge tube(s).

Once the gettering bed is saturated, it is isolated and regenerated by externally heating to 700°C with nitrogen. The hydrogen isotopes are released and swept from the bed with a minimal quantity of helium and sent to isotope separation. A small quantity of tritium is irretrievably lost in the charcoal adsorbers [30]. The TBR must be adjusted accordingly to compensate.

## Isotope Separation

Hydrogen isotopes ( $Q = \text{H, D, T}$ ) recovered from the getters are separated by the established technique of cryogenic distillation [36,37]. Helium contamination must be <10% of the isotope stream before introduction for effective distillation [38]. A simplified diagram of the isotope separation and storage process is presented in Figure 3-17. The isotopes released from the gettering beds are mixed:  $\text{D}_2$ ,  $\text{DT}$ , and  $\text{T}_2$  from the fusion chamber and  $\text{H}_2$ ,  $\text{HT}$ , and  $\text{T}_2$  from the fluoride salt. This generalized hydrogen isotope mixture,  $Q_2$ , is processed through a series of distillation columns. The tritium and deuterium cuts are sent to storage. Residual gas, consisting primarily of  $\text{H}_2$  contaminated with helium, is returned to the sparge tube(s).

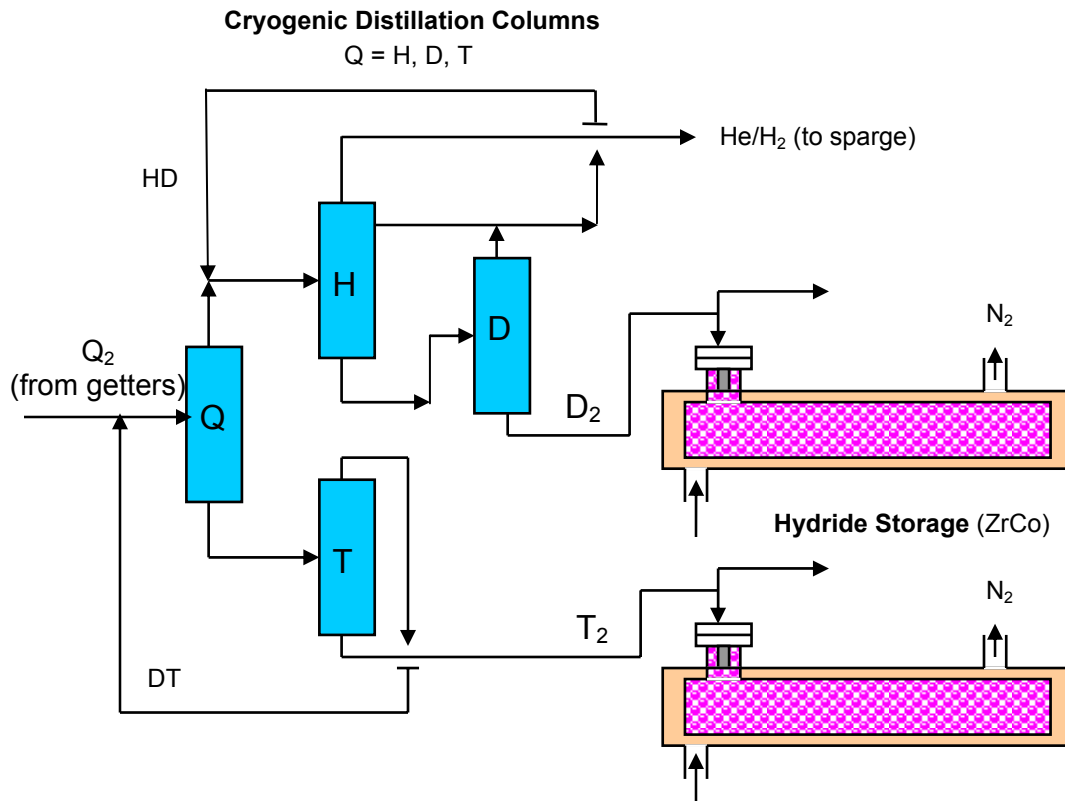


**Figure 3-17: Distillation and Storage**

## Tritium Storage

Zirconium-cobalt (ZrCo) intermetallic hydride beds are selected for long term storage of deuterium and tritium as done with ITER [39]. Isotopes are liberated by externally heating the bed to  $\sim 330^\circ\text{C}$  using nitrogen [40]. The bed also serves as a filter for the tritium decay product  $^3\text{He}$ . This contaminant becomes trapped in the metal lattice and physically damages the bed over time. Bed replacement is considered acceptable to maintain the tritium purity requirements ( $>99.5\%$ ) for fusion target capsule manufacture.

The stored quantity is no less than one week of power plant operation or 90 g of tritium (900,000 Curies) and 60 g of deuterium. Each bed will store up to 100 g of isotopes dedicated to either tritium or deuterium.

## Discussion

One key aspect of the In-Zinerator power plant design is the use of a proven method of tritium extraction from helium. In fact, the FSV helium coolant purification system encountered significant operational problems including water contamination from the water-lubricated bearings in the helium circulators and nitrogen poisoning of the titanium sponge gettering beds were serious problems [41,42]. Fortunately, water ingress is not an issue for the In-Zinerator design.

The titanium sponge bed has been retained despite its eventual replacement at FSV with copper-oxide [41]. It is important to note that the original FSV design called for capturing tritium and venting it through a gaseous waste system; later adoption of the ALARA concept eliminated this disposal route [30]. Consequently, the focus shifted to solid low level waste disposal of the titanium sponge. This development, combined with nitrogen poisoning from leaks elsewhere in the purification loop, contributed to the switch to copper-oxide. Copper-oxide is an effective hydrogen scavenger and was probably less expensive to acquire and discard [43]. Improved methods of quality control diminish the possibility of titanium sponge bed poisoning in the In-Zinerator design.

As for the PRISM® membrane system and its industry equivalents, it does not appear that hydrogen isotope enrichment possibilities have been fully investigated. The indication is that development costs would be high and unattractive as a significant market for tritium does not yet exist.

### **3.3.3 Safety Issues**

#### **Tritium Control**

Tritium presents many safety issues that must be taken into consideration for design purposes. The primary two safety concerns are tritium buildup and the resulting explosions (similar to hydrogen) and the diffusion of tritium through materials and the resulting radiation concerns..

Hydrogen buildup in light water reactors (LWRs) is a major safety concern. Most LWRs have implemented the use of hydrogen igniters to prevent the buildup of hydrogen in containment and prevent uncontrolled hydrogen explosions from occurring. The explosive nature for hydrogen also exists for tritium, although some research suggests that tritium is less explosive than hydrogen [44]. Thus, using standardized hydrogen constants to calculate explosion concerns with tritium results in a conservative, if not an overly conservative analysis. Fortunately the tritium levels in the actinide mixture should be well monitored since tritium is being extracted in this design. Systems must also be put in place to monitor tritium buildup in the environment [45].

Tritium, like hydrogen, can easily diffuse through most materials. When choosing which materials to use, the ease at which tritium can diffuse through the material must be considered, especially in the actinide loop. Material choices must be made to prevent large amounts of tritium from escaping the system and accumulating in the environment. Tritium is a beta emitter, so minimum shielding will be needed to protect personnel. However, personnel must be protected from inhaling diffused tritium, since beta particles can deliver large amounts of localized radiation to the lung tissue. Research is being done on the use of ceramic coatings to decrease tritium diffusion; this may prove to be a valuable option [46]. Other options would be the use of aluminide coatings, carbides, nitrides, silicon and even glasses [47]. Tritium control and containment will need to be examined in more detail in future work.

## 3.4 Thermal Analyses

The heat cycle and power conversion systems were not investigated in detail for this work since it is not viewed as a major engineering challenge. There is a tremendous amount of past work on designing heat cycles using a molten metal (lead) coolant that can be applied when the time is appropriate. Potential heat cycles include the Rankine cycle using water or the Brayton cycle using either helium or supercritical CO<sub>2</sub>.

A much greater challenge with this design is in adequately removing the heat from the near-instantaneous energy deposition. These sections examine this issue and discuss alterations to the baseline design that may be required.

### 3.4.1 Heat Generation

The results of the pulse modeling work (described in section 6.1.2) show that the energy deposition of the fusion pulse and subsequent fission multiplication all occurs within 10 ms. This is virtually instantaneous on the time scales required for heat removal. For a baseline design of 3,000 MWth, this equates to an instantaneous energy deposition in the actinide mixture of 30 GJ once every 10 seconds.

All components within the chamber are power producing components, meaning the nuclear heating recovered from the FW, blanket, actinide tubes, reflector, and surrounding structures will be high grade heat. A small fraction (< 0.1%) leaks from the back wall and top/bottom structures. The breakdown of the heating indicates 3, 180, 2800, and 16 MW deposited in the FW, Pb coolant, actinide tubes, and Pb reflector, respectively, totaling 3000 MW for the entire system. Most of the power (93%) is generated in the 1146 tubes submerged in the Pb coolant. This means the fission process within the blanket accounts for the majority of the produced power. The radial heating across the six rows of tubes is almost uniform. It peaks at 2.6 MW in the third row and drops slightly to 2.4 MW per tube of the first or last rows.

Peak heating values were calculated for the actinide mixture, the steel wall of the tubes, and the chamber steel wall. Total heating values were calculated for the Pb coolant and reflector. For lack of better data, the thermal characteristics of Flibe were used in the calculations, which is a serious limitation of this work. Table 3-6 gives the heating values and the resulting temperature rise per pulse. The heating values are based on steady state time between pulses. The actinide tube region was split into 6 “rows” with row 1 representing tubes closest to the Z-Pinch target and row 6 referring to tubes farthest away.

It is apparent that the heating in the actinide mixture is excessive, although experimental data of the thermal properties of the mixture will be required to get more confident results. Either way, this magnitude of a thermal rise will likely be very difficult to engineer, so techniques will need to be examined in future work to minimize this rise. The easiest way to cut the temperature rise is to increase the total amount of actinide mixture while keeping the total actinide content constant. The boiling temperature of many molten salts is >1400°C at atmospheric pressure, and obviously greater at higher pressure. Therefore, it appears that although these temperature increases are high, there may be some room to work within their domain.

Component	row	Peak Heating (MW/cm <sup>3</sup> )	Mass (kg)	Peak ΔT (°C)	Avg. ΔT (°C)
Flibe	1	3.64e-4	15.2	760	633
	2	3.83e-4	“	814	679
	3	4.12e-4	“	858	715
	4	4.13e-4	“	860	717
	5	3.97e-4	“	827	689
	6	3.77e-4	“	786	655
Tube	1	1.16e-5	2.89	31	26
	2	1.22e-6	“	33	27
	3	1.28e-5	“	35	29
	4	1.29e-5	“	35	29
	5	1.23e-5	“	33	27
	6	1.16e-5	“	31	26
Avg. Heating (MW/cm <sup>3</sup> )					
Chamber wall		9.88e-8	28,183		0.27
Pb coolant		5.52e-6	356,655		31.4
Pb reflector		3.60e-7	511,388		2.05
Equilibrated Pb			868,043		14.1

**Table 3-6: Nuclear Heating and Temperature Rise**

The nuclear heating of the chamber wall is very small and not an area of concern. The heating of the tubes is reasonable, but the large temperature rise of the actinide mixture will increase the tube temperature significantly. The melting temperature of Hastelloy-N is 1370°C, but the recommended maximum temperature for this alloy would be 2/3 of melting, or 913°C. Future work must examine how to minimize the temperature rise in the actinide mixture.

### 3.4.2 Other Thermal Issues

Sudden and instant energy deposition will result in instant pressurization and disassembly with possible high speed acceleration of fluid masses inside the chamber. This phenomenon is referred to as isochoric heating. Isochoric heating should be investigated since the duration of the pulse is so short, but the Gruneisen parameter for Flibe is on the order of 1.0, so it may not be a major issue.

Lastly, compatibilities of the materials at the high temperatures have to be investigated. Hastelloy-N is believed to perform adequately up to 700 °C, but corrosion may become an issue at higher temperatures [3].

### 3.5 References

1. C.L. Olson et al., “Z-Pinch IFE Program Final Report for FY04,” SAND2005-2742P (April, 2005).
2. C.L. Olson et al., “Z-Inertial Fusion Energy : Final Report FY 2006,” SAND Report to be printed October, 2006.
3. D.F. Williams, L.M. Toth, and K.T. Clarno, “Assessment of Candidate Molten Salt Coolants for the Advanced High-Temperature Reactor (AHTR),” ORNL/TM-2006/12 (March, 2006).
4. S. Fetter, E.T. Cheng, and F.M. Mann, “Long Term Radioactive Waste from Fusion Reactors: Part II,” *Fusion Engineering and Design*, **13**, 239 (1990).
5. Nuclear Regulatory Commission, “10CFR61, Licensing Requirements for Land Disposal of Radioactive Waste,” *Federal Register*, FR47, 57446 (1982).
6. B.B. Cipiti, “RTL Manufacturing Plant Options,” published in the Z-IFE FY05 Year End Report (September, 2005).
7. E. Rodriguez-Vieitez, E. Greenspan, J. Ahn, and Y. Hirose, “Molten-Salt Type Effect on Once-Through Molten-Salt Transmuters Characteristics,” University of California-Berkeley, unpublished.
8. J.P.M. van der Meer et al., “Thermodynamic Modeling of LiF-LnF<sub>3</sub> and LiF-AnF<sub>3</sub> Phase Diagrams,” *Journal of Nuclear Materials*, **335**, 345-352 (2004).
9. M. Hron, “Project SPHINX Spent Hot Fuel Incinerator by Neutron Flux (The Development of a New Reactor Concept with Liquid Fuel Based on Molten Fluorides),” *Progress in Nuclear Energy*, **47**(1-4), 347 (2005).
10. V. Ignatiev, R. Zakirov, and K. Grebenkine, “Molten Salts as Possible Fuel Fluids for TRU Fuelled SYSTEMS: ISTC #1606 Approach,” RRC-Kurchatov Institute.
11. Y. Orlov, P. Marytnov, and V. Gylevsky, “Issues of Lead Coolant Technology,” State Scientific Center of Russian Federation, Institute of Physics and Power Engineering.
12. A.M. Weinberg, “Preface: Molten-Salt Reactors,” *Nuclear Applications and Technology*, **8**(2), (February, 1970).
13. M.E. Whatley et al., “Engineering Development of the MSBR Fuel Recycle,” *Nuclear Applications and Technology*, **8**(2), 170 (February, 1970).
14. I.M. Ferris et al., “Equilibrium Distributions of Actinide and Lanthanide Elements between Molten Fluoride Salts and Liquid Bismuth Solutions,” *Journal of Inorganic Nuclear Chemistry*, **32**, 2019 (1970).
15. D.G. Schweitzer and J.R. Weeks, “Liquid-Metal Fuel Constitutions – III and IV,” *Transactions of the ASM*, **54**, 185 (1961).
16. D. Lexa, “Preparation and Physical Characteristics of a Lithium Beryllium-Substituted Fluorapatite,” *Metallurgical and Materials Transactions*, **30A**, 147 (1999).
17. G. Silva, “Study on Immobilizing Radionuclides in Apatite-Based Host Phase Material,” Master’s Thesis, University of Nevada, Las Vegas (December, 2005).
18. R.C. Ewing and L.M. Wang, “Phosphates as nuclear waste forms,” *Phosphates: Geochemical, Geobiological, and Materials Importance Reviews in Mineralogy & Geochemistry*, **48**, 673 (2002).
19. T.R. Johnson, J.K. Fink, and L. Leibowitz, “Evaluation and Analysis of Zeolite Ion Exchange Studies,” ANL-06/21, Argonne National Laboratory (in press).

20. M.F. Simpson & M. Dunzik-Gougar, "Two-site Equilibrium Model for Ion Exchange between Monovalent Cations and Zeolite-A in a Molten Salt," *Industrial & Engineering Chemistry Research*, **42**, 4208 (2003).
21. M.A. Lewis, M.C. Hash, W.L. Ebert, A. Hebden, and S.M. Oliver, "Results of Physical Characterizations and Product Consistency Tests with Ceramic Waste Form Products Prepared at Six Temperatures and Six Hold Times," ANL-NT-178, Argonne National Laboratory (May, 2001).
22. Chemical Technology Division Annual Report to May 1970, ORNL-4572, p 19.
23. Chemical Technology Division Annual Report to March 1971, ORNL-4682, p. 21-23.
24. T.R. Johnson et al., Chemical Engineering Division Semiannual Report, January – June 1965, ANL-7055, p 44.
25. D.T. Ingersoll et al., "Status of Preconceptual Design of the Advanced High-Temperature Reactor (AHTR)," ORNL/TM-2004/104 (2004).
26. Hydrogen Recovery and Purification. <http://www.airproducts.com/Products/Equipment/PRISMMembranes/page08.htm>
27. S.A. Rogers, Air Products and Chemicals, Inc, Allentown, PA., Personal communication (2006).
28. M. Nishikawa, H. Kido, K. Kotoh, and M. Sugisaki, "Titanium-Sponge Bed to Scavenge Tritium from Inert Gases," *Journal of Nuclear Materials* **115**, 101 (1983).
29. H.G. Olson, "The Fort St. Vrain High Temperature Gas-Cooled Reactor I: Low Power Physics Tests," *Nuclear Engineering Design*, **53**, 117 (1979).
30. H.G. Olson, H.L. Brey, and F.E. Swart, "The Fort St. Vrain High Temperature Gas-Cooled Reactor VI: Evaluation and Removal of Primary Coolant Contaminants," *Nuclear Engineering Design*, **61**, 315 (1980).
31. G.C. Bramblett, C.R. Fisher, and F.E. Swart, "Operational Experience at Fort St. Vrain," IAEA Conference, Lausanne, Switzerland (1980). [http://www.iaea.org/inis/awsh/tgr/abstracts/abst\\_iwggr1\\_01.html](http://www.iaea.org/inis/awsh/tgr/abstracts/abst_iwggr1_01.html)
32. G.L. Wessman and T.R. Moffette, "HTGR Plant Safety Design Bases," *Nuclear Engineering Design*, **26**, 78 (1974).
33. J.I. Shin, "Conceptual Design of an HTGR System for a Total Energy Application," Thesis, Nuclear Engineering Department, Massachusetts Institute of Technology (1975).
34. G.R. Longhurst, R.A. Anderl, and R.S. Willms, "Tritium Loss in Molten FLiBe Systems," *Fusion Technology*, **38**, 376 (2000).
35. D.K. Sze, "Counter Current Extraction System for Tritium Recovery from  $^{17}\text{Li}$ - $^{83}\text{Pb}$ ," *Fusion Technology*, **8**, 887 (1985).
36. J.R. Robins et al., "Tritium Purification System for TFTR," 15<sup>th</sup> IEEE/NPSS Symposium on Fusion Engineering, **1**, 69 (1993).
37. J.L. Anderson and K. Okuno, "Tritium Handling and Processing Experience at TSTA," Los Alamos National Laboratory, LA-UR-94-1868 (1994).
38. D. Zhang, A. Kodama, M. Goto, and T. Hirose, "Recovery of Trace Hydrogen by Cryogenic Adsorption," *Separation and Purification Technology*, **35**, 105 (2004).
39. H. Yoshida, D. Murdoch, M. Nishi, V. Tebus, and S. Willms, "ITER R&D: Auxiliary Systems: Tritium Systems," *Fusion Engineering and Design*, **55**, 313 (2001).
40. R.D. Penzhorn, M. Devillers, and M. Sirch, "Evaluation of ZrCo and Other Getters for Tritium Handling and Storage," *Journal of Nuclear Materials*, **170**, 217 (1990).
41. H.L. Brey, "Fort St. Vrain Operations and Future," *Energy*, **16**, 47 (1991).



42. R.D. Burnette and N.L. Baldwin, "Primary Coolant Chemistry of the Peach Bottom and Fort St. Vrain High Temperature Gas-Cooled Reactors," IAEA conference, Juelich, Federal Republic of Germany (1980). [http://www.iaea.org/inis/aws/htgr/abstracts/abst\\_iwggcr2\\_19.html](http://www.iaea.org/inis/aws/htgr/abstracts/abst_iwggcr2_19.html)
43. M.S. Yao, R.P. Wang, Z.Y. Liu, X.D. He, and J. Li, "The Helium Purification System of the HTR-10," *Nuclear Engineering and Design*, **218**, 163 (2002).
44. L. Cadwallader and D. Petti, "Deuterium and Tritium Safety Issues in Target Fabrication," *Fusion Science and Technology*, **41**, 635 (2002).
45. S. O'hira et al., "Safety Design Concepts for ITER-Tritium Facility," *Fusion Science and Technology*, **41**, 642 (2002).
46. M. Nakamichi, H. Kawamura, and T. Teratani, "Development of Ceramic Coatings as Tritium Permeation Barrier," *Fusion Science and Technology*, **41**, 939 (2002).
47. Shelby, J., *Handbook of Gas Diffusion in Solids and Melts*. Materials Park, OH: ASM International, 1996, 116-117.

## 4.0 Advanced Nuclear Fuel Cycle

The previous chapter described the engineering of the In-Zinerator concept for transmuting actinides, but it is important to understand the integration of the In-Zinerator with the fuel cycle to determine how it compares to alternatives. This chapter examines the currently proposed fuel cycle as part of the Global Nuclear Energy Partnership (GNEP) along with how the In-Zinerator can fit in. Attention is given to a comparison of Fast Reactors (FRs) and In-Zinerators for waste reduction.

The purpose of an advanced nuclear fuel cycle is to close the fuel cycle and make it sustainable. The once-through cycle is currently not sustainable since multiple repositories will be required over the next century. It is unlikely that multiple repositories will be possible in the U.S, so the goals of an advanced fuel cycle are to [1]:

1. Significantly minimize nuclear waste destined for the repository.
2. Create a sustainable nuclear energy future.
3. Design an economically-competitive fuel cycle.
4. Achieve the above goals in a proliferation resistant manner.

### 4.1 GNEP Fuel Cycle

The GNEP fuel cycle is shown in Figure 4-1. In this scenario, spent LWR fuel is reprocessed according to the UREX+1a concept. Uranium is separated and can be re-enriched or stored as a strategic resource. All transuranic isotopes are pulled out together and fabricated into FR fuel for burning. Spent FR fuel then goes through pyroprocessing to recycle the actinides and segregate the fission products. All fission products from both reprocessing plants go to the repository. The figure also shows the expected mass flow rates for the system per metric ton of reprocessed LWR fuel.

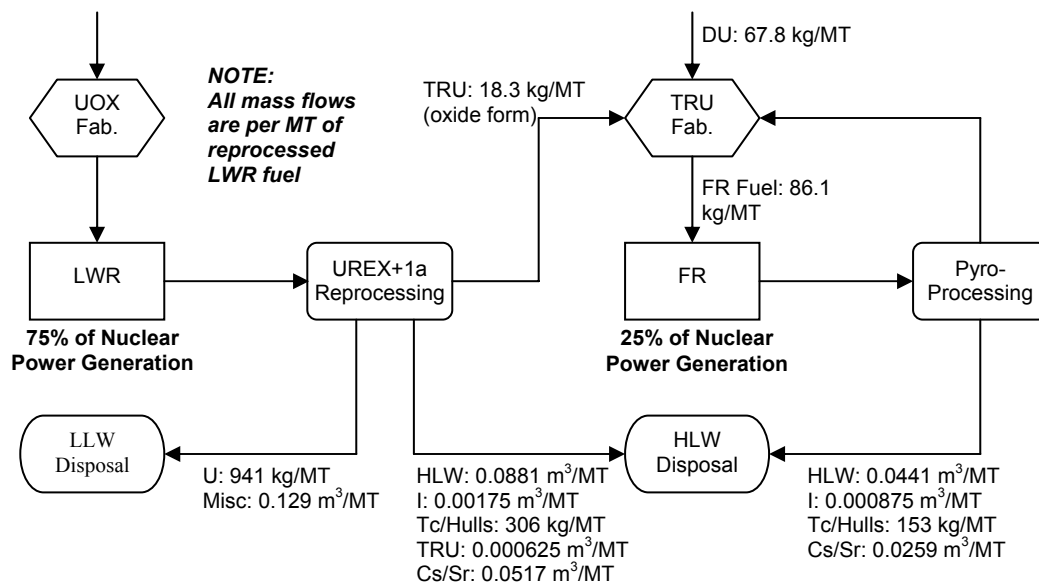


Figure 4-1: GNEP Fuel Cycle [1,2,3]

A large, 2,000 MT/yr reprocessing plant produces about 24,600 kg/yr of TRU, so the FRs shown in Figure 4-1 will be designed to burn this amount of TRU per year. The support ratio of FRs to LWRs is 1:3 as indicated by the percentages under the reactor blocks. The percentages refer to the total electrical power output of LWRs and FRs in order to burn up the TRU in FRs as fast as the LWRs produce it.

The support ratio is dependent on the conversion ratio that can be achieved in a FR, and the conversion ratio is the ratio of TRU produced divided by the amount of TRU burned. For example, if a burner is only burning TRU and not producing any, the conversion ratio is zero. In the case of a breeder reactor that produces just as much plutonium as it burns, the conversion ratio is one. A burner reactor will produce TRU if the fuel contains fertile material like  $^{238}\text{U}$  which can undergo neutron capture reactions. The support ratio shown in Figure 4-1 requires a conversion ratio of 0.25, which is likely to be a best case scenario for a fast reactor.

There are a number of concerns about this fuel cycle. The first is that FRs will cost more than LWRs, so the building of many will drive up the overall cost of the fuel cycle. Reaching a conversion ratio of 0.25 or lower will require significant fuels development and require more refueling of the reactor. These facts will both push off the development time and increase costs. Higher conversion ratios are more near-term, but will result in a lower efficiency for burning actinides, thus requiring more FRs. Finally, the TRU fuel fabrication and required pyroprocessing will be expensive.

## 4.2 Integration of the In-Zinerator in the Fuel Cycle

### 4.2.1 Complete TRU Burning

Figure 4-2 shows an alternative fuel cycle scenario if fusion transmutation could replace FRs for TRU burning. The In-Zinerator concept does not require fuel fabrication since the actinides are in a fluid form. This eliminates a costly processing step. In addition, because the conversion ratio for the In-Zinerator is zero, the support ratio (1:5) is better than for the FR scenario. The current LWR fleet would require about 20 In-Zinerators to balance the TRU production.

The technological readiness of a fusion transmutter is at an immature level, and likely such a unit would be more expensive than a FR. However, due to the better support ratio and the elimination of fuel fabrication, there could be some overall cost benefit to the In-Zinerator concept.

The FR plan and the In-Zinerator plan both give alternative energy options in the future. FRs can lead to sustainable energy growth through the use of Pu breeding. The In-Zinerator could lead to hybrid reactor designs and eventually pure fusion energy power plants given more research and development.

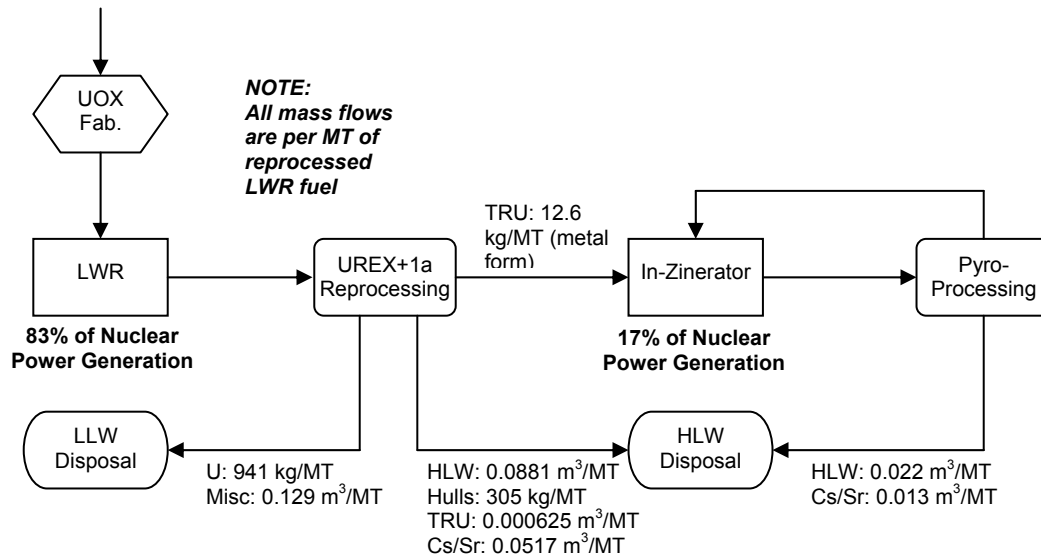


**Figure 4-2: Advanced Fuel Cycle with Complete In-Zineration of TRU [1,2,3]**

For this report, an In-Zinerator was designed and optimized for burning all TRU. This was chosen as a starting point in order to align with and compare to the proposed GNEP fuel cycle. Splitting up the TRU elements and examining different strategies introduces more uncertainty into the fuel cycle. In addition, keeping the TRU together is currently seen as desirable for increased proliferation resistance. That being said, the following section briefly examines an alternative strategy that could be studied in future work.

### 4.2.2 Alternative Burning Strategies

The In-Zinerator can also be configured to burn only specific minor actinides, such as Am/Cm or Np/Am/Cm mixtures. Preliminary work this year discovered that these fueling configurations will operate similarly to complete TRU burning, although it was not examined in great detail. A minor actinide In-Zinerator could be useful in a fuel cycle scenario that burned up Pu or Pu/Np in LWRs.

It is possible that a future fuel cycle in the U.S. will co-extract U and Pu together to form mixed oxide fuels (MOX) for burning in LWRs. Since Pu dominates the TRU, this option is one way to reduce the majority of the TRU in the current fleet of reactors. However, MOX burning is only a temporary solution as only 1 or 2 recycles will be practical before the fuel is unsuitable for LWR use [4]. On the other hand, this fuel cycle option does provide time to develop fast neutron systems for more complete actinide burning. In this situation, the minor actinides will still need to be burned up, and an In-Zinerator could be designed solely for that purpose. Figure 4-3 shows what this fuel cycle could look like.

The major advantage of a Np/Am/Cm In-Zinerator is that it would only take 1-2 units to burn up these species at the rate of production from the current LWR fleet. It would be much more realistic for the government to support the building and testing of one unit as opposed to an entire fleet of transmutation reactors. This fuel cycle could meet all the waste reduction goals to

increase the storage capacity of Yucca Mountain for about 50-75 years, but then the number of In-Zinerators would have to be expanded to burn up spent MOX fuel. Future work will examine this fuel cycle and the required In-Zinerator design in more detail.

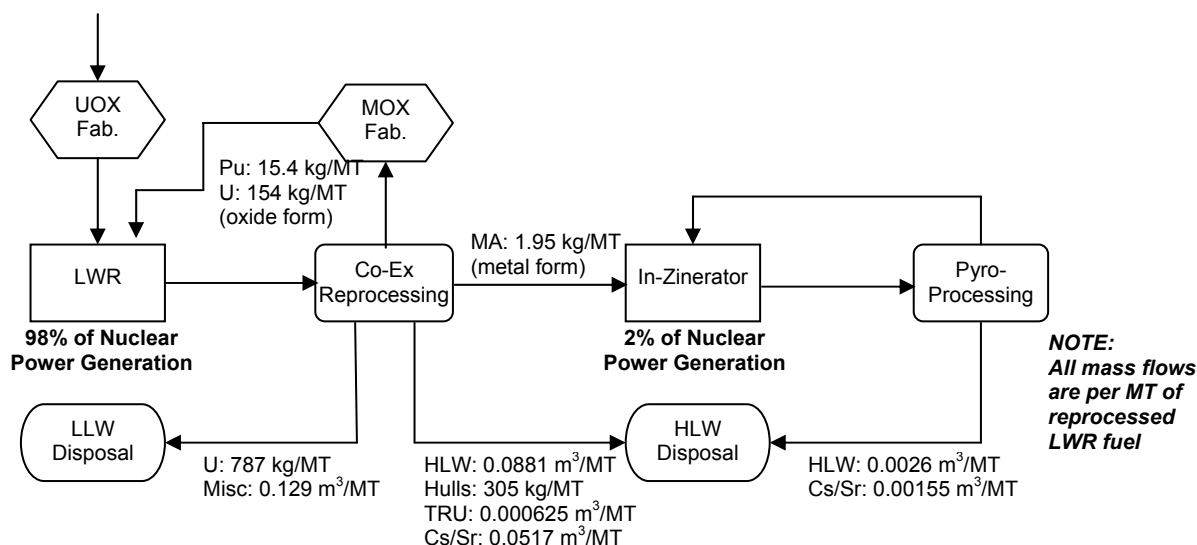


Figure 4-3: MOX Fuel Cycle with In-Zineration of Minor Actinides [1,2,3]

### 4.2.3 In-Zinerator vs. Fast Reactor Technical Comparison

Fast reactor (FR) deployment has been the preferred strategy for transmutation of actinides since they have been built in the past. Of the different transmutation options, FRs are at the highest level of technological readiness. In addition to cost, there are a number of concerns with large-scale deployment including:

1. The realistically-achievable support ratio required to balance the fuel cycle
2. FR Fuel fabrication requirements
3. Multi-recycle and multi-transport of radiologically hot fuel

#### Support Ratio

The largest uncertainty with FRs is their efficiency for burning up actinides. As described above, transmutation efficiency is measured as conversion ratio, which depends on the amount of fertile material (like <sup>238</sup>U) that is present in the fuel. In practice, the design of a TRU or minor actinide (MA) burner core is constrained by performance and safety parameters, such as the reactivity swing during burn-up, coolant void reactivity effect, Doppler coefficient, effective delayed-neutron fraction, etc. In particular, for a sodium-cooled FR core, the substitution of normal MOX fuel by TRU- or MA-dominated fuel has an unfavorable influence on several of these parameters. To ensure that a FR core performs satisfactorily and has acceptable safety parameters, it is usually necessary to blend fertile materials, like uranium, with the TRU or minor actinides [5]. Neutron capture of <sup>238</sup>U produces higher order actinides, so the net result is a lowering of the overall transmutation rate. There is some debate as to the lowest conversion

ratio that can be practically achieved, but it is likely to lead to a FR:LWR support ratio between 1:2 and 1:3 [6,7]. Lower conversion ratio reactor designs would likely be more expensive and require much longer development times.

In this context, sub-critical systems offer interesting additional parameters of freedom by removing the criticality constraint and increasing the safety margin to prompt criticality. The In-Zinerator blanket can be fueled with TRU with no fertile material, which allows for a better support ratio. Sub-critical systems would be particularly useful for minor actinides burners, which are difficult to control as critical systems because the effective delayed-neutron fraction is only about half of that of a normal FR [5].

## **Multi-Recycle**

Experimental and theoretical work which has been performed on the irradiation of MAs or on a mixture of Pu + MAs suggest that multi-recycling is necessary to achieve a significant inventory reduction factor. Burnups of 150 GWd/tHM could be achieved but even at this level yield a TRU depletion of only 17%, which corresponds to a situation in which 83% TRU fraction is still present in the target or fuel [5]. The fuel must be reprocessed and re-fabricated into new fuel over and over again. Thus, FR transmutation will require a significant amount of robotic handling and shuffling of the fuel around the fuel cycle, and this could be problematic with concerns over transportation of highly radioactive materials. If the cladding and hulls need to be disposed of as HLW after each reprocessing step, multi-recycling of TRU in FRs could generate a lot of secondary wastes. It may not be advantageous to burn up long-lived TRU if the end result is the production of more low level wastes.

The advantage of continuous processing with the In-Zinerator design is that the TRU product from the reprocessing plant comes in, fission product waste comes out, and no more shuffling of the TRU back and forth to the reprocessing plant is required. It also eliminates the generation of cladding wastes or the requirement to recycle cladding materials.

## **Fuel Fabrication**

There are still a number of questions to answer regarding FR fuel. FR fuel fabrication has issues related to the maximum amount of minor actinides that can be present, the self-heating of the fuel, and the most desirable fuel form (metal vs. ceramic). Fuel fabrication facilities will be completely robotic due to the heat content, and the cost of these facilities is very uncertain at this point. In addition, the recycling of FR fuel will require pyroprocessing which requires further cost. Proponents of a LWR-FR fuel cycle will have to prove that these additional fuel cycle costs required to get the full repository benefit will not be show-stoppers.

### **4.2.4 In-Zinerator vs. Fast Reactor Economic Comparison**

The In-Zinerator provides two services: electricity production and waste reduction. The economic analysis of the In-Zinerator should then include both of these economic bases. The value of electricity is straight-forward, but the value of reducing waste is much more vague. This section discusses the different ways to examine the In-Zinerator economics.

## Unit to Unit LCOE Comparison

The levelized cost of electricity (LCOE) was compared for LWRs, FRs, and the In-Zinerator using assumptions listed in Table 4-1. The costs are based on the assumption of the building of an nth of a kind plant. The capital cost of a FR is expected to be more than a LWR, while the cost of an In-Zinerator is expected to be higher than a FR (although this economic estimation has not been done yet). The operation and maintenance costs are assumed to be the same. The fuel cost for a LWR accounts for mining, conversion, enrichment, and fuel fabrication. The fuel cost for FRs includes a TRU reprocessing cost of \$2,000 per kg and a fuel fabrication cost of \$2,600 per kg of heavy metal [3,8]. The fuel cost for the In-Zinerator only includes reprocessing since fuel fabrication is not needed. The different capacity factors are used to represent the increasing engineering complexity in going from LWRs to FRs to In-Zinerators.

Using the assumptions shown in Table 4-1, the LCOE was calculated to be 5.29 c/kWh for LWRs, 6.35 c/kWh for FRs, and 6.54 c/kWh for In-Zinerators *if the In-Zinerator capital cost was the same as a FR*. In the following section this analysis is carried out as an average over the entire fuel cycle to determine what an In-Zinerator may cost to be competitive with FRs.

	Capital (\$/kW)	Fixed O&M (\$/kW)	Variable O&M (\$/kWh)	Fuel (\$/Mbtu)	Years to Con- struct	Average Capacity Factor (%)	LCOE (c/kWh)
Light Water Reactor	1694	60.06	0.00044	0.43	6	90.0	5.29
FR	2100			0.40		85.0	6.35
In- Zinerator	2100+			0.17		80.0	6.54+

**Table 4-1: Reactor Cost Assumptions**

In comparing a FR to an In-Zinerator, the majority of the plant will require the same technologies, and similar-sized components. Both require either molten salt or molten metal coolants, both reactor vessels are of the pool-type design, the power conversion systems will be similar, and both will require some type of pyro-processing step to remove fission products and reuse the actinides. The major difference is the requirement of a fusion driver for the In-Zinerator. This will lead to additional capital costs for the pulsed power LTD driver and all the robotics associated with inserting the RTL/target assemblies and removal and recycling of the debris.

With the additional capital costs, the In-Zinerator does not compete with a FR as a stand-alone unit. However, the fuel cycle must be examined as a whole to get the full story due to the differences in transmutation efficiency (support ratio) between the two options. What is more difficult to account for is the value of transmuting waste.

## Fuel Cycle Averaged LCOE Comparison

The reason that the fuel cycle averaged LCOE must be examined for this comparison is because of the difference in support ratios between FRs and In-Zinerators. When one considers adding transmutation technology into the fleet of nuclear reactors, the LCOE of the fleet as an average will change. The default assumption for this analysis is that the ratio for FRs to LWRs is somewhere between 1:2 and 1:3, while the ratio for In-Zinerators to LWRs is 1:5.

Table 4-2 shows the Fleet Average LCOE for the FR option and the In-Zinerator option as a function of support ratio. For example, if a FR fleet is used to transmute the LWR TRU, and if the support ratio for the fast reactors is 1:2, the average LCOE across the entire fuel cycle will be 5.63 c/kWh, about 0.35 c/kWh higher than with only LWRs and a once-through fuel cycle. As the support ratio gets better, the fleet averaged LCOE decreases since less transmuters are needed. Since the In-Zinerator can achieve the highest support ratio of 1:5, and since the FR will have a hard time even reaching 1:3, the In-Zinerator has an advantage. It needs to be noted that the assumptions used to calculate Table 4-2 come from Table 4-1 above, so they do not take into account the fact that an In-Zinerator could cost more than a FR.

Support Ratio	LCOE (c/kWh)	
	Fast Reactor	In-Zinerator
1:2	5.63	5.68
1:3	5.54	5.58
1:4	5.49	5.52
1:5	5.46	5.48

**Table 4-2: Fleet Average LCOE (cents/kWh)**

Figure 4-4 shows the allowable stand-alone In-Zinerator LCOE in order for the In-Zinerator to be competitive with FRs. If a support ratio of 1:3 is the best that can be achieved by a FR fleet, then the percentage of FR electrical output will be 25%. In that case, a fleet of In-Zinerators operating at a 1:5 support ratio can produce power for 6.88 c/kWh and cost the same (averaged across the fleet). Since LCOE roughly scales with the capital cost, this means that the In-Zinerator could cost about 8% more than a FR. If a more realistic FR support ratio is at 40% FRs and 60% LWRs, the In-Zinerator could cost 23% more than a FR at 7.83 c/kWh.



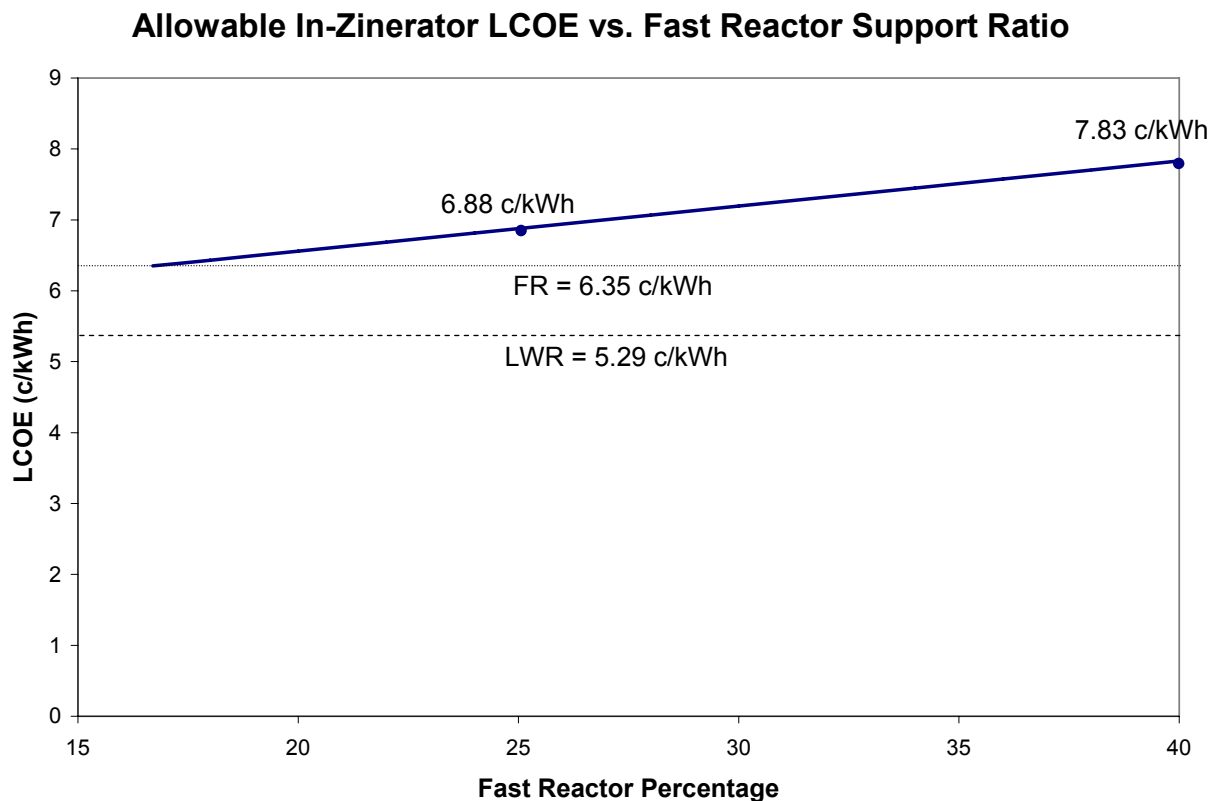


**Figure 4-4: Allowable In-Zinerator LCOE to be Competitive with FRs**

The purpose of this analysis is to show that by reaching the best support ratio with the In-Zinerator, the concept can afford to cost more and still be competitive with a FR fuel cycle. This also sets a maximum that the In-Zinerator should cost, which in turn provides a goal for the cost of the fusion driver that must be obtained.

### Value of Transmutation

It is evident from the previous analysis that either a FR or an In-Zinerator fuel cycle will not compete with the current once-through fuel cycle based on this LCOE comparison. However, this comparison does not account for the value of transmuting actinides.

Based on Table 4-2, if it were possible to build a FR with the maximum 1:5 support ratio, the fleet averaged LCOE would be 5.48 c/kWh, about 3.6% higher than the once-through fuel cycle. In some ways this does not seem like a great deal of increase, and it requires an increase of about 2 mil/kWh added to the cost of nuclear power across the board. This is about twice what is currently charged to nuclear reactors for the nuclear waste fund.

Regardless of the fuel cycle, a repository will still be required, so it is likely that the current nuclear waste fund fee of 1 mil/kWh will still be required for long-term disposal. The question for policy-makers and the public is whether it is worth an additional 2 mil/kWh to drastically minimize nuclear waste and provide a path to sustainable energy in the future. If the relative cost

increase of reprocessing and transmutation is correct, then it will also be up to policy-makers to determine how an added 2 mil/kWh tax will be used to subsidize the building and operation of these facilities.

The added cost of 2 mil/kWh may not seem like a lot considering the average cost a person pays for electricity, but applied to the entire nuclear fuel cycle, it quickly adds up to very large amounts. The building of 20 In-Zinerators or 33 FRs, each somewhere in the range of \$2-3 billion dollars is an incredibly huge undertaking. There will have to be a well-proven and large payoff in waste reduction in order to justify either of these advanced fuel cycles.

#### 4.2.5 Summary Comparison

Table 4-3 provides a general summary comparison of In-Zinerator transmutation to FRs and LWR thermal recycle, which has been examined in the past. It is possible to burn up some actinides in a thermal spectrum, but there are a number of other actinides that will buildup. Only fast spectrum systems have the potential to burn up all TRU.

Aspect	In-Zinerator	GNEP	Thermal Recycle
Safety (power excursion)	Reactors are subcritical, no chance of a runaway chain reaction	Fast reactors have short neutron lifetimes, it is possible that an excursion could be worse than LWR	Possibility of a power excursion, core damage, & slight chance of radioactive release
Safety (Coolant supply under loss of power)	Pool-type has inherent safety features	Pool-type has inherent safety features	Current LWRs require extensive safety systems, ALWRs less so
Safety (Coolant supply during depressurization)	Lead has low vapor pressure, small chance of "boiling dry"	Sodium has low vapor pressure, small chance of "boiling dry"	Energy release from depressurizing LWRs causes major design difficulties; supply of emergency cooling is also an issue.
Refueling	A continuous process with no separation of TRU materials and no TRU transportation	Batch process requiring reactor shutdown, transportation of separated TRU, and fuel fabrication step.	Batch process requiring reactor shutdown, transportation of separated TRU, and fuel fabrication step.
Energy	The fission device is able to multiply the energy output substantially, but loses some power to the fusion driver.	Fission power is a net producer of energy at current state of development. Energy input is only a few percent of plant output.	Fission power is a net producer of energy at current state of development. Energy input is only a few percent of plant output.

Economics	Likely to cost more than a FR as a stand-alone unit, but better support ratio requires less units. Cost savings by eliminating fuel fabrication. Will cost more than the once-through fuel cycle.	It is not yet clear a fast reactor with associated added facilities (separations plant, fuel remote fabrication plant, decay storage facilities, transportation, etc.) can surpass the economics of the "once-through" ALWR, which is the "standard" advanced nuclear systems must achieve.	As with the fast systems, thermal recycle systems are not yet shown to be economic compared to the "once-through" ALWR, which is the "standard" advanced nuclear systems must achieve.
TRU Destruction	Much more efficient than a FR—leads to a better support ratio.	Fast reactors are effective in destroying the higher TRU nuclides, but efficiency may be limited	Some TRU isotopes cannot be burned up in LWRs

**Table 4-3: In-Zinerator vs. FR vs. Thermal Recycle**

## 4.3 References

1. "Spent Nuclear Fuel Recycling Program Plan," Report to Congress, U.S. Department of Energy (March, 2006).
2. "Scoping Study for the Spent Fuel Treatment Facility," Washington Group International (January, 2004).
3. "Accelerator-Driven Systems (ADS) and Fast Reactors (FR) in Advanced Nuclear Fuel Cycles: A Comparative Study," OECD Nuclear Energy Agency (2002).
4. J.A. Stillman et al. "Follow-Up Analyses for the ANTT Review," ANL-AFCI-132 (September 30, 2004).
5. P.V. Tsvetkov & A.B. Alajo, "Assessment of System Performance Characteristics for a Complete Ultimate Incineration of Aggregated TRU Vectors with Minimum Recycling," Texas A&M University unpublished report (September, 2006).
6. E.E. Morris & M.A. Smith, "Development of Low Conversion Ratio Fast Reactors for Transmutation," ANL-AAA-057 (October 18, 2002).
7. R. Hill, Argonne National Laboratory, private communication (May 23, 2006).
8. M. Bunn et al., "The Economics of Reprocessing vs. Direct Disposal of Spent Nuclear Fuel," DE-FG26-99FT4028, Harvard University (December, 2003).

## 5.0 Modeling Methodology

A few different computer codes were used to help design and optimize the In-Zinerator systems and to calculate the transmutation rates. MCNP was used for a majority of the neutronics calculations including determining  $k_{\text{eff}}$ , multiplication, heating rates, dpa calculations, tritium breeding ratio, pulse modeling, and neutron spectrum analysis. The MCISE simulation model was used to calculate transmutation rates and fission product production rates. The ORIGEN code was used to calculate activities and heat loads of the products along with helping to verify the transmutation results. The model theory and development will be described in this chapter.

### 5.1 MCNP Model

An iterative optimization process was used to develop an initial working design for the In-Zinerator. The issues that were considered include neutron criticality, transmutation rates, heat transfer, energy multiplication, tritium breeding, and safety.

The actinide blanket must remain in a sub-critical configuration at all times in reactor operation. Insuring sub-criticality adds an inherent safety feature because there is no risk of an uncontrolled rise in power. However, in order for this system to be effective at energy production and transmuting nuclear waste it must be close to a critical configuration with a high energy multiplication. Tritium breeding from the presence of Li is required to provide fuel for the fusion targets.

It was assumed that a reasonable design basis model for the In-Zinerator would be a hollow cylindrical core with liquid fuel separated into tubes surrounded by a liquid-metal coolant. The liquid fuel was chosen to be the eutectic  $(\text{LiF})_2\text{-AnF}_3$ , and the coolant was chosen to be molten lead. A parametric study was used to find potential reactor geometries based on the multiplication factor. MCNP5.0 was used in order to calculate  $k_{\text{eff}}$  for the different models under consideration.

Figure 5-1 shows the initial baseline design as modeled in MCNP. The fusion chamber is 2 m in radius and 5 m tall. Argon at 10 torr is used as a background gas for the model, and a Z-Pinch fusion neutron energy distribution is used as a point source in the center of the chamber. The inner and outer walls of the chamber are 5 cm thick and modeled using the composition of Hastelloy-N. The blanket region is a total of 107 cm thick with the actinide tubes only in the first 57 cm. The tubes are also modeled using Hastelloy-N with 4.8 cm outer diameter and 4.4 cm inner diameter. The actinide mixture is contained within the tubes, and lead fills the rest of blanket region. The tubes are arranged in a hexagonal array with a pitch of 9 cm between tube centers. Because there are a lot of uncertainties about the RTL insertion at the top and debris removal system at the bottom, these areas were ignored and modeled as 20 cm thick Hastelloy-N. This was partly done to keep the model simplified and partly because the design is expected to change in the future.

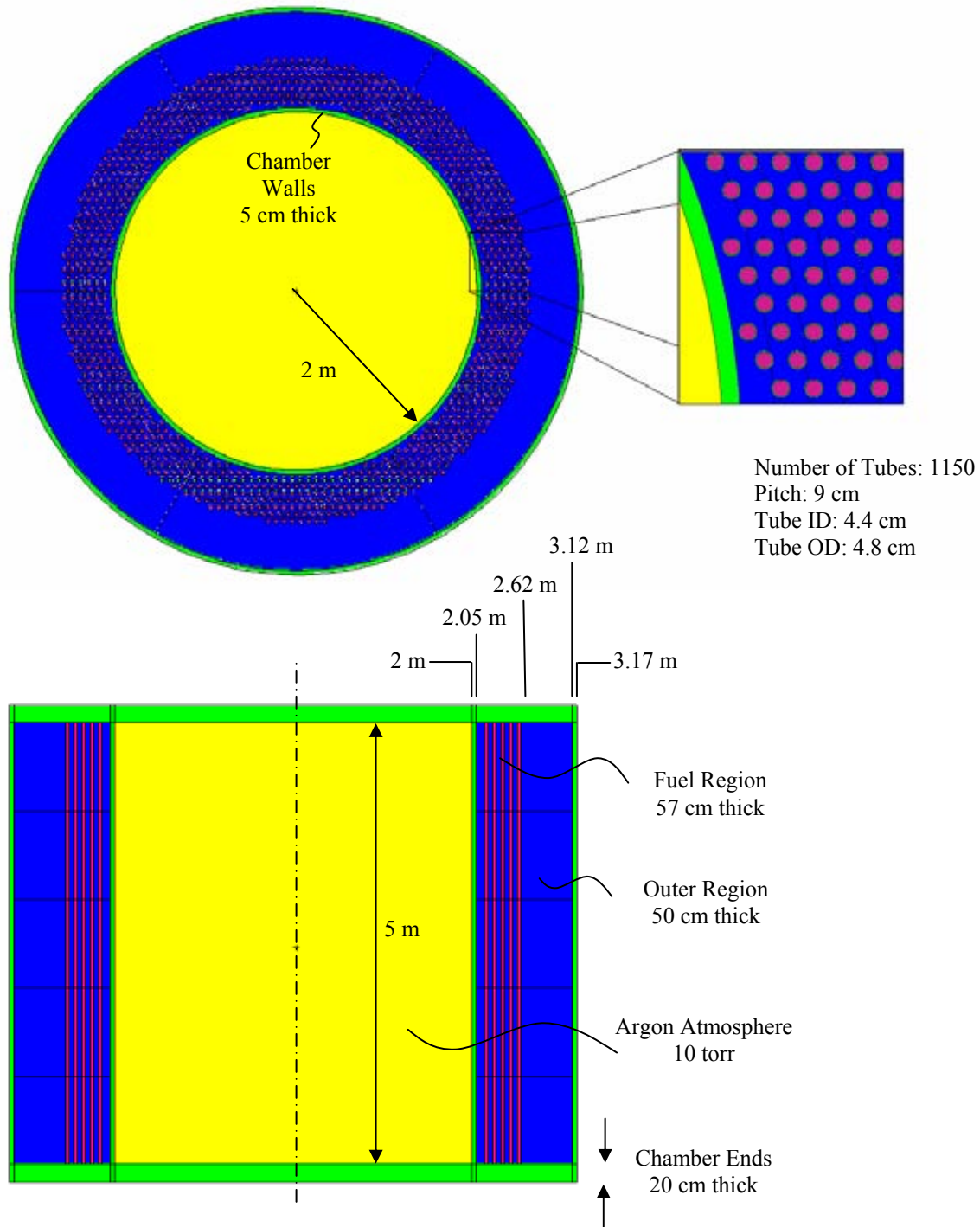


**Figure 5-1: In-Zinerator MCNP Model**

The optimization study varied the following parameters: fuel tube pitch, fuel tube diameter, fuel blanket region thickness, outer reactor chamber wall radius,  $^6\text{Li}$  enrichment, and inner wall thickness. The number of fuel tubes was calculated and the fuel tube centers were found using an algorithm given a pitch, first wall outer radius, and maximum fuel region radius. The minimum distance from the wall to the first tube was assumed to be 1 cm.

A combination of a Fortran code and Matlab script were used to generate the MCNP input files for the different parameters. The Matlab script was used to run MCNP for each input file and extract the results from the output. Several hundred runs were completed, and the outputs were sorted by hand to find the most likely designs. Tritium production tallies were also used to determine which of the likely designs had an appropriate tritium breeding ratio.

The current state of the optimization is far from complete. Additional constraints based on heat transfer and energy deposition in the fuel from fission should also be considered in future work. However, it will not be possible to complete a thorough optimization based on heat transfer until the thermal properties of the actinide mixture are established.

### **5.1.1 Modeling Data**

The modeling in MCNP and MCise is dependent on the quality of data used. This section provides a few comments on the nuclear data files that can be used when performing neutronics transmutation modeling calculations. Also presented is an examination of the TRU vector, or isotopic distribution, used for fueling and re-fueling of the blanket.

#### **Analysis of Nuclear Data**

Reactor designs with the MA-bearing fuel compounds require more accurate nuclear data for TRUs. The data of main interest are fission and capture cross-sections, fission neutron yields, fission neutron spectra and scattering cross sections. Due to current research interests and needs of many national programs including AFCI/GNEP and Generation IV programs, the status of nuclear data for MAs has been extensively evaluated in many studies including this project. In many independent assessments it was concluded that the currently available experimental data are insufficient to produce the accurate evaluated data for MAs, and new measurements are needed. On the other hand the current data sets are useful for scoping-level work.

The experimental post-irradiation benchmark studies indicated that the current JENDL, ENDF/B-VI and JEF libraries yield significant discrepancies in the predicted amounts of MAs and multiplication factors [1]. The fission and capture cross-sections between different data libraries are fairly consistent for low neutron energies up to about 0.1 eV. However, at high energies, there are order-of-magnitude or greater discrepancies in cross-sections. Neutron yields also vary considerably, which leads to concern in designing a sub-critical blanket with a  $k_{\text{eff}}$  close to 1.0.

#### **TRU Vectors**

The TRU vector refers to the distribution of actinides present in spent fuel that would be the output from a reprocessing plant. Factors such as fuel type, burnup, and fuel age all affect the final composition of spent fuel and can change the isotopic composition of the fueling going into the In-Zinerator. These factors were investigated to determine the range of fueling composition that a future transmuter may need to deal with.

Table 5-1 shows the effect of fuel burnup on the TRU vector. The isotopic distributions are given as percentages of the total actinide content. Data is given for both BWR and PWR fuel. As expected, the minor actinide inventory increases with burnup. However, the sum of the minor actinides (Np, Pu, Am, Cm) does not increase at the same scaling as the burnup. As LWRs reach higher burnups, less total fuel is consumed per unit of output power. The total minor actinide content as a function of electrical output then decreases slightly. This is an interesting result as it means that less In-Zinerators will be required as burnup increases.

PWR	Burnup (GWd/t HM)								
	20	30	45	50	60	70	80	90	100
U <sup>235</sup>	2.0819%	1.4059%	0.7000%	0.5391%	0.3082%	0.1694%	0.0907%	0.0478%	0.0249%
U <sup>236</sup>	0.3444%	0.4541%	0.5459%	0.5591%	0.5650%	0.5510%	0.5254%	0.4941%	0.4611%
U <sup>238</sup>	96.9094%	97.2468%	97.5878%	97.6582%	97.7437%	97.7732%	97.7690%	97.7491%	97.7251%
Np <sup>237</sup>	0.0203%	0.0391%	0.0720%	0.0827%	0.1015%	0.1156%	0.1246%	0.1289%	0.1295%
Pu <sup>238</sup>	0.0028%	0.0085%	0.0258%	0.0338%	0.0518%	0.0703%	0.0868%	0.1000%	0.1095%
Pu <sup>239</sup>	0.4564%	0.5127%	0.5364%	0.5386%	0.5403%	0.5407%	0.5407%	0.5406%	0.5405%
Pu <sup>240</sup>	0.1344%	0.2103%	0.2768%	0.2880%	0.3002%	0.3049%	0.3065%	0.3069%	0.3070%
Pu <sup>241</sup>	0.0434%	0.0941%	0.1586%	0.1723%	0.1890%	0.1964%	0.1993%	0.2003%	0.2007%
Pu <sup>242</sup>	0.0058%	0.0221%	0.0689%	0.0880%	0.1263%	0.1601%	0.1868%	0.2068%	0.2211%
Am <sup>241</sup>	0.0007%	0.0022%	0.0050%	0.0057%	0.0066%	0.0069%	0.0068%	0.0067%	0.0065%
Am <sup>242m</sup>	0.0000%	0.0000%	0.0001%	0.0001%	0.0002%	0.0002%	0.0002%	0.0002%	0.0002%
Am <sup>243</sup>	0.0005%	0.0029%	0.0156%	0.0229%	0.0417%	0.0634%	0.0849%	0.1040%	0.1197%
Cm <sup>242</sup>	0.0001%	0.0006%	0.0019%	0.0024%	0.0032%	0.0038%	0.0041%	0.0043%	0.0043%
Cm <sup>244</sup>	0.0000%	0.0005%	0.0052%	0.0091%	0.0224%	0.0443%	0.0743%	0.1104%	0.1498%
Sum MA	0.6644%	0.8931%	1.1662%	1.2435%	1.3831%	1.5064%	1.6149%	1.7090%	1.7889%

BWR	Burnup (GWd/t HM)								
	20	30	45	50	60	70	80	90	100
U <sup>235</sup>	2.0462%	1.3560%	0.6445%	0.4865%	0.2657%	0.1391%	0.0708%	0.0355%	0.0177%
U <sup>236</sup>	0.3502%	0.4609%	0.5492%	0.5599%	0.5599%	0.5398%	0.5089%	0.4737%	0.4378%
U <sup>238</sup>	96.9614%	97.3170%	97.6700%	97.7401%	97.8214%	97.8457%	97.8386%	97.8192%	97.7986%
Np <sup>237</sup>	0.0197%	0.0392%	0.0735%	0.0845%	0.1035%	0.1169%	0.1245%	0.1272%	0.1261%
Pu <sup>238</sup>	0.0027%	0.0088%	0.0282%	0.0371%	0.0570%	0.0765%	0.0931%	0.1054%	0.1135%
Pu <sup>239</sup>	0.4368%	0.4886%	0.5093%	0.5110%	0.5123%	0.5125%	0.5125%	0.5124%	0.5123%
Pu <sup>240</sup>	0.1321%	0.2059%	0.2681%	0.2780%	0.2882%	0.2918%	0.2929%	0.2932%	0.2932%
Pu <sup>241</sup>	0.0431%	0.0930%	0.1540%	0.1663%	0.1805%	0.1864%	0.1885%	0.1893%	0.1897%
Pu <sup>242</sup>	0.0060%	0.0229%	0.0716%	0.0913%	0.1300%	0.1631%	0.1885%	0.2070%	0.2201%
Am <sup>241</sup>	0.0011%	0.0033%	0.0071%	0.0081%	0.0091%	0.0094%	0.0093%	0.0090%	0.0088%
Am <sup>242m</sup>	0.0000%	0.0000%	0.0001%	0.0001%	0.0001%	0.0001%	0.0001%	0.0001%	0.0001%
Am <sup>243</sup>	0.0005%	0.0031%	0.0167%	0.0246%	0.0444%	0.0668%	0.0883%	0.1068%	0.1217%
Cm <sup>242</sup>	0.0002%	0.0007%	0.0021%	0.0026%	0.0034%	0.0038%	0.0040%	0.0041%	0.0042%
Cm <sup>244</sup>	0.0001%	0.0006%	0.0057%	0.0099%	0.0245%	0.0482%	0.0799%	0.1169%	0.1563%
Sum MA	0.6423%	0.8660%	1.1364%	1.2134%	1.3530%	1.4755%	1.5816%	1.6715%	1.7459%

**Table 5-1: TRU Vectors as a Function of Burnup [1]**

The effect of fuel age was also investigated. Table 5-2 shows a comparison of LWR fuel at a burnup of 60 GWD/MT and 4.03% initial enrichment for both 5-year and 50-year cooled. The most significant differences are that there is much less  $^{241}\text{Pu}$  and much more  $^{241}\text{Am}$  in the 50 year old fuel due to the decay of  $^{241}\text{Pu}$ . The  $^{244}\text{Cm}$  content is also lower in older fuel. Most of the rest of the isotopes do not change much with age, so there is little expected effect of reprocessing older fuel.

LWR Fuel, 60 GWD/t HM, 4.03% Initial Enrichment						
	5 yr old			50 yr old		
	g/MTHM	moles/MTHM	Ratios	g/MTHM	moles/MTHM	Ratios
<b>Np</b> <sup>236</sup>	1.19E-03	5.04E-06	0.0000%	1.19E-03	5.04E-06	0.0000%
<b>Np</b> <sup>237</sup>	1.12E+03	4.73E+00	6.7601%	1.20E+03	5.06E+00	7.3435%
<b>Np</b> <sup>238</sup>	6.27E-07	2.63E-09	0.0000%	5.10E-07	2.14E-09	0.0000%
<b>Np</b> <sup>239</sup>	2.97E-04	1.24E-06	0.0000%	2.96E-04	1.24E-06	0.0000%
<b>Pu</b> <sup>238</sup>	6.22E+02	2.61E+00	3.7385%	4.37E+02	1.84E+00	2.6630%
<b>Pu</b> <sup>239</sup>	7.50E+03	3.14E+01	44.8899%	7.49E+03	3.13E+01	45.4519%
<b>Pu</b> <sup>240</sup>	4.21E+03	1.75E+01	25.0932%	4.35E+03	1.81E+01	26.2873%
<b>Pu</b> <sup>241</sup>	1.34E+03	5.56E+00	7.9538%	1.53E+02	6.35E-01	0.9208%
<b>Pu</b> <sup>242</sup>	9.57E+02	3.95E+00	5.6569%	9.57E+02	3.95E+00	5.7354%
<b>Pu</b> <sup>243</sup>	2.26E-12	9.30E-15	0.0000%	2.26E-12	9.30E-15	0.0000%
<b>Pu</b> <sup>244</sup>	1.86E-01	7.62E-04	0.0011%	1.86E-01	7.62E-04	0.0011%
<b>Am</b> <sup>241</sup>	4.33E+02	1.80E+00	2.5701%	1.53E+03	6.35E+00	9.2075%
<b>Am</b> <sup>242</sup>	3.34E+00	1.38E-02	0.0197%	2.72E+00	1.12E-02	0.0163%
<b>Am</b> <sup>243</sup>	3.46E+02	1.42E+00	2.0368%	3.44E+02	1.42E+00	2.0531%
<b>Cm</b> <sup>242</sup>	2.01E-02	8.31E-05	0.0001%	6.58E-03	2.72E-05	0.0000%
<b>Cm</b> <sup>243</sup>	1.38E+00	5.68E-03	0.0081%	4.62E-01	1.90E-03	0.0028%
<b>Cm</b> <sup>244</sup>	1.99E+02	8.16E-01	1.1667%	3.55E+01	1.45E-01	0.2110%
<b>Cm</b> <sup>245</sup>	1.46E+01	5.96E-02	0.0852%	1.46E+01	5.96E-02	0.0864%
<b>Cm</b> <sup>246</sup>	3.30E+00	1.34E-02	0.0192%	3.28E+00	1.33E-02	0.0193%
<b>Cm</b> <sup>247</sup>	6.34E-02	2.57E-04	0.0004%	6.34E-02	2.57E-04	0.0004%
<b>Cm</b> <sup>248</sup>	7.32E-03	2.95E-05	0.0000%	7.32E-03	2.95E-05	0.0000%

**Table 5-2: TRU Vectors as a Function of Fuel Age**

The ratios of actinides for the 50-year-old fuel as shown in Table 5-2 was used for the fueling of the In-Zinerator in the model. These ratios were also assumed for the continuous reloading of the fuel. This data was chosen because the 60 GWD burnup was felt to be an average value of burnup between legacy fuel and future fuel. The 50 year cooling time seemed reasonable for the age of current spent fuel by the time these technologies could come on line.

### 5.1.2 MCNP Transmutation Modeling

Initially, MCNP5.0 was used to determine the neutron multiplication and total transmutation rates for all actinides in the blanket. The MCise model (described in the next section) is a much



more thorough model that has more capabilities, so the results shown in this report are MCise results. However, the MCNP modeling results were useful as a check on the MCise results to help validate the data.

In the MCNP model, the total loss for each isotope was calculated using the sum of all fission and (n,x) reactions. Then the total gain was calculated by considering the reactions (n,2n), (n,nd), (n,d), (n, $\gamma$ ), and (n, $\alpha$ ) on all of the actinides. The decay of actinides with relatively short half-lives was also taken into account. This method provided a simplified calculation that could be expanded in the future, but the MCise code includes many more reactions.

## 5.2 MCise Transmutation Model

### 5.2.1 Theory

A Monte Carlo inventory simulation engine (MCise) has been developed and implemented for modeling activation of materials with complex processes and irradiation histories [2]. This tool is specifically aimed at systems with flows that separate into multiple streams, each one subject to different processes or irradiation environments before rejoining into a common stream. Monte Carlo (MC) techniques based on following the history of individual atoms allows these atoms to (a) follow randomly determined flow paths, (b) enter or leave the system at arbitrary locations and (c) be subjected to radiation or chemical processes at different points in the flow path. Many elements of the methodology for MC inventory analysis have direct analogs to neutral particle MC radiation transport, where neutral particles traveling through space and changing their energy are replaced by isotopes traveling through time and changing their isotopic identity.

The current implementation of MCise includes the capability to simulate simple, complex, loop flows, and any combination of these. These advanced capabilities can later be used to implement features of real systems including sources, sinks, post-irradiation decay and extraction processes. In addition, some basic variance reduction techniques have been employed to enhance the analog simulation. These capabilities make MCise a suitable tool for an activation calculation of the eutectic fuel in the In-Zinerator because of the need to account for the on-line constant addition of fresh fuel and extraction of fission products.

The basic methodology of MCise can be summarized as follows. The total effective reaction rate coefficient,  $\lambda_{eff}$ , of an isotope at an arbitrary time can be determined by collapsing the total transmutation cross-section with the neutron flux and adding the decay constant,

$$\lambda_{eff} = \lambda + \int \phi(E) \sigma_{tot}(E) dE .$$

The probability of this isotope undergoing a reaction within time  $dt$  is

$$p(t)dt = e^{-\lambda_{eff}t} dt .$$

Using the inverse transformation of the cumulative distribution of  $p(t)$ , the time until the next reaction, defined as  $t_{rxn}$ , can be determined from a random variable  $\xi$  by

$$t_{rxn} = \frac{-\ln \xi}{\lambda_{eff}} = n_{rxn} \tau_{eff},$$

where  $\tau_{eff}$  is the mean reaction time ( $1/\lambda_{eff}$ ) and  $n_{rxn}$  is the randomly determined number of mean reaction times until the next reaction, if  $\xi$  is uniformly distributed between 0 and 1. If the remaining amount of time in the current irradiation environment, expressed in a unit of the number of mean reaction times

$$n_{rem} = t_{rem} \lambda_{eff},$$

is more than  $n_{rxn}$ , a new isotope is sampled from the possible reaction pathways. The relative probability of the new isotope is calculated from the individual pathway cross-sections weighted by the current neutron flux and/or decay rates. Also, the amount of the remaining time is decremented appropriately by

$$t_{rem} = t_{rem} - t_{rxn}.$$

The new isotope is then followed in the same way as the previous isotope. On the other hand, if the remaining amount of time is less than  $n_{rxn}$ , the particle moves to another environment and  $\lambda_{eff}$  is updated for the flux at this new point. The number of mean reaction times until the next reaction is decremented to,

$$n_{rxn} = n_{rxn} - n_{rem}.$$

For a calculation at a single time point, this second condition indicates the end of the history of an atom and a new atom is sampled. By appropriately counting the isotopic species each history represents at a given time of interest, an expected value of the isotopic composition can be determined.

## 5.2.2 Modeling Requirements

To fully specify an MCise model of a nuclear system requires describing the network of irradiation environments and flow paths between them and then including the sources of atoms.

An irradiation environment in MCise is defined by a *control volume*. The control volume is characterized by a neutron flux and a residence time,  $t_r$ . The neutron flux is expressed as a multi-group spectrum and is assumed to be constant throughout the control volume. The number of energy groups and energy group structure for the neutron flux must conform with those of the nuclear data format. The residence time represents the average amount of time any atom spends in the control volume and is defined by the engineering performance requirements of the system.

For example, it can be based on a minimum required flow rate through a system for adequate heat removal or on a maximum flow rate through a chemical extraction system.

Since the flow rate leaving a control volume is defined by its residence time, the flow paths between control volumes are defined only by the relative distribution of the flow to downstream control volumes using a simple discrete probability distribution function (PDF). The flow distribution can act on all isotopes equally, representing a bulk material flow, or can act differentially on specific isotopic or atomic species, representing extraction processes.

Another necessary component of an MCise model is a set of one or more atom sources. In MCise, each atom source is associated with a single control volume and has a time-independent isotopic composition and a time-dependent function  $r(t_{sim})$  characterizing the source strength. The total strength of each source,  $R_s$ , is defined by integrating  $r(t_{sim})$  over the total simulation time  $T_{sim}$ , i.e.,

$$R_s = \int_0^{T_{sim}} r(t_{sim}) dt_{sim}.$$

The set of total source strengths defines a discrete PDF which can be sampled to determine from which source a new atom comes. Once a particular source is chosen, its initial control volume is explicitly defined. Its isotopic identity can be randomly sampled from the discrete PDF representing the isotopic mix and its birth time can be randomly sampled from the continuous PDF,  $r(t_{sim})/R_s$ .

Another initial parameter for new atoms is the remaining time in its initial control volume. Some sources introduce atoms to the system as the beginning of the control volume, representing a flow from outside the network of control volumes into the system. Other sources represent inventories of atoms that are initially present in the system, some of which may leave their initial control volume immediately and others of which are resident in their initial control volume for the full residence time of that control volume. PDFs can easily be constructed to be sampled for the initial remaining residence time,  $t_{rem}$ .

### 5.2.3 MCise Model

A schematic of MCise model of the In-Zinerator is illustrated in Figure 5-2. The two control

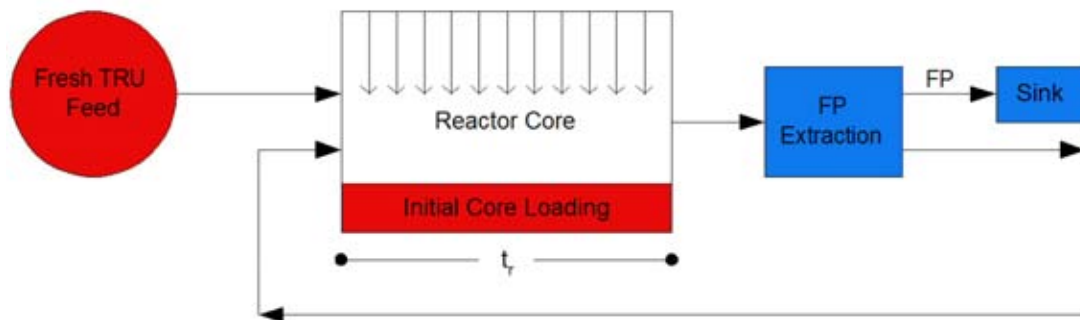


Figure 5-2: Schematic of In-Zinerator MCise Model

volumes in this schematic are the reactor core and fission product extraction environments. The reactor core is characterized by the average neutron flux that the eutectic fuel experiences while the second control volume has a neutron flux of zero. For the purpose of this analysis, a residence time of 100 days in the reactor was chosen corresponding the processing of 1% of the total inventory per day in the fission product extraction step. The residence time of the FP extraction represents a processing period of the fuel and was chosen to be zero during the initial stages of this study.

All of the flow leaving the reactor core goes to the FP extraction process, but the flow leaving the FP extraction process is divided into two streams based on the atomic species. All fission products flow to the sink and all actinides (and Li and F) are returned to the reactor core. This model was chosen to represent an ideal separations process and the flow distribution of each species can be adjusted to represent the real separations efficiencies.

There are two atom sources in the In-Zinerator model. Isotopic distributions of both sources are summarized in Table 5-3. Note that these distributions were calculated from the data in Table 5-2 from section 5.1.1 for 50-year-old fuel, but the initial core loading also includes Li and F.

The first one is the source representing the isotopic mix of the initial core loading and is assigned to the reactor core control volume. Mathematically, its time-dependent source strength is defined as

$$r_1(t_{sim}) = R_I \delta(0),$$

where  $R_I$  is the total number of atoms at the initial core loading. Since the atoms sampled from this source would start their history uniformly inside the reactor core, a PDF describing their remaining residence time is given by:

$$p_1(t_{rem}) = 1/t_r$$

The other source accounts for the addition of fresh fuel (TRU) to replace the consumed fuel. For this model, it was assumed that actinides could only be added as rapidly as fission products were being removed, to maintain a constant inventory in the reactor. More precisely, since each actinide fission results in two fission products, the rate of addition of actinides should be  $\frac{1}{2}$  the rate of removal of fission products. The fission product removal rate is determined by the inventory of fission products in the system. Under the assumption of a constant power level in the reactor, this can be calculated analytically.

$$\dot{F} = \kappa P - \frac{\epsilon \dot{C}}{I} F,$$

$$F(0) = 0,$$

where

$F$  = a total inventory of fission products [atoms]

$P$  = a desired power level [energy/time]

$\kappa$  = a number of fission products produced for an average fission energy released

Isotope	Initial Core Loading (atomic fraction)	Feed Stream (atomic fraction)
Li-6	1.2501E-02	-
Li-7	2.3753E-01	-
F-19	6.2507E-01	-
Np-236	9.0012E-09	7.3147e-08
Np-237	9.0761E-03	7.3435E-02
Np-238	-	3.1085E-11
Np-239	-	1.7966E-08
Pu-236	-	1.4384E-12
Pu-238	3.3129E-03	2.6630E-02
Pu-239	5.6632E-02	4.5452E-01
Pu-240	3.2879E-02	2.6288E-01
Pu-241	1.1576E-03	9.2095E-03
Pu-242	7.2382E-03	5.7352E-02
Pu-243	1.4127E-06	1.3491E-16
Pu-244	-	1.1055E-05
Am-241	1.1576E-02	9.2075E-02
Am-242	2.0627E-05	1.9542E-09
Am-242m	-	1.6305E-04
Am-243	2.6003E-03	2.0530E-02
Am-244		1.5457E-20
Cm-242	4.9754E-08	3.9434E-07
Cm-243	3.5004E-06	2.7573E-05
Cm-244	2.6878E-04	2.1100E-03
Cm-245	1.1051E-04	8.6423E-04
Cm-246	2.4878E-05	1.9336E-04
Cm-247	4.8005E-07	3.7225E-06
Cm-248	5.5381E-08	4.2804E-07
Bk-249	1.2501E-10	-
Cf-249	1.2501E-10	-
Cf-250	1.2501E-10	-

**Table 5-3: Loading Rates**

$$\approx \frac{2}{180MeV} [\text{atoms/energy}]$$

$\varepsilon$  = an efficiency of a fission product separation process [dimensionless]

$\dot{C}$  = a processing capacity rate [atoms/time]

$I$  = a total initial inventory [atoms]

Therefore,

$$F(t) = \frac{\kappa PI}{\varepsilon \dot{C}} \left( 1 - e^{-\varepsilon \dot{C} t / I} \right).$$

The feed rate of fresh TRU needed is also equivalent to the time-dependent source strength of the second source in the MCise simulation and given by:

$$r_2(t_{sim}) = \frac{1}{2} \frac{\varepsilon \dot{C}}{I} F(t_{sim}) = \frac{\kappa P}{2} \left( 1 - e^{-\frac{\varepsilon \dot{C} t_{sim}}{I}} \right), \quad 0 < t < t_{sim}.$$

Since the feed stream always enters at the beginning of the reactor control volume, a PDF describing the remaining residence time of the feed is defined with a delta function,

$$p_2(t_{rem}) = \delta(t_r).$$

The CINDER90 nuclear data library is used in this study. It uses a 63 group energy structure and includes both transmutation reactions and fission reactions with fission product yields. The fission product yields are not explicitly dependent on the neutron flux spectrum, but are defined for a number of representative spectrum types: thermal, fast and high-energy. For some isotopes, spontaneous fission product yields are also given. CINDER does not provide fission yields for all possible fission reactions. In such cases, when a fission reaction occurs, the product isotopes will be assigned a placeholder isotopic identity, *unknown fission product*. This isotope is stable and neutronically transparent and will accumulate. An accumulation of this isotope could result in underestimating decay heat and specific activity of the system.

Now that all necessary MCise components are defined, MCise employs the following algorithm to generate results.

1. A source is randomly chosen between two specified sources.
2. An initial atom is randomly sampled from a prescribed isotopic composition. Its entry time to and remaining residence time in the reactor core are determined from their respective PDF.
3. As the simulated atom travels through the reactor core, its history is tracked according to the methodology described in the previous section. The history ends when the total simulation time is reached.
4. Upon exiting the reactor core, the simulated atoms go into the fission product extractor. All fission product atoms enter the sink and have their histories terminated. The other atoms continue their histories in Step 3.

## 5.2.4 Analysis Methodology

As in any fissile system, a calculation of the long term isotopics requires a tight coupling between the neutron transport calculation and the changing isotopics. In this system, justified in part by the constant replenishment of TRU fuel, the system was modeled with a constant neutron flux, both magnitude and energy spectrum, and assumed to have a constant power level. The validity of those assumptions as well as improvements for the analysis methodology in the next phase of this study will be discussed later.

Parameter	Value	Description
P	3.7233e3 MW <sub>th</sub>	A F6 tally in MCNP is used to detect energy absorption in the reactor structure. The fusion source strength is taken to be 7.1e18 s <sup>-1</sup> .
I	2.8293e29	A total number of atoms from the initial core loading
E	100%	Assumed
C	I/100 day <sup>-1</sup>	Assumed
$t_{sim}$	20,000 days	Assumed
$t_r$	100 days	I/C

**Table 5-4: Analysis Parameters**

In addition to these assumptions, several key parameters must be assumed to initiate an MCise simulation. Those parameters are summarized in Table 5-4. The neutron flux at the initial core loading can be obtained from MCNP.

Based on these assumptions and parameters, an MCise simulation was performed with a constant neutron flux in the reactor core for 20,000 days of operation, with isotopic inventory results recorded every 20 days.

### 5.3 Activity and Heat Load Reduction Calculations

ORIGEN 2 version 2.2 was used to calculate the activity and heat load of the various results. The MCNP and MCise models were useful for determining the actual mass of actinides that were burned or fission products produced, but this data needed to be converted into an activity or heat load to see the effect of transmutation on waste reduction. ORIGEN provided this capability.

ORIGEN is typically used for burnup, depletion, and activation studies, and these capabilities were used to check the transmutation modeling results. However, ORIGEN can also be used to determine the net activity and heat load from a given distribution of isotopes. It can also track the change in isotopes and activity as a function of time. The transmutation results from the MCise model were input into ORIGEN to determine the net effectiveness of transmutation.

### 5.4 References

1. P.V. Tsvetkov & A.B. Alajo, "Assessment of System Performance Characteristics for a Complete Ultimate Incineration of Aggregated TRU Vectors with Minimum Recycling," Texas A&M University unpublished report (September, 2006).
2. P.P.H. Wilson and P. Phruksarojanakun, "Analog Monte Carlo methods for simulating isotopic inventories in complex systems." *Nucl.Sci.Eng.*, **152**, 243-255. (2006)

## 6.0 Modeling and Transmutation Results

The following sections show the results from the modeling work. The neutron energy spectrum for the In-Zinerator is shown along with the results from the pulse analysis. This spectrum was used to calculate the transmutation rates for the individual actinide isotopes. Results shown include the burnup/buildup rates, change in isotopic inventories with time, and fission product production. The key result from this work is the overall transmutation effectiveness that shows the decrease in heat load as a result of transmuting actinides into fission products. Lastly, results are presented on the effects of some of the parameters that were changed in the optimization process.

### 6.1 Neutron Spectrum Analysis

#### 6.1.1 Neutron Energy Spectrum

The average neutron energy spectrum calculated at the beginning of reactor life is shown in Figure 6-1. This spectrum is typical of a fast spectrum with the majority of neutrons between 10 keV and 1 MeV due to the high multiplication with this design—the majority of neutrons in the system are the result of a fast fission.

This spectrum was used for the MCise modeling and was believed to stay roughly the same as the isotopic ratios changed. The spectrum shape stayed about the same as a function of depth into the blanket; however, the magnitude of the spectrum changes with position in the reactor. This will be examined in more detail in future work.

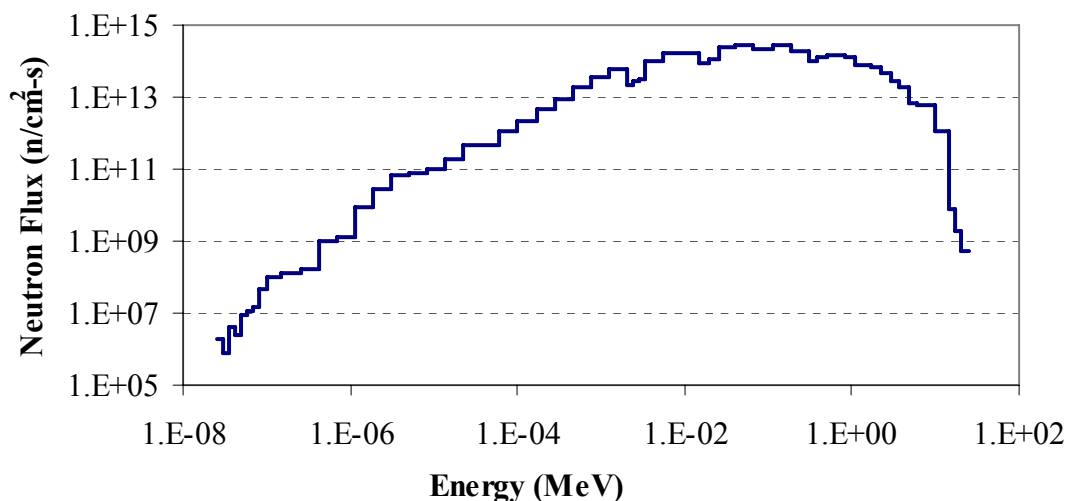


Figure 6-1: Neutron Energy Spectrum with Initial Core Loading Isotopics



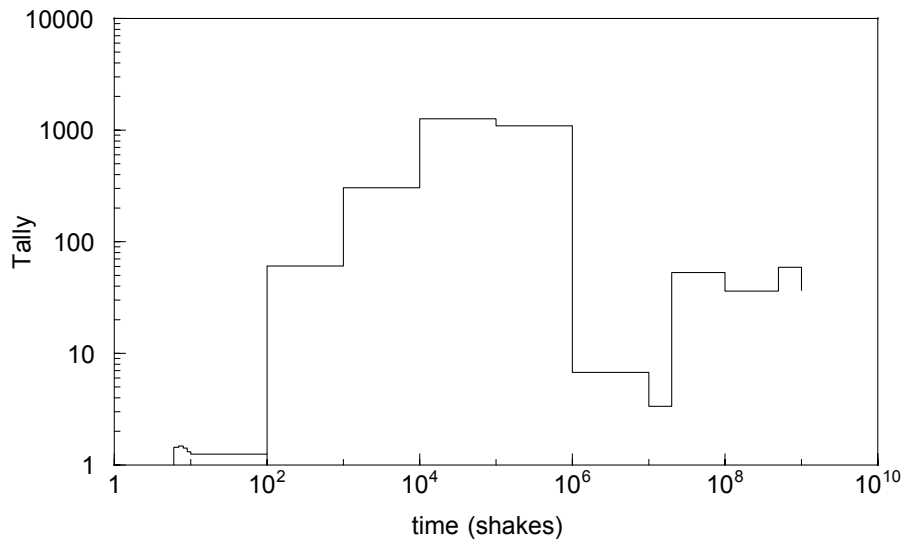
## 6.1.2 Pulse Modeling

The time dependence of the neutron pulse in the blanket was also investigated using MCNP5. The pulse is triggered by the initial fusion neutrons from the fusion pellet and results from the blanket neutron multiplication factor ( $\sim 30$ ). Because of this high factor, most of these neutrons are fast fission neutrons, not fusion neutrons; consequently, the neutron spectrum is more like a FR than a fusion reactor.

The baseline MCNP input deck was modified to include delayed neutrons and a time-dependent tally. Twenty time bins were used going out to 10 seconds. The first ten bins use a  $10^{-8}$  s time interval to examine the fusion neutrons, and the last 10 bins are divided exponentially. Delayed neutrons have typical half-lives in the range 0.2 – 55 sec, with peak yields being in the 2 – 5 sec range [1]. Hence the bin structure provides time coverage over the most probable delayed neutron deposition times.

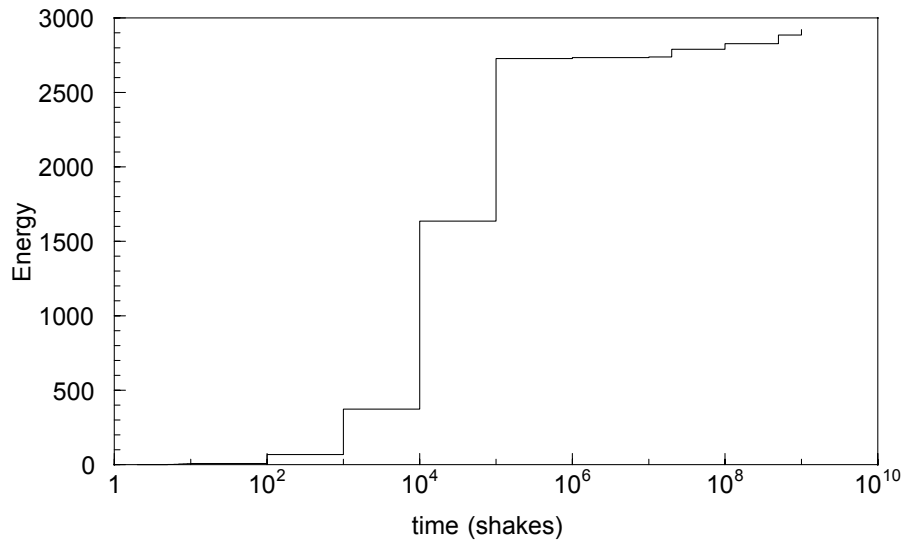
The initial neutron pulse from the fusion pellet was modeled as a square pulse of 3 ns width with mono-energetic fusion neutrons. The fusion energy spectrum was modeled as the expected spectrum coming from a Z-Pinch fusion target. The deck was run with 10,000 particle histories, which gave acceptable statistics in most bins.

Figure 6-2 shows the result plotted in units of shakes (1 shake =  $10^{-8}$  seconds). The result shows an initial delay of  $\sim 4$  shakes before the pulse begins. This delay is consistent with the velocity of fusion neutrons and the dimensions of the reactor. Three pulses can be seen: the initial pulse from the fusion neutrons, a second much broader pulse from the blanket prompt fissions, and a third smaller pulse. The third pulse centered at  $\sim 1$  s is due to the delayed neutrons. This third pulse has little effect on the total energy produced. All tallies shown are un-normalized and indicate relative height and timing only, not actual energy or power.



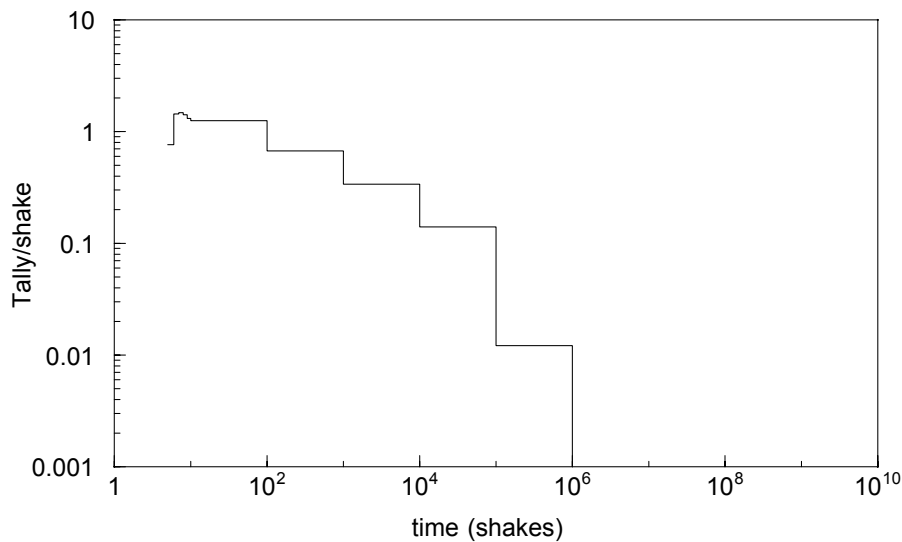
**Figure 6-2: In-Zinerator Neutron Pulse**

Figure 6-3 shows the integrated energy deposition as a function of time. The numbers on the y-axis should only be used as a relative scale and depend on the assumed fusion source used. The energy deposition curve indicates that most of the energy is deposited in the second pulse over about 10 ms, with the additional energy from the delayed neutrons being about a 5% effect.



**Figure 6-3: Relative Energy Deposition vs. Time**

An indication of the actual power levels during the pulses is shown in Figure 6-4 by plotting tallies per unit time. This graph shows that the first pulse from the fusion neutrons has the highest power, with the power tailing off from there. However, since the first pulse is very short, the energy deposition is much less than for the much longer secondary pulse.



**Figure 6-4: Power vs. Time**

The reason for the blanket neutron pulse being much wider than the initial fusion pulse is the high blanket multiplication factor – most of the neutrons are due to fission in the blanket, not

fusion, so the pulse width is more related to fast neutron lifetimes in the blanket than to the fusion neutron pulse. The energy deposition curve shown in Figure 6-3 makes it clear that the deposition is mostly from the lower, wider secondary blanket pulse.

Another point is that the delayed neutrons have little effect on either the overall multiplication factor or on the energy deposition. This is apparent from examining the MCNP multiplication results with and without delayed neutrons and from the small effect of the delayed pulse in Figure 6-2.

## Discussion

The results of the pulse modeling indicate that; (1) the energy is mostly deposited in about 10 ms after a shot, and (2) delayed neutrons do not have a significant effect on either the neutron multiplication factor or on the energy deposition (5% effect). The energy deposition time is similar to that for pulse reactors, which have been studied extensively; thermal and structural engineering considerations in pulse reactor design may have application to the blanket design.

## 6.2 Transmutation Rates

The focus of the initial modeling effort was on designing an In-Zinerator that burns all TRU species, as opposed to just specific minor actinides. Therefore the results shown in this section are for a TRU burner. Using the neutron flux generated from MCNP for the baseline In-Zinerator design, the MCISE model was used to determine the transmutation rates. This section presents the change in actinide inventory as a function of time, the burnup and buildup rates of actinides in the system, and the buildup of fission products. The final result shown is a comparison of how well the In-Zinerator reduces nuclear waste after 50 years of operation.

### 6.2.1 Actinide Inventory Change

The actinide ratios in the actinide mixture change with time due to the large number of fissions, captures, and decays. This change was tracked to determine if it would lead to an undesirable change of  $k_{\text{eff}}$  during operation. Figure 6-5 shows the change in isotopic inventories with time.

A total of 25 actinides were plotted, though a more detailed listing was tracked in the code. The plot groups elements by the same color. Pu (shown in red) makes up the majority of the actinide mixture, and most of these isotopes did not change considerably. Most of the Pu isotopes were able to reach a steady-state level after about 10-15 years. The Np isotopes (shown in purple) decrease with time but also level out after about 15 years. The Am isotopes (shown in blue) do not change significantly and level out after about 10 years. It is the higher order isotopes (Cm, Bk, and Cf) that rise more considerably with time.

The change in total activity and heat load in the blanket was examined at beginning and end of life. Figure 6-6 shows this comparison for the heat load. At the end of life, the total heat load of actinides in the In-Zinerator blanket has grown to about 2.5 times the heat load of the initial

mixture. Since the total mass of actinides in the blanket was kept constant, this increase is only due to the change in ratios with time. The heat load from Np has decreased slightly, while the heat load from Cm has increased substantially. This makes sense because Cm built up significantly during the simulation.

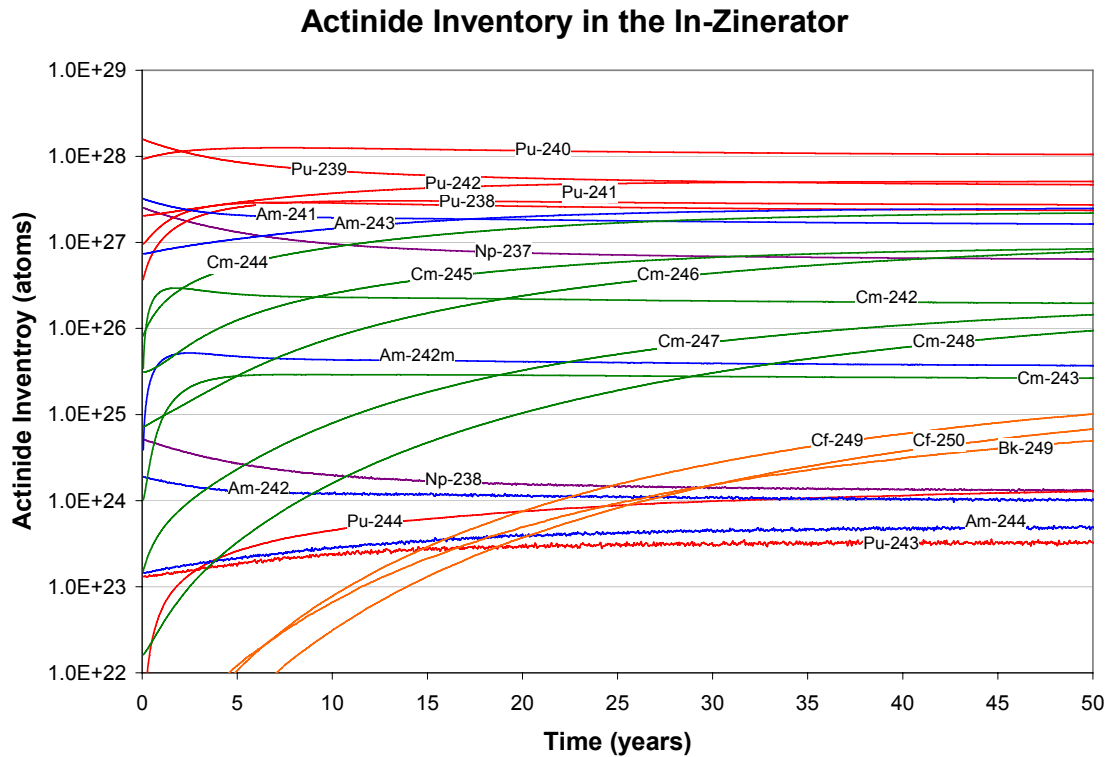


**Figure 6-5: Actinide Ratio Change in the In-Zinerator**

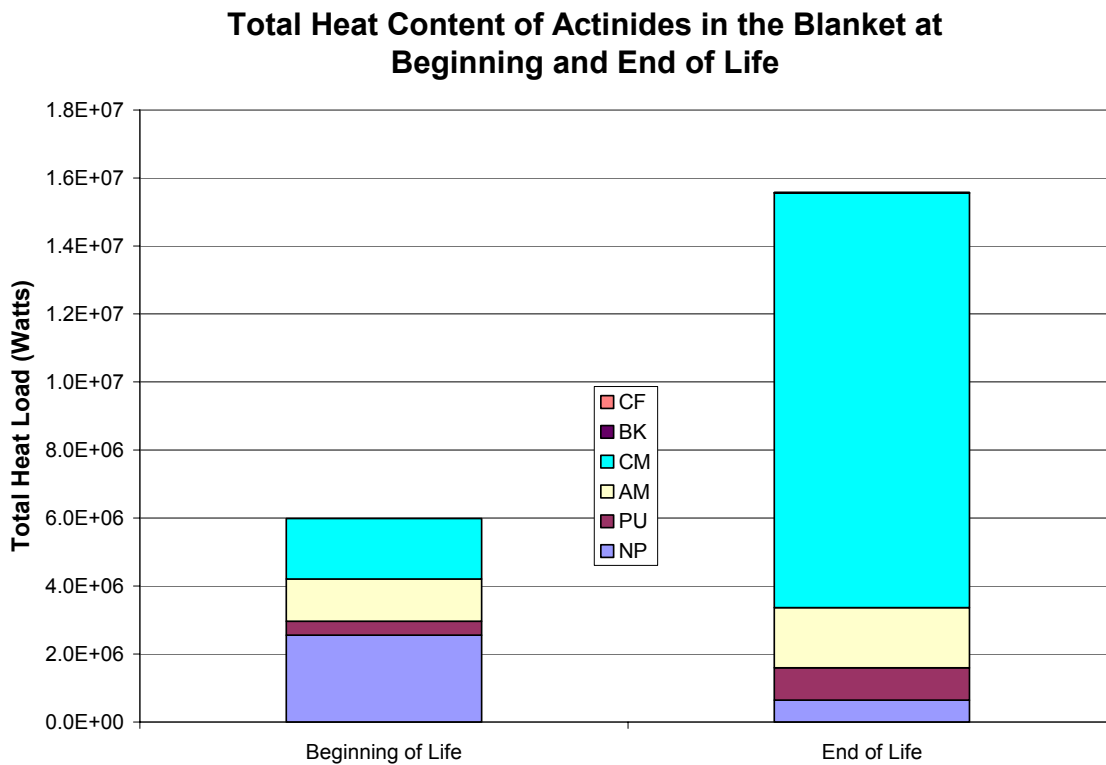


**Figure 6-6: Beginning of Life and End of Life Comparison of Blanket Radioactivity**

### 6.2.2 Actinide Burnup/Buildup Rates

The results of the MCise model were used to plot the actinide burnup rates for each isotope of interest coming from the reprocessing feed. The burnup rates change with time as the actinide ratios change. Figure 6-7 shows the burnup rates after 1 year of operation. The positive values on the graph represent a net burn, while the negative numbers indicate those isotopes that are building up.  $^{239}\text{Pu}$  strongly dominates the burnup early in the reactor life. A number of isotopes are building up at this point, though.  $^{238}\text{Pu}$ ,  $^{241}\text{Pu}$ , and the Cm isotopes are the more noticeable species. It should be noted that the energy produced from this reactor was about 3,850 MWth. This was a slightly higher energy output than what was desired, but the burnup rates scale directly as the energy changes.

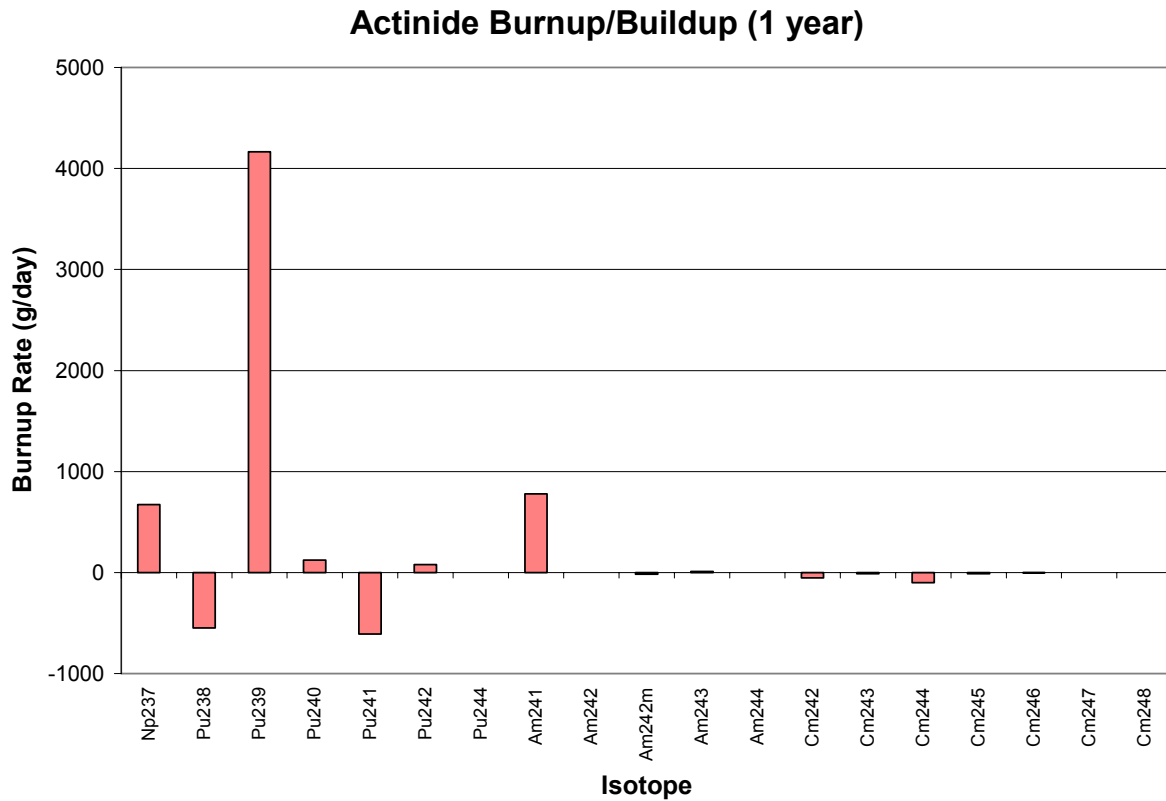


**Figure 6-7: Actinide Burnup/Buildup after 1 Year of Operation**

At the end of the reactor life, the results are considerably different as shown in Figure 6-8. At the end of 50 years,  $^{239}\text{Pu}$  and  $^{240}\text{Pu}$  dominate the burnup. Most of the isotope inventories have stabilized by this point, so even the Cm isotopes are remaining mostly constant with the exception of  $^{247}\text{Cm}$  and  $^{248}\text{Cm}$ . What is useful about this result and the graph in Figure 6-7 is that it shows that there is an initial buildup of higher order actinides in the blanket, but the levels stabilize after about 50 years. This means that continued transmutation in the fuel cycle will keep the actinide levels stable. In reality it may mean that after a transmutation reactor has to be shut down, the actinide mixture will be transferred to a new reactor.

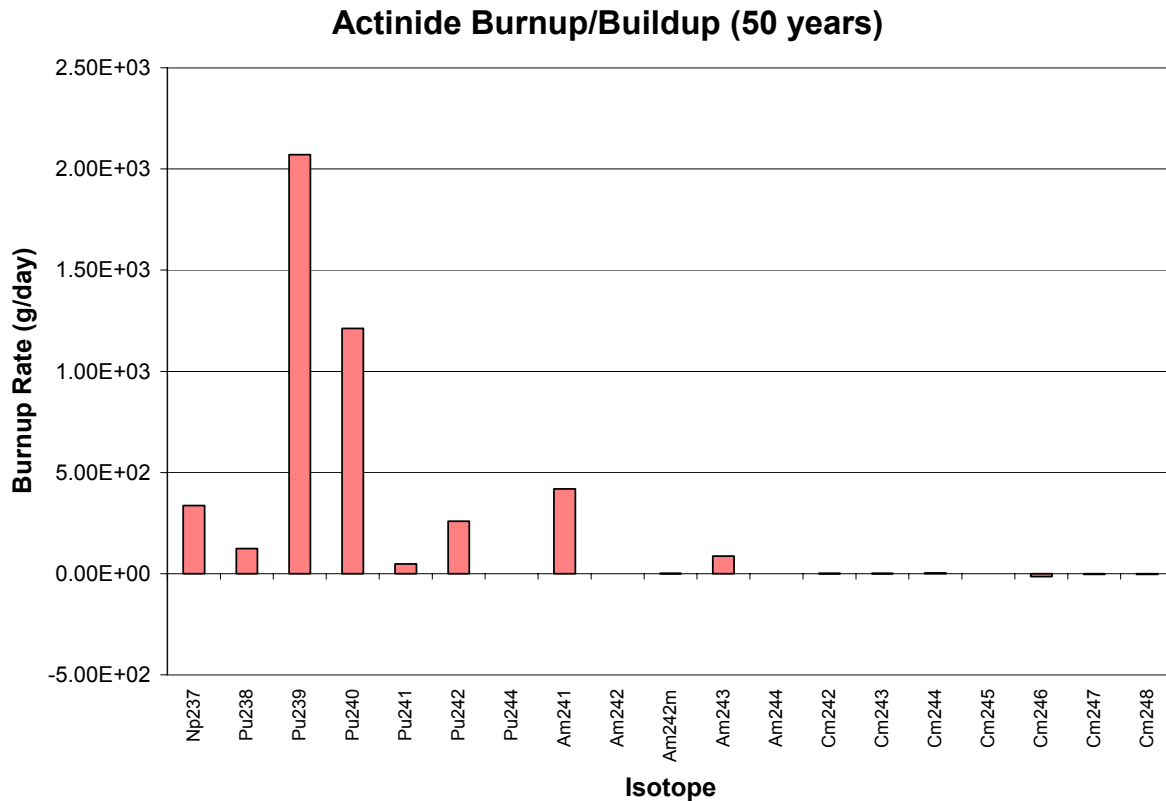


**Figure 6-8: Actinide Burnup/Buildup after 50 Years of Operation**

Summing over all of the isotopes, there was a net burn of 4,480 g/day at the beginning of life, and 4,540 g/day at the end of life at a constant power output of 3,850 MWth. If the plant was designed to produce 3,000 MWth, the net burn is about 3,500 g/day or 1,280 kg/yr. The fusion driver was assumed to be 20 MW, or a 200 MJ target fired once every ten seconds.

The effect of the neutron energy spectrum on the buildup/burnup was evaluated by changing the  $k_{\text{eff}}$  of the system. This was done to determine if more higher-energy fusion neutrons will change the transmutation substantially in the blanket. Figure 6-9 shows the result for three different  $k_{\text{eff}}$ , 0.97, 0.9, and 0.58. The fusion neutron source was increased to make up for the loss in neutrons (so the results are somewhat normalized). The burnup/buildup follows the same trend for the different multiplications, which suggests that moving towards a higher-energy fusion neutron regime may not have much of an effect on the In-Zinerator results. This is a useful result because it shows that there may be no advantage to using a higher-yield fusion target for transmutation. A low  $k_{\text{eff}}$  system would be very impractical.

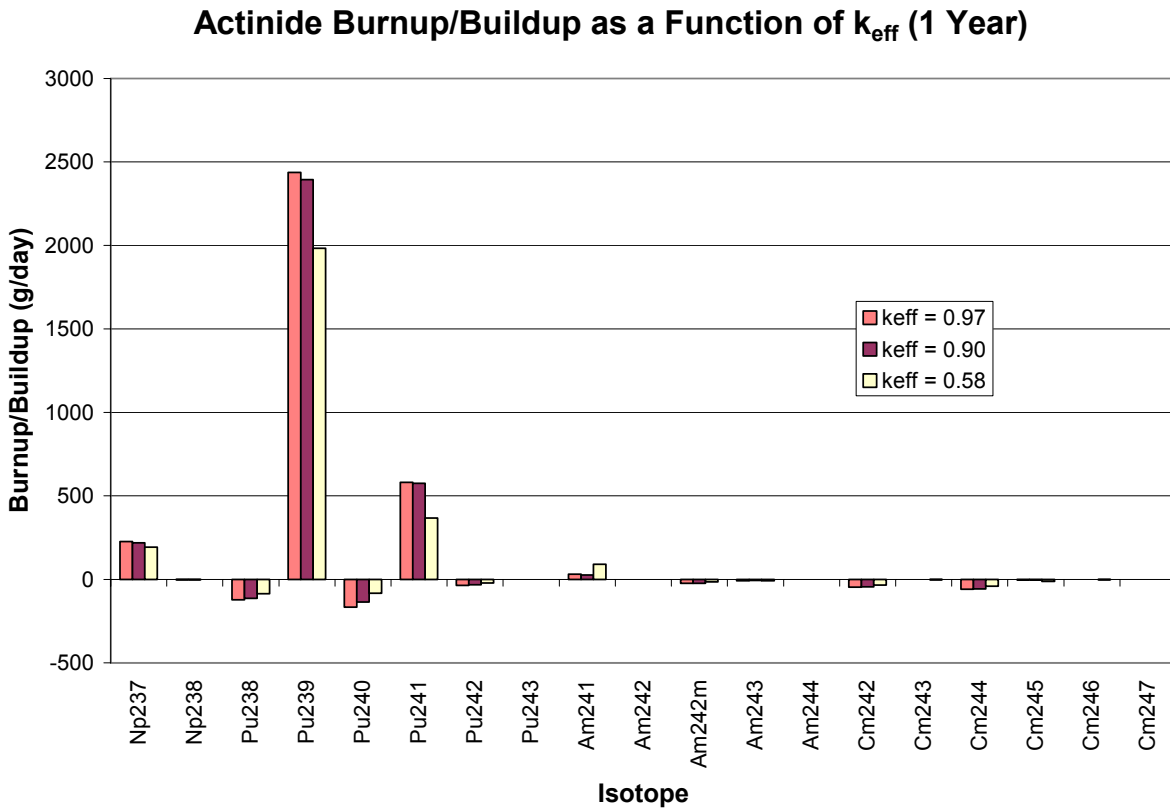


**Figure 6-9: Actinide Burnup/Buildup as a Function of  $k_{\text{eff}}$**

### 6.2.3 Fission Product Buildup

The MCise code also calculated the fission product production in the actinide blanket during the 50 year reactor life. It can be assumed that the fission product production rate is constant over the life of the reactor as long as the power output is constant. Table 6-1 shows the total fission products accumulated in moles over 50 years of run time. These values refer to the total amount of the actinides produced, and do not include the effects of decay during the 50 years of operation.

The results of this table were used to determine the amount of fission products that needed to be extracted in the extraction systems. These results were also used to determine the amounts of fission product gases that need to be removed from the actinide mixture.



Isotope	Moles	Isotope	Moles	Isotope	Moles	Isotope	Moles	Isotope	Moles	Isotope	Moles	Isotope	Moles	Isotope	Moles	Isotope	Moles
Ni 64	4.26E-13	Kr 86	2.43E+03	Nb 98m	4.44E-02	Rh 114	3.78E-08	Sn 112	8.51E-13	I 131	1.41E+03	La 148	9.23E-06	Sm 161	2.46E-05		
Ni 66	2.50E-04	Kr 87	2.26E+00	Nb 99	3.14E-02	Rh 115	8.51E-13	Sn 114	3.94E-03	I 132	2.40E+01	La 149	7.02E-08	Eu 151	2.83E+00		
Cu 67	1.92E-10	Kr 88	6.77E+00	Nb 99m	2.21E-01	Pd 102	9.36E-05	Sn 115	1.45E+01	I 132m	2.34E-01	Ce 138	1.13E-04	Eu 152	1.03E-01		
Zn 66	1.93E-03	Kr 89	1.35E-01	Nb 100	3.77E-03	Pd 103	1.21E-03	Sn 116	2.09E+00	I 133	2.96E+02	Ce 139	1.16E-01	Eu 152m	2.00E-03		
Zn 67	1.43E-03	Kr 90	2.33E-02	Nb 100m	7.17E-04	Pd 104	1.08E+02	Sn 117	1.63E+02	I 133m	2.78E-03	Ce 140	1.59E+04	Eu 153	1.74E+03		
Zn 68	7.60E-03	Kr 91	4.51E-03	Nb 101	2.21E-02	Pd 105	2.02E+04	Sn 117m	7.79E-02	I 134	1.41E+01	Ce 141	7.64E+03	Eu 154	6.81E+01		
Zn 70	6.05E-02	Kr 92	9.15E-07	Nb 102	4.93E-03	Pd 106	1.92E+03	Sn 118	1.28E+02	I 134m	1.26E-01	Ce 142	1.73E+04	Eu 154m	4.29E-03		
Zn 71m	4.26E-13	Kr 93	1.15E-04	Nb 102m	4.81E-03	Pd 107	1.48E+04	Sn 119	1.18E+02	I 135	9.37E+01	Ce 143	3.17E+02	Eu 155	8.41E+02		
Zn 72	8.05E-03	Rb 83	6.84E-04	Nb 103	5.04E-04	Pd 107m	9.26E-04	Sn 119m	5.19E-01	I 136	1.20E-01	Ce 144	1.27E+04	Eu 156	1.45E+02		
Ga 69	2.21E-02	Rb 84	5.88E-03	Nb 104	6.48E-03	Pd 108	1.16E+04	Sn 120	1.06E+02	I 136m	4.64E-02	Ce 145	3.32E-01	Eu 157	4.12E+00		
Ga 71	1.23E-01	Rb 85	1.32E+03	Nb 104m	1.70E-10	Pd 109	6.67E+01	Sn 121	1.63E+00	I 137	4.44E-02	Ce 146	1.25E+00	Eu 158	1.54E-01		
Ga 72	8.87E-04	Rb 86	2.11E+00	Nb 105	1.97E-03	Pd 109m	3.68E-06	Sn 121m	7.44E+00	I 138	8.29E-03	Ce 147	8.56E-02	Eu 159	2.43E-02		
Ga 73	2.61E-03	Rb 87	3.11E+03	Nb 106	9.26E-04	Pd 110	4.85E+03	Sn 122	1.32E+02	I 139	2.50E-03	Ce 148	4.40E-02	Eu 160	4.21E-04		
Ga 74	1.69E-10	Rb 88	6.97E-01	Mo 94	1.21E-02	Pd 111	6.38E-01	Sn 123	2.15E+01	I 140	6.65E-12	Ce 149	3.31E-03	Eu 161	2.29E-04		
Ga 75	1.06E-13	Rb 89	7.57E-01	Mo 95	2.72E+03	Pd 111m	1.57E-01	Sn 123m	3.68E-02	Xe 126	2.68E-03	Ce 150	9.84E-04	Eu 162	5.34E-04		
Ge 70	4.73E-09	Rb 90	1.21E-01	Mo 96	9.57E+01	Pd 112	1.78E+01	Sn 124	2.12E+02	Xe 128	1.02E+01	Ce 151	4.03E-05	Gd 152	3.01E-02		
Ge 72	2.62E-01	Rb 90m	8.91E-02	Mo 97	1.77E+04	Pd 113	1.17E-02	Sn 125	1.79E+01	Xe 129	4.24E-02	Ce 152	9.47E-04	Gd 153	3.09E-05		
Ge 73	6.64E-01	Rb 91	7.45E-02	Mo 98	1.94E+04	Pd 114	8.30E-03	Sn 125m	2.15E-02	Xe 129m	4.62E-04	Ce 153	3.09E-05	Gd 154	5.04E-01		
Ge 74	1.40E+00	Rb 92	7.47E-03	Mo 99	8.41E+02	Pd 115	1.03E-03	Sn 126	5.28E+02	Xe 130	3.08E+01	Ce 141	1.09E+04	Gd 155	1.69E+01		
Ge 75	2.32E-03	Rb 93	3.96E-03	Mo 100	2.30E+04	Pd 116	2.69E-04	Sn 127	1.08E+00	Xe 131	1.07E+04	Pr 142	5.83E-01	Gd 156	4.97E+02		
Ge 76	7.34E+00	Rb 94	9.51E-04	Mo 101	3.14E+00	Pd 117	4.26E-13	Sn 127m	1.35E-02	Xe 131m	2.58E+01	Pr 142m	2.19E-03	Gd 157	4.52E+02		
Ge 77	5.60E-02	Rb 96	2.46E-05	Mo 102	2.52E+00	Pd 118	2.86E-05	Sn 128	1.10E+00	Xe 132	1.69E+04	Pr 143	3.11E+03	Gd 158	3.20E+02		
Ge 77m	1.19E-08	Sr 84	2.81E-04	Mo 103	2.78E-01	Ag 107	1.15E-03	Sn 128m	1.21E-03	Xe 133	1.81E+03	Pr 144	5.78E-01	Gd 159	2.18E+00		
Ge 78	5.70E-02	Sr 85	1.82E-09	Mo 104	1.88E-01	Ag 108m	2.77E-02	Sn 129	5.19E-02	Xe 133m	2.36E+01	Pr 144m	9.90E-03	Gd 160	1.06E+02		
Ge 79	3.10E-05	Sr 86	3.31E+00	Mo 105	1.01E-01	Ag 109	7.91E-03	Sn 129m	6.73E-02	Xe 134	2.76E+04	Pr 145	4.03E+01	Gd 161	1.68E-03		
Ge 79m	3.94E-06	Sr 87	6.36E-02	Mo 106	8.41E-03	Ag 109m	6.45E-02	Sn 130	6.62E-02	Xe 135	1.44E+02	Pr 146	2.27E+00	Gd 162	6.87E-04		
Ge 80	1.03E-03	Sr 87m	4.26E-13	Mo 107	4.45E-03	Ag 110	3.96E-06	Sn 130m	3.06E-02	Xe 135m	8.53E-01	Pr 147	1.08E+00	Gd 163	2.57E-04		
Ge 81	1.19E-08	Sr 88	4.13E+03	Mo 108	1.01E-03	Ag 110m	5.60E+00	Sn 131	1.11E-02	Xe 136	2.48E+04	Pr 148	1.26E-01	Gd 164	9.87E-04		
Ge 82	4.26E-13	Sr 89	2.81E+03	Tc 97	4.26E-13	Ag 111	2.76E+02	Sn 131m	7.99E-03	Xe 137	8.14E-01	Pr 148m	1.11E-02	Gd 165	4.59E-19		
As 75	3.30E+00	Sr 90	6.46E+03	Tc 98	1.74E-01	Ag 111m	2.16E-02	Sn 132	1.00E-02	Xe 138	2.81E+00	Pr 149	1.34E-01	Tb 157	2.45E-06		
As 76	1.55E-03	Sr 91	4.34E+01	Tc 99	2.02E+04	Ag 112	2.75E+00	Sn 133	3.85E-05	Xe 139	1.06E-01	Pr 150	6.90E-03	Tb 158	1.01E-03		
As 77	4.04E-01	Sr 92	1.48E+01	Tc 99m	6.75E+01	Ag 113	2.90E+00	Sb 121	1.05E+02	Xe 140	9.01E-03	Pr 151	8.78E-03	Tb 159	1.76E+02		
As 78	5.93E-02	Sr 93	8.38E-01	Tc 100	1.64E-04	Ag 113m	4.25E-03	Sb 122	6.36E-02	Xe 141	1.81E-03	Pr 152	1.34E-03	Tb 160	4.40E+00		
As 79	6.14E-03	Sr 94	1.42E-01	Tc 101	3.07E+00	Ag 114	5.29E-04	Sb 123	1.18E+02	Xe 142	1.19E-04	Pr 153	3.46E-04	Tb 161	5.90E+00		
As 80	1.37E-04	Sr 95	4.75E-02	Tc 102	1.23E-02	Ag 115	3.53E-02	Sb 124	5.75E-01	Cs 131	2.60E-08	Nd 142	1.96E+01	Tb 162	2.38E-03		
As 81	2.40E-03	Sr 96	1.41E-04	Tc 102m	3.81E-03	Ag 115m	9.34E-04	Sb 124m	4.26E-13	Cs 132	4.03E-02	Nd 143	1.26E+04	Tb 162m	4.45E-04		
As 82	4.56E-04	Sr 98	1.95E-04	Tc 103	1.94E-01	Ag 116	5.96E-03	Sb 125	2.61E+02	Cs 133	2.18E+04	Nd 144	1.71E-03	Tb 163	3.34E-03		
As 82m	3.62E-04	Y 87	4.26E-13	Tc 104	4.30E+00	Ag 116m	1.12E-04	Sb 126	7.39E-01	Cs 134	1.72E+02	Nd 145	1.11E+04	Tb 164	7.73E-05		
As 83	4.05E-04	Y 88	2.42E-03	Tc 105	1.61E+00	Ag 117	7.59E-04	Sb 126m	1.74E-03	Cs 134m	4.72E-02	Nd 146	9.47E+03	Tb 165	7.18E-06		
As 84	9.28E-04	Y 89	2.37E+03	Tc 106	1.05E-01	Ag 117m	5.00E-09	Sb 127	7.66E+01	Cs 135	2.61E+04	Nd 147	1.22E+03	Tb 166	1.89E-10		
As 85	8.51E-13	Y 90	1.79E+00	Tc 107	4.97E-02	Ag 118	1.46E-09	Sb 128	9.74E-01	Cs 135m	7.14E-03	Nd 148	6.54E+03	Tb 167	4.26E-13		
Se 76	3.46E-02	Y 91	4.45E+03	Tc 108	9.73E-03	Ag 119	3.76E-08	Sb 128m	2.09E-01	Cs 136	5.53E+01	Nd 149	5.26E+00	Dy 159	9.39E-08		
Se 77	1.78E+01	Y 91m	2.23E+00	Tc 109	1.47E-04	Cd 108	2.82E-02	Sb 129	1.10E+01	Cs 136m	4.82E-07	Nd 150	4.05E+03	Dy 160	1.52E+01		
Se 78	5.39E+01	Y 92	1.96E+01	Tc 110	9.39E-08	Cd 109	5.07E-05	Sb 130	1.31E+00	Cs 137	2.35E+04	Nd 151	3.61E-01	Dy 161	5.06E+01		
Se 79	9.98E+01	Y 93	7.12E+01	Ru 99	6.76E-01	Cd 110	1.03E+02	Sb 130m	2.06E-01	Cs 138	7.10E+00	Nd 152	2.47E-01	Dy 162	2.98E+01		
Se 79m	6.46E-03	Y 93m	2.76E-04	Ru 100	2.43E+02	Cd 111	2.29E+03	Sb 131	2.17E+00	Cs 138m	3.84E-02	Nd 153	1.55E-02	Dy 163	1.77E+01		
Se 80	2.11E+02	Y 94	2.51E+00	Ru 101	2.15E+04	Cd 111m	8.27E-04	Sb 132	2.38E-01	Cs 139	1.93E+00	Nd 154	6.31E-03	Dy 164	8.23E+00		
Se 81	8.17E-02	Y 95	1.61E+00	Ru 102	2.27E+04	Cd 112	1.44E+03	Sb 132m	1.29E-01	Cs 140	1.74E-01	Nd 155	2.09E-03	Dy 165	5.25E-03		
Se 81m	2.76E-02	Y 96	8.66E-03	Ru 103	1.12E+04	Cd 113	9.14E+02	Sb 133	1.65E-01	Cs 141	5.29E-02	Nd 156	4.03E-04	Dy 165m	1.21E-04		
Se 82	6.05E-02	Y 96m	1.12E-02	Ru 104	2.32E+04	Cd 113m	1.83E-01	Sb 134	3.76E-08	Cs 142	3.30E-03	Pm 145	2.94E-06	Dy 166	6.13E-02		
Se 83	1.06E-01	Y 97	3.22E-03	Ru 105	5.53E+01	Cd 114	5.43E+02	Sb 134m	3.66E-03	Cs 143	4.22E-04	Pm 146	9.18E-02	Dy 167	1.10E-07		
Se 83m	1.69E-03	Y 97m	3.75E-04	Ru 106	1.69E+04	Cd 115	9.74E+00	Sb 135	1.12E-04	Ba 132	7.25E-04	Pm 147	6.18E+03	Dy 168	3.76E-07		
Se 84	4.69E-02	Y 98	2.07E-04	Ru 107	5.58E-01	Cd 115m	6.58E+00	Te 122	7.80E-01	Ba 133	9.27E-08	Pm 148	1.15E+01	Ho 163	3.18E-04		
Se 85	5.29E-03	Y 98m	4.59E-04	Ru 108	5.35E-01	Cd 116	2.06E+02	Te 123	1.09E-03	Ba 134	4.95E+00	Pm 148m	3.93E+01	Ho 165	3.35E+00		
Se 85.1	1.51E-03	Y 99	1.79E-03	Ru 109	2.38E-02	Cd 117	2.11E-01	Te 123m	3.91E-03	Ba 135	2.57E-02	Pm 149	1.60E+02	Ho 166	2.81E-02		
Se 85m	2.07E-03	Y 100	2.46E-05	Ru 109m	8.25E-03	Cd 117m	4.98E-02	Te 124	4.15E-01	Ba 135m	9.20E-04	Pm 150	2.69E-02	Ho 166m	8.75E-03		
Se 87	3.88E-04	Y 101	2.20E-04	Ru 110	1.10E-02	Cd 118	7.63E-02	Te 125	7.39E+00	Ba 136	2.15E+02	Pm 151	5.22E+01	Ho 167	5.52E-04		
Se 88	1.93E-04	Zr 90	2.14E+01	Ru 111	5.57E-04	Cd 119	1.79E-03	Te 125m	1.34E+00	Ba 137	8.68E+01	Pm 152	9.52E-02	Ho 168	6.58E-07		
Br 79	3.87E-04	Zr 91	3.14E+03	Ru 112	2.60E-05	Cd 119m	9.05E-05	Te 126	8.08E+00	Ba 137m	2.62E-03	Pm 152m1	4.04E-03	Ho 169	4.26E-13		
Br 80m	8.51E-13	Zr 92	9.29E+03	Ru 113	6.99E-05	Cd 120	6.04E-04	Te 127	6.96E+00	Ba 138	2.28E+04	Pm 152m2	4.21E-03	Ho 170	4.26E-13		
Br 81	4.28E+02	Zr 93	1.18E+04	Ru 114	3.76E-07	Cd 121	1.12E-04	Te 127m	1.70E+02	Ba 139	1.80E+01	Pm 153	1.03E-01	Er 164	4.94E-07		
Br 82	1.67E-01	Zr 94	1.34E+04	Rh 102	1.14E-02	Cd 121m	4.26E-13	Te 128	2.15E+03	Ba 140	3.64E+03	Pm 154	2.40E-02	Er 166	1.44E+00		
Br 82m	2.45E-04	Zr 95	9.39E+03	Rh 102m	2.05E-02	In 113											

## 6.2.4 Net Transmutation Effectiveness

The most important result from this work is the net transmutation effectiveness of using the In-Zinerator. The purpose of the In-Zinerator is to transmute long-lived actinides into short-lived fission products. To do an accurate comparison of the effectiveness, the total heat load of TRU in spent fuel was compared to the total heat load of the fission products that were produced after running the In-Zinerator.

The data from the MCise results was used to show this effect. First the data was used to determine the total amount and isotopic distribution of TRU that would be transmuted over 50 years of In-Zinerator operation. Then the fission product yields were examined to determine the total amount of fission products produced over 50 years.

This isotopic data was then input into ORIGEN2 to determine the activity and thermal powers as a function of time. Note that ORIGEN2 was not used to determine burnups, it was only used to decay the isotopes out in time and calculate the activity and thermal powers.

Figure 6-10 shows the final heat load result comparing un-irradiated TRU to the byproducts of running the In-Zinerator. The blue line represents the heat production of 64 MT of TRU from spent LWR fuel if nothing is done to it. 64 MT is the total amount of TRU that is transmuted in the baseline In-Zinerator design in 50 years assuming a full capacity factor at 3,000 MWth. The green line shows the heat production for the sum of the fission products produced over 50 years assuming Cs and Sr are removed from the fission product waste. The removal of Cs/Sr from the fission product waste makes a big difference just like with LWR spent fuel. This was assumed to have alignment with the current GNEP proposed fuel cycle.

The initial FP byproducts from running the In-Zinerator will be substantially hotter than if the TRU was left alone, but after about 3 years of cooling the by-products reach the cross-over point. This is expected since transmutation of TRU turns a long-lived isotope into more active, short-lived fission products. After just 10 years of cooling the heat load of the by-products is decreased by a factor of 10, and after 50 years the total heat load of the by-products decreases by a factor of 500, a substantial savings.

This important result verifies the theory behind the purposes of transmutation. The effect of transmutation can be seen after only a few years, and significant reductions in heat load are seen beyond 10 years. When only the fission products from LWR fuel along with these burned fission products from the In-Zinerator are placed in the repository, the repository capacity could increase dramatically.

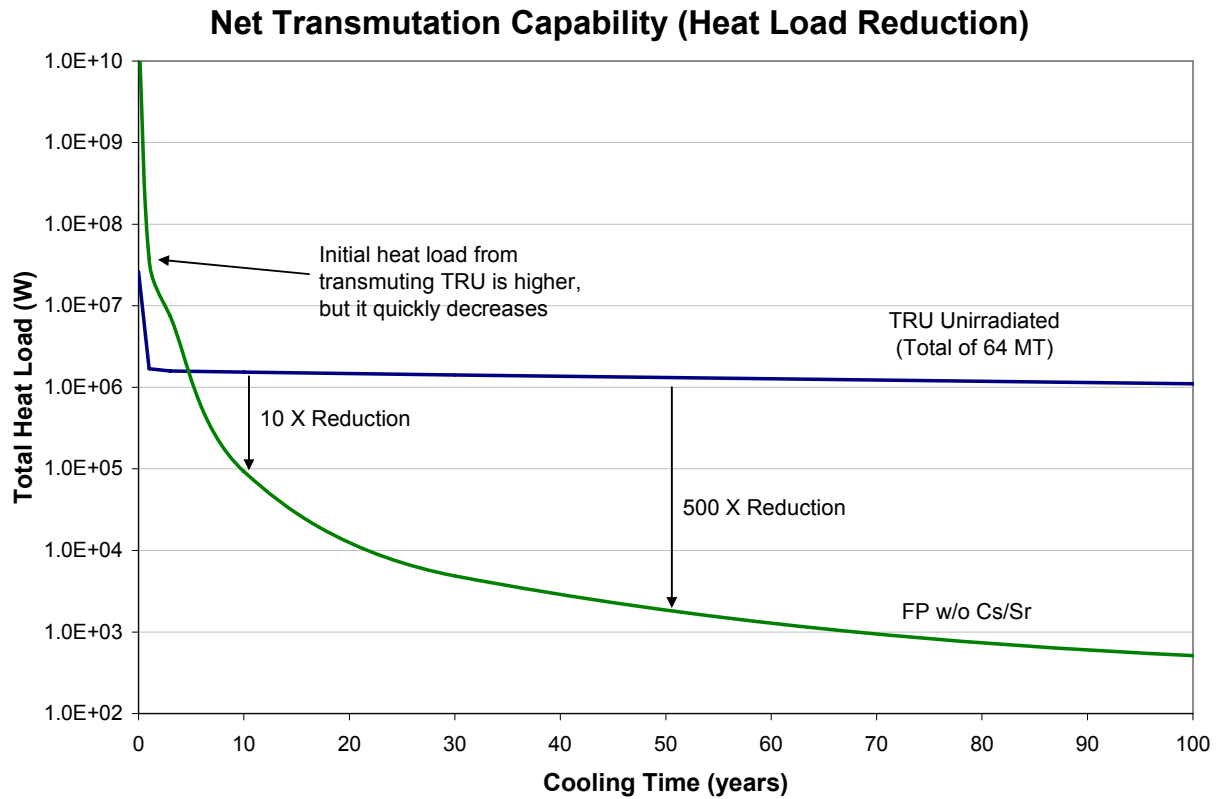


**Figure 6-10: In-Zinerator Net Transmutation Capability**

The previous figure did not show the effect of buildup TRU that is produced in the In-Zinerator during operation. However, as described earlier, the buildup TRU reaches a saturation point during the lifetime of the In-Zinerator, and then most of the isotopes stabilize. After the stabilization point, the In-Zinerator does have the effect shown in the previous figure—it turns actinides into fission products.

Figure 6-11 shows a similar plot of the transmutation effectiveness out to 1,000 years. On this plot, the blue line again represents unburned TRU. The dotted pink line represents the sum of the buildup TRU that is produced over the life of the reactor and all the fission products. The dotted green line shows the sum of all fission products (with Cs/Sr), and the solid green line shows the fission products without Cs/Sr. The purpose of showing this information is to give a more complete picture of how the device operates. Some actinides do buildup over the life of the reactor, and Cs/Sr removal will be an important part of the disposal of these fission products.

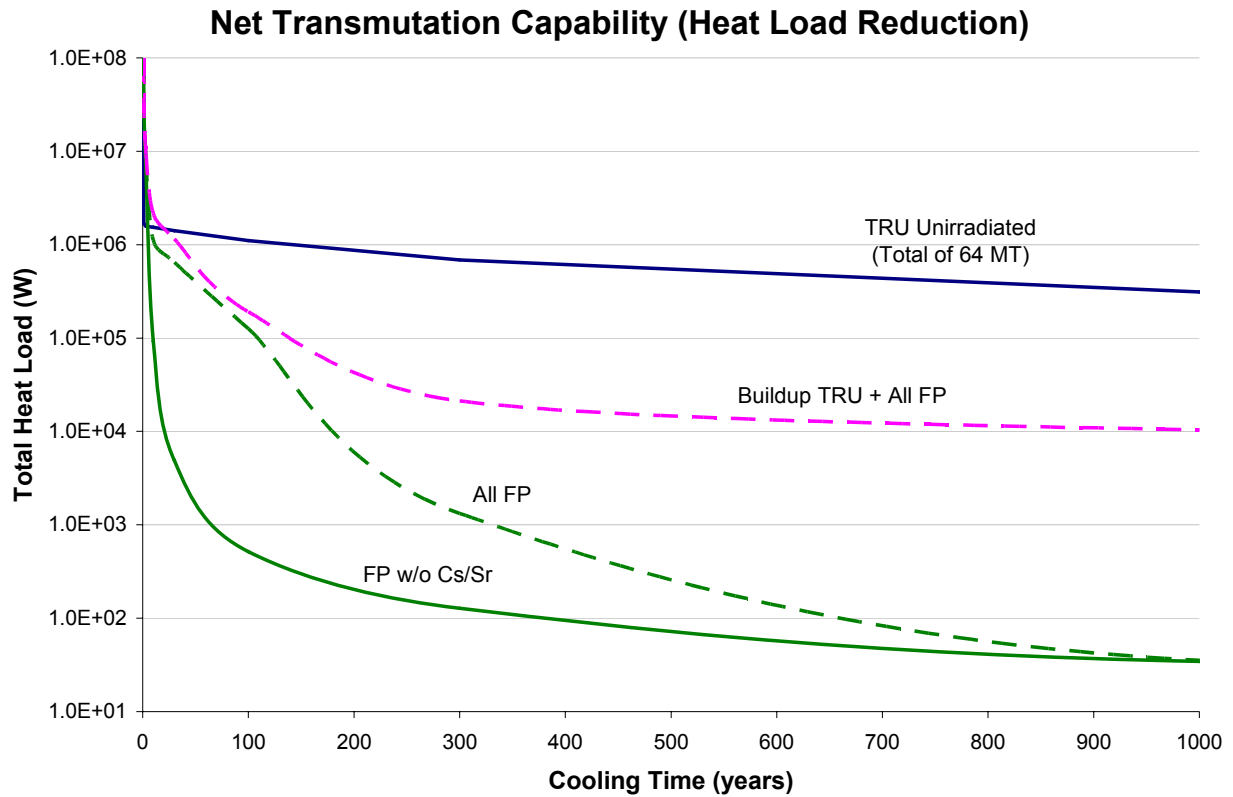


**Figure 6-11: Effect of TRU Buildup and Cs/Sr**

The effectiveness of transmutation is only possible if transmutation technologies are continuously used across the entire fuel cycle for an indefinite amount of time. If a transmutation facility comes on line and then gets shut down after 10-20 years due to political changes or external world events, it is likely that the facility will have had little or no effect on long term radionuclide inventories.

### 6.3 Design Optimization Variables

The In-Zinerator design and operation is sensitive to a number of parameters including chamber geometry, first wall thickness, reflector thickness,  $^6\text{Li}$  enrichment, and actinide ratio change. There is not much control over the actinide ratio change with time, but after a baseline chamber design is chosen, the additional parameters are “knobs” that can be tweaked to optimize the energy multiplication,  $k_{\text{eff}}$ , and tritium breeding ratio. This section present results that give some insight into the sensitivity of these parameters on the In-Zinerator operation.

### 6.3.1 $^6\text{Li}$ Enrichment

The energy multiplication and  $k_{\text{eff}}$  were calculated as a function of time and shown in Figures 6-12 and 6-13 respectively. Error bars in the figures represent  $1\sigma$  statistical errors. These were calculated using MCNP with material compositions based on the results of MCise. Original results (shown in the blue lines on both graphs) based on a replenishment of only TRU did not take into account the substantial depletion of  $^6\text{Li}$  during the operation, whereas the red lines show the effect of maintaining a constant  $^6\text{Li}$  inventory. Due to the actinide ratio change, the energy multiplication and  $k_{\text{eff}}$  drop off initially with time but then level out if the  $^6\text{Li}$  inventory is maintained. If the  $^6\text{Li}$  is depleted, the multiplication and  $k_{\text{eff}}$  increase gradually with time. This result demonstrates the sensitivity that the In-Zinerator has on  $^6\text{Li}$  enrichment.

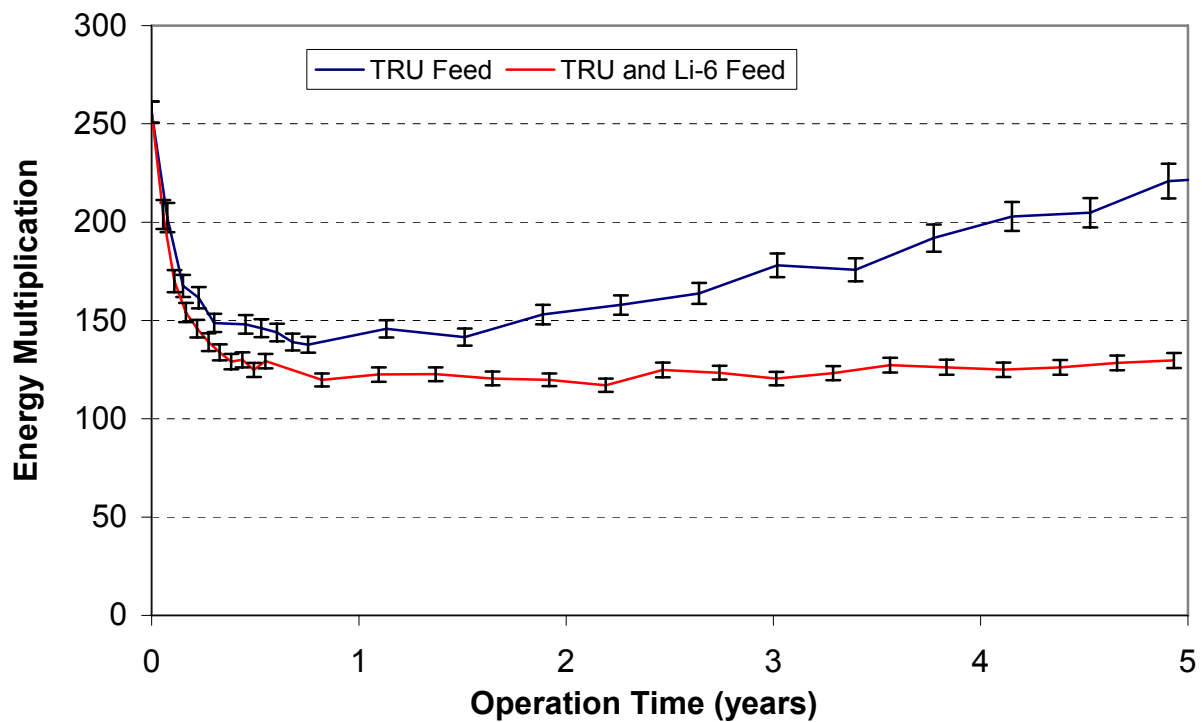
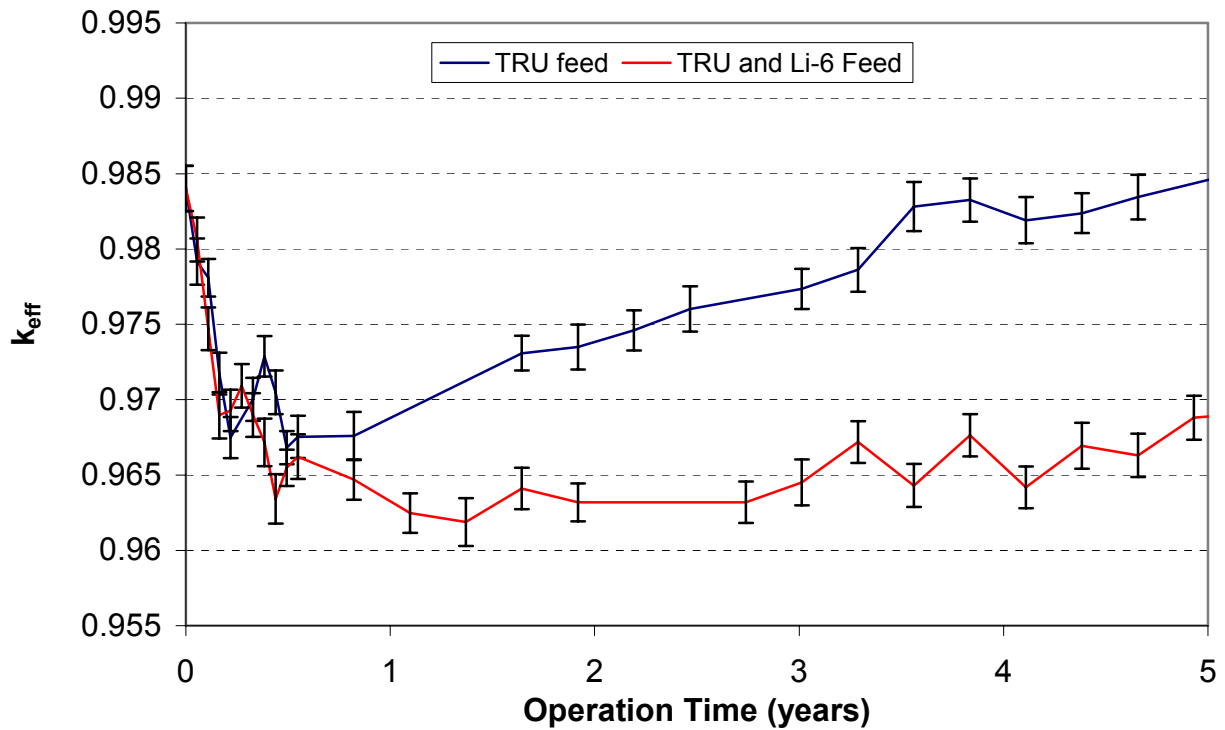
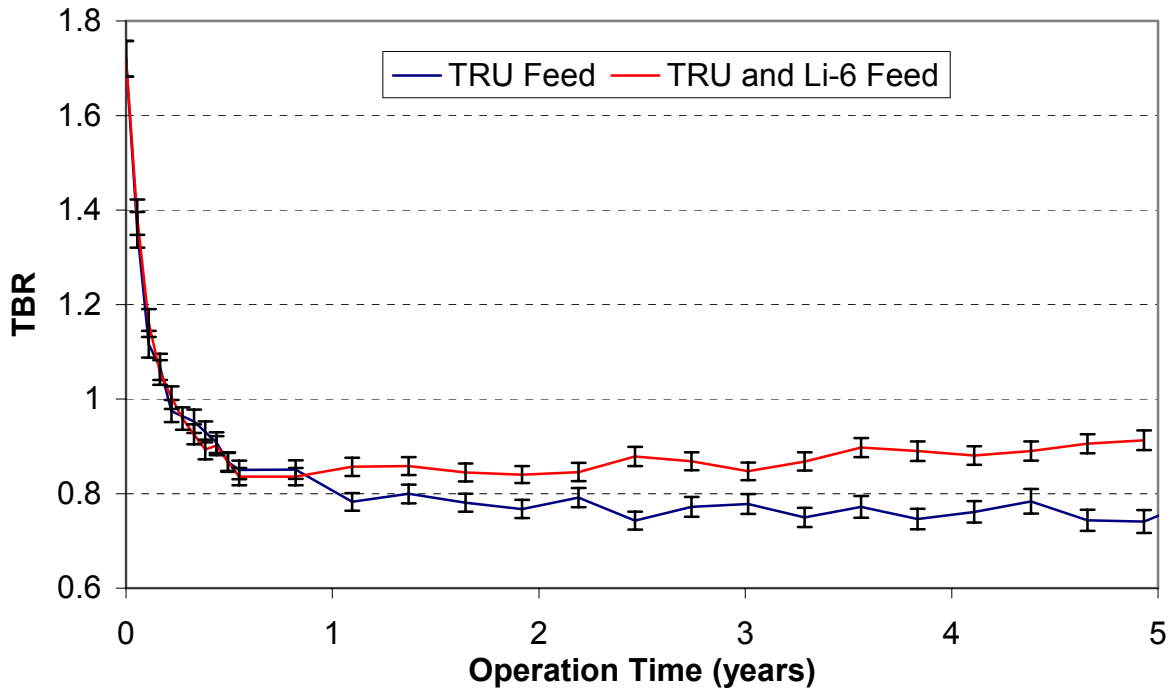


Figure 6-12: Energy Multiplication vs. Time with and without  $^6\text{Li}$  Replenishment



**Figure 6-13:  $k_{eff}$  vs. Time with and without  $^6\text{Li}$  Replenishment**

The tritium breeding ratio (TBR) as a function of time is shown with and without  $^6\text{Li}$  replenishment in Figure 6-14. Note that the TBR drops off quickly as multiplication drops off as expected. For this design the TBR leveled off below 1, but the goal was 1.2, so the design will require some optimization or control during operation.



**Figure 6-14: Tritium Breeding Ratio (TBR) with and without Replenishment of  $^6\text{Li}$**

These results demonstrate that reactivity control mechanism will be necessary to ensure a constant energy multiplication over the life of the system. If such a mechanism were to preserve the neutron energy spectrum and magnitude, then the modeling assumptions made here would continue to be valid. However, preliminary results show that this may not be the case, requiring a tighter coupling between the neutronics, isotopics, and reactivity configuration of the system.

### 6.3.2 First Wall Thickness

There are a number of uncertainties about the final design requirements for the first wall thickness due to concerns over the interaction with the RTL debris. The RTL debris may require a thicker first wall, or it may require a shield in front of the first wall that will add to the overall neutron attenuation.

Figure 6-15 shows the results of varying first wall thickness on the baseline In-Zinerator design. Hasetlloy-N was used as the material for the first wall, and MCNP was used to perform this study. The baseline design at 5 cm has a  $k_{\text{eff}}$  just below 1, but even increasing the thickness to 10 cm results in a  $k_{\text{eff}}$  of 0.98. Therefore it does not seem that first wall thickness has a major impact on the operation of the device up to 10 cm. These small variations in  $k_{\text{eff}}$  can be made up for with slight geometry modifications or  $^6\text{Li}$  enrichment.

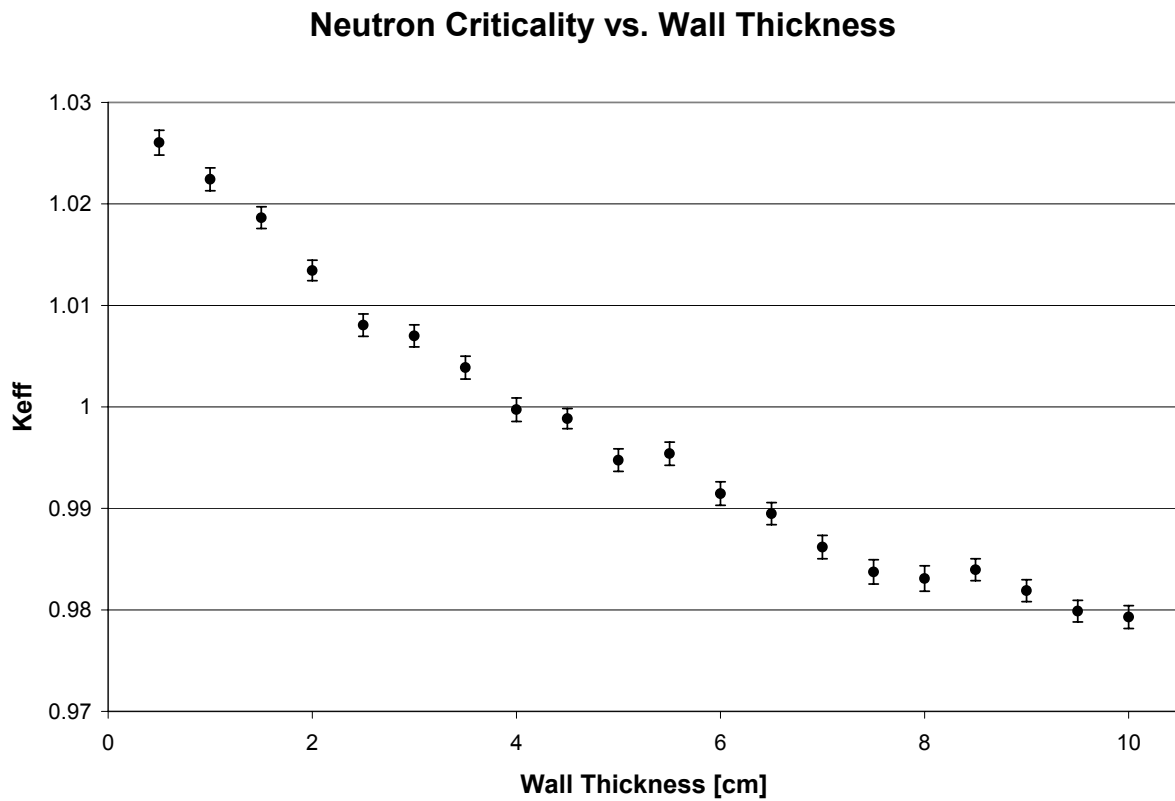


**Figure 6-15: Effect of First Wall Thickness on Criticality**

## 6.4 References

1. J. R. Lamarsh, *Nuclear Reactor Theory*, Addison-Wesley Publishing (1966).



## 7.0 Conclusion

The baseline In-Zinerator design produces 3,000 MWth while burning up 1,280 kg of TRU per year. The required Z-Pinch target yield is 200 MJ if the target is fired once every 10 seconds for a  $k_{\text{eff}}$  near 0.97. The actinide ratios do change during operation of the In-Zinerator, but the change results in a lowering of the  $k_{\text{eff}}$  with time. Increased reflectivity will be needed to maintain a constant power level. A buildup of some higher-order actinides occurs in the blanket, but after about 30 years the actinide levels stabilize. The buildup results in an increase in the total heat content of the blanket inventory by a factor of 2.5 over 50 years of operation.

The In-Zinerator effectively transmutes long-lived actinides into fission products with much shorter half-lives. When TRU is transmuted, the resulting fission product heat load is reduced by a factor of 10 after 10 years and a factor of 500 after 50 years. Thus, transmutation can effectively increase the repository capacity based on thermal limits. However, the effect of packing more fission product waste into the repository has not been examined yet.

The current LWR fleet produces on the order of 24,600 kg of TRU per year, so about 20 In-Zinerators would be required to burn up all of the TRU at the rate of production. Because In-Zinerators have a better support ratio (as compared to FRs), they may have an economic advantage, even if the stand-alone cost is higher. However, whether transmutation is accomplished with FRs or In-Zinerators, reprocessing and transmutation technologies will add at least 2 mil/kWh to the cost of nuclear power. It will be up to policy-makers to decide if this cost should be legislated in order to help clean-up nuclear waste.

As compared to the Z-Pinch Power Plant, there are some key differences of the transmutation application. The fusion yield requirement is over an order of magnitude lower, with the requirement of only one chamber at a 0.1 Hz repetition rate. In addition, the transmutation of actinides provides Z-Pinch with a useful application while at the same time producing power and gaining valuable experience on developing fusion energy systems.

A sub-critical blanket driven by fusion makes the burning of actinides safer than a fast reactor without the possibility of a prompt-critical excursion. In addition, a sub-critical configuration allows unique actinide mixtures to be burned safely without the need to worry about reactor control issues. This gives the In-Zinerator flexibility to fit into any advanced fuel cycle.

The fluid fuel form allows for the actinides to be continuously reprocessed and prevents the need for costly fuel fabrication. It eliminates the multiple handling and transportation of very hot reactor fuel back and forth through the fuel cycle. Fluid fuel also eliminates the production of a large amount of cladding and hulls waste that solid fuel will produce.

Compared to other fusion designs, Z-Pinch may offer the most compact fusion source due to the unique power delivery system. The solid transmission line comes in from the top of the reactor, which means that the sides and bottom are left clear for installation of a blanket. Unique shock mitigating techniques using aerosols will be possible since the chamber atmosphere does not need to be clean for the driver to work.

## Challenges

First and foremost, Z-Pinch must continue to make strides in fusion yield production. Experimental facilities capable of testing the engineering issues of developing a pulsed power reactor will be required to make long-term progress in this research.

More theoretical and experimental validation will be required for the shock mitigation technique. The recyclable transmission line destruction, remanufacturing, rep-rated installation, and interaction with the solid first wall need to be investigated further.

The energy deposition from the fusion pulse and subsequent fission energy multiplication occurs almost instantaneously. Removing the heat, and engineering the device for large temperature changes will be challenges for future work. This will require experimental investigation of the thermal properties of the actinide mixture.

The high neutron flux will cause damage to the chamber first wall and actinide pipes over time which could require periodic replacement of components. This issue will need to be addressed by either limiting the power level or examining high temperature operation that extends the lifetime of components.

There are a number of safety and control concerns with using a fluid fuel (even in a sub-critical configuration) that will need to be more fully explored.

This concept will have all the components and challenges of FR technology, plus the added cost of the fusion driver. Compared side by side, the In-Zinerator will likely cost more than a FR of the same power output. It is not clear if the better transmutation efficiency of the In-Zinerator will make up for this deficit.

## Path Forward

Reprocessing and transmutation technologies can make it possible to drastically reduce the volume and heat load of waste destined for a repository. However, these technologies will have to be used across the entire fuel cycle indefinitely in order to realize the long-term benefits. The long-term vision required to get these facilities built and keep them running makes these options very uncertain given our current political environment. If only one In-Zinerator could reduce the waste from the entire LWR reactor fleet, it might be possible to keep the reactor up and running. The requirement of 20 In-Zinerators or even more FRs would require a tremendous amount of political support. The poorer economics of fast spectrum reactors is ultimately what will hold an advanced fuel cycle back. It will likely require fast spectrum systems that have the same costs and uncertainties as LWRs in order for this nuclear future to be realized.

It is much more realistic to only build one or two of these reactors in the next few decades as opposed to building an entire fleet. One reactor will allow the device to be tested and the problems to be worked out. For this reason, it would be useful to focus on alternative actinide burning strategies in the future that minimize the number of In-Zinerators required. A minor actinide burner that is fueled with Np, Am, and Cm may be able to satisfy this goal. This reactor

would make sense if Pu was co-extracted with U to form a MOX fuel that can be burned in the existing fleet of LWRs. Focusing on this design in future work will give the research flexibility as the GNEP program changes directions.

Future work will also examine the transmutation of specific fission products like  $^{129}\text{I}$  and  $^{99}\text{Tc}$  in the In-Zinerator. These products will require thermal neutrons to optimize the effectiveness, so outer blankets or target regions will be examined. If an advanced fuel cycle leads to the concentration of fission product wastes in the repository, these long-lived fission products could be a potential long-term hazard. It would be useful to have a technology designed to transmute these species as well.

In parallel to this work, Z-Pinch is also being examined as an external driver for a nuclear assembly (ZEDNA) for use in high-intensity neutron irradiation test programs []. This compact assembly, fueled with less than 20% enriched uranium can allow for continued radiation effects testing at Sandia National Laboratories in the near term. However, it also could help to build experience with fusion driven sub-critical assemblies that will be useful in reaching the transmutation goal. A roadmap has been developed to discuss how Z-Pinch can evolve through the ZEDNA concept, transmutation, and fusion energy for future planning purposes [].

Fusion transmutation of waste is a useful application for a technology that has a difficult time reaching economical competitiveness. The In-Zinerator provides an intermediate step on the path towards pure fusion energy development, which will be required for long-term energy sustainability. Fast reactors can also lead to energy sustainability; however, fast reactors will always produce fission product waste and will always have the risk of a criticality excursion. Only fusion has the long-term potential to provide sustainable energy without the criticality concerns and without the production of large amount of high level waste.

## 7.1 References

1. E.J. Parma et al., “An Externally Driven Neutron Multiplier Assembly Concept Using a Z-Pinch 14-MeV Neutron Source (ZEDNA),” Sandia National Laboratories Report (not yet published).
2. C.W. Morrow et al., “Roadmaps and Containment Concepts for Early Z-Pinch Fusion Applications,” Sandia National Laboratories Report (not yet published).

## Distribution

- 2 Paul Wilson  
University of Wisconsin  
1500 Engineering Dr.  
Madison, WI 53706
- 2 Pavel Tsvetkov  
Department of Nuclear Engineering  
129 Zachry Engineering Center, 3133 TAMU  
Texas A&M University  
College Station, TX, 77843-3133
- 2 Remy Gallix  
General Atomics, Energy Group  
P.O. Box 85608  
San Diego, CA 92186-5608
- 1 Wayne Meier  
Lawrence Livermore National Lab  
P.O. Box 808, L-641  
Livermore, CA94551
- 1 Mahmoud Youssef  
UCLA MAE  
BOX 951597, 46-128C Engr IV  
Los Angeles, CA 90095-1597
- 1 Weston Stacy  
Room 0405, 801 Ferst Drive N.W.  
Georgia Institute of Technology  
Atlanta, Georgia 30332-0405
- 1 Mike Cappiello  
Los Alamos National Laboratory  
P.O. Box 1663  
Los Alamos, NM 87545
- 2 Francis Thio  
Office of Fusion Energy Sciences  
SC-24/Germantown Building  
U.S. Department of Energy  
1000 Independence Avenue, SW  
Washington, D.C. 20585-1290

- 2 Tom Drennen  
Hobart & William Smith Colleges  
314 Stern Hall  
300 Pultney St.  
Geneva, NY 14456
- 2 Jim Willit  
Argonne National Laboratory  
9700 S. Cass Ave  
Argonne, IL 60439
- 1 Al Trivelpiece  
14 Wade Hampton Trail  
Henderson, NV 89052-6635
- 1 David Hammer  
Cornell University  
Room 369 Upson Hall  
Ithaca, NY 14853
- 1 Barrett Ripin  
U.S. Department of State  
OES-STC  
Washington, DC 20522
- 1 Ehsan Khan  
U.S. Department of Energy  
SC-5/Forrestal Building  
1000 Independence Ave., SW  
Washington, DC 20585
- 1 Ted Hardebeck  
SAIC  
6825 Pine St.  
MS B-10  
Omaha, Nebraska, 68106
- 1 John Nuckolls  
Lawrence Livermore National Laboratory  
MS L-001, P.O. Box 808  
Livermore, CA 94551
- 1 Paul White  
Los Alamos National Laboratory  
MS A148, P.O. Box 1663  
Los Alamos, NM 87545

1 William Martin  
University of Michigan  
1941 Cooley Building  
2355 Bonisteel Blvd.  
Ann Arbor, MI 48109-2104

1 Wil Gauster  
2 Templeton Ct.  
Avon, CT 06001-3950

1 MS0125 Pace Vandevender, 12101  
1 MS0425 Jon Rogers, 0245  
1 MS0513 Rick Stulen, 1000  
1 MS0701 Peter Davies, 6700  
1 MS0724 Les Shephard, 6000  
1 MS0727 Tom Sanders, 6020  
1 MS0736 John Kelly, 6770  
1 MS 0736 Ron Lipinski, 6771  
1 MS0736 JD Smith, 6772  
10 MS0748 Ben Cipiti, 6763  
1 MS0748 Virginia Cleary, 6761  
1 MS0748 Jason Cook, 6763  
1 MS0748 Sam Durbin, 6763  
1 MS0748 Rodney Keith, 6763  
1 MS0748 Charlie Morrow, 6763  
1 MS0748 Gary Rochau, 6763  
1 MS0748 Mike Young, 6763  
1 MS0771 Dennis Berry, 6800  
1 MS0839 Karl Braithwaite, 7000  
1 MS0839 Linda Branstetter, 7000  
1 MS0839 Darryl Drayer, 7000  
1 MS0839 Gerold Yonas, 7000  
1 MS1136 Ed Parma, 6771  
1 MS1136 Paul Pickard, 6771  
1 MS1186 Mark Herrmann, 1674  
10 MS1186 Tom Mehlhorn, 1674  
1 MS1190 Keith Matzen, 1600  
1 MS1190 Craig Olson, 1600  
1 MS1191 John Porter, 1670  
1 MS1193 Dan Sinars, 1673  
1 MS1219 Charlie Craft, 5923  
1 MS1374 Joe Saloio, 6723  
2 MS9018 Central Technical Files, 8944  
2 MS0899 Technical Library, 4536  
1 MS0123 Donna Chavez, 1011